博士論文

A Comprehensive Numerical System for Predicting Airborne Chloride Generation and its Ingression into Concrete Under Actual Environmental Conditions

（実環境下における飛来塩分発生およびコンクリート内部への浸透を予測する包括的数値解析システム）

Wattanapornprom Rungrawee

ワッタナポーンプロム　ルンラウィー

A Comprehensive Numerical System for Predicting Airborne Chloride Generation and its Ingression into Concrete Under Actual Environmental Conditions

実環境下における飛来塩分発生およびコンクリート内部への浸透を予測する包括的数値解析システム

Rungrawee Wattanapornprom

Supervisor

Professor Tetsuya Ishida

Department of Civil Engineering

The Graduated School of Engineering

The University of Tokyo

September, 2016

A Comprehensive Numerical System for Predicting Airborne Chloride Generation and its Ingression into Concrete Under Actual Environmental Conditions

実環境下における飛来塩分発生およびコンクリート内部への浸透を予測する包括的数値解析システム

Rungrawee Wattanapornprom

Ph.D. Thesis – Civil Engineering
August, 2016

ABSTRACT

In a marine environment, deterioration of reinforced concrete structures is caused by airborne chloride attack and thereby many infrastructures used in the coastal area sometimes require repair or reconstruction due to the corrosion of reinforcing steel bars. The recent JSCE standard specification presents a simple method for durability design of marine environment structure. However, the proposed method has been formulated based on the limited number of measured data and it needs to be improved for reasonable durability design. Therefore, a reliable prediction model to calculate airborne chloride penetration into concrete structures is necessary to evaluate the service life of concrete structures and to realize rational maintenance.

However, there are some difficulties in predicting the chloride ingression into concrete structure due to airborne chloride, since chloride concentration on the concrete surface depends on the amount of airborne chloride supply, which varies due to wind direction, wind speed, wave height, obstacles, distance from the seashore, etc. In addition, when a structure is exposed to airborne chloride environment, chloride and water ingression do not occur uniformly on the concrete surface. Consequently, the chloride ingress model for the direct exposure case, such as submerged condition or cyclic wetting and drying condition, cannot be used to predict chloride penetration in case of airborne chloride attack. Furthermore, under actual environmental conditions, the chloride concentration on the concrete surface can be affected by rainfall, which means pure water can wash chloride out from the concrete surface and chloride inside the structure gradually diffuses out. As a result,

the reduction of the total amount of chloride in the concrete structure takes place. Hence, a new model to predict chloride ingress into concrete structure under complex airborne chloride environment is needed.

Against the above background, this study proposed a comprehensive system for calculating the amount of chloride generation, transportation, and ingression. The system is consists of three numerical models, which are airborne chloride generation and transportation model, moisture and chloride flux model at the boundary surface and chloride ion transport model in cementitious materials. By connecting each calculation model together, the proposed framework will be able to determine the amount of chloride ingression under the actual environmental condition without recorded airborne chloride data. Firstly, the amount of airborne chloride at the specified position can be calculated by using the airborne chloride generation and transportation model. After the airborne chloride amount has been calculated, the data will be given as the input for the airborne chloride surface flux model. Each model in the comprehensive system has been verified by the experiment and/or onsite measurement data to confirm the validity of the model.

The moisture and chloride flux model at the surface has been formulated as a time-dependent computational model for predicting the amount of airborne chloride ingress into concrete under the actual environmental conditions. The proposed model calculates the amount of chloride penetration by considering the amount of advection and diffusion of airborne chloride on the concrete surface. To compute the amount of airborne chloride, the proportion of dry and wet sections on the concrete surface is assumed, and to ensure accurate prediction of chloride penetration into concrete structures under actual environment conditions, the washout effect of rainfall is also taken into account in the calculation.

To verify the moisture and chloride surface flux model, the experimental series are conducted under controlled conditions in a laboratory. From the verification, the proposed model can predict the chloride ingression under airborne chloride condition, water ingression and washout chloride amount under specified condition. Moreover, the onsite measurement data were also used to verify airborne chloride ingression under actual environmental condition. From the verification, it is shown that the proposed model can appropriately simulate the chloride penetration and washout effect of mortar specimen under actual environment conditions. In some cases, the analysis gives the dissimilar value compared with the exposure testing result. This may be due to the limitation of the meteorological data, and/or the fact that the assumptions used in the proposed model do not correspond to the actual exposure conditions.

The airborne chloride generation and transportation model can be used to predict the amount of airborne chloride at the specified position by input the data of breaking wave

height, wind direction, wind speed, obstacles, distance from the coastline etc. The calculated airborne chloride data from the airborne chloride generation and transportation model have been verified by onsite measurement data. From the verification, the chloride generation and transportation model can predict the amount of airborne chloride at each location under different exposure condition.

Finally, after the verifications of each model, the overall system also has been verified by onsite measurement data at Okawa Bridge. The verification results showed that the proposed system can calculate the total chloride amount when the structure subjected to the rainfall (flange position). However, the analysis results at web position are not well predicted. The reason may be due to the limitation of the proposed system which cannot calculate the chloride penetration in unsaturated concrete. Thus, the future modification of the chloride ion transportation should be considered.

Acknowledgement

First of all, I would like to express my sincere thanks of gratitude to my supervisor, *Professor ISHIDA Tetsuya*, for his enthusiasm and effort to guide me. Without his great vision and encouragement, this research cannot be completed. He kindly gave me the support and advice, not only in the research work but also in my student life and future career.

Secondly, I would also like to extend my sincere gratitude to *Professor MAEKAWA Koichi* for his kind encouragement since at the beginning of my study life in Concrete Laboratory. In every discussion, he always comes up with the meaningful comments and thoughtful suggestions which help me very much in supporting my life and research in Japan.

Besides, I would like to acknowledge my supervising committee members: *Professor KISHI Toshiharu, Professor TAJIMA Yoshimitsu* and *Professor SAEKI Tastuhiko* (Niigata University) for their valuable suggestion and comment which assisted me to improve my research work.

I'm sincerely thankful to *Associate Professor Boonchai STITMANNAITHUM*, for always being my inspiration and motivation. Although he is very busy but he never leaves his students behind and always pushes me when I am feeling tired. Special thanks to *Associate Professor Withit PANSUK*, who makes my life in Japan becomes much more interesting with his special style of teaching and continuously inspire me to challenge myself in doing something new. *Associate Professor Phoonsak PHEINSUSOM*, who always spends his time in listening to my stupid story during his vacation in Japan and kindly give me the encouragement. *Chulalongkorn University faculty members* who kindly came and visit Thai student in Tokyo.

I would like to extend my appreciation to *Dr. Ahmed Mohammad Youssef Mohammad, Dr. Ali Ahmed* who helped me a lot during my experimental work. *Concrete Laboratory members* and *Civil engineering department staffs* for their good support during my study. Especially, *Dr. Youssef* who spent his time walking with me and sent me near my accommodation when I finished my research late at night. I'm also thankful to *Chulalongkorn University Concrete Club members, Thai student in the University of Tokyo, Thai Waseda Members* and *Yanaka House Members* for the best friendship, help and encouragement in every way. *CPAC lab members* and *SCG staffs* who always trust and give me so many support/opportunity, even though I've already changed my work place.

I also would like to express my gratitude to *The Ministry of Education, Culture, Sports, Science and Technology (MEXT) of Japan*, for supporting the scholarship during my study.

At last, I would like to thank my lovely family for their endless help and mental support Especially, *Khun Aung (Dr. Watcharee)*, my sister for being the best supporter.

Rungrawee Wattanapornprom

Table of content

List of figures

List of Tables

Abbreviations

AMEDAS	Automated Meteorological Data Acquisition System
ASTM	American Society of Testing Materials
DuCOM	Durability Concrete Model
FA	Fly ash
ISO	International Organization for Standardization
JIS	Japanese Industrial Standards
JSCE	Japan Society of Civil Engineers
MF	Magnified Factor (to increase the water absorption capacity when the concrete surface is exposed to rainfall)
NowPhas	The Nationwide Ocean Wave information network for Ports and HArbourS
OPC	Ordinary Portland Cement
PC	Pre-stressed Concrete
PWRI	Public Works Research Institute
RC	Reinforced Concrete (members)
RH	Relative Humidity
W/B	water-to-binder ratio in concrete
W/C	water-to-cement ratio in concrete

Chapter 1
Introduction

1.1. Introduction

Concrete is a composite material and is most commonly used for infrastructure. However, concrete structures can be damaged through many processes, including physical effects, deleterious chemical effects, alkali-aggregate reactions, sulfate attacks, and the corrosion of steel embedded in concrete [1].

Chloride ingress into concrete is also one of the most important factors in the deterioration of reinforced concrete (RC) structures. Many infrastructures require repair or reconstruction due to the corrosion of reinforcing steel bars [2]. The corrosion of reinforcement in concrete not only reduces the reinforcement diameter but also causes damage on covering concrete.

Airborne chloride or sea salt aerosols can also be the cause of deterioration in concrete structures. The chloride from airborne chloride accumulates on the surface of infrastructure, diffuses, and accelerates the corrosion of embedded steel bars.

Figure 1-1 Corrosion and spalling of reinforced concrete (RC) structure in Rayong province, Thailand caused by airborne chloride.

To prolong the service of concrete infrastructures in marine environment, deterioration from airborne chloride should be carefully considered especially the structure near the seashore.

1.2. Problem Statement

In marine environment, RC structures deteriorate because of airborne chloride attacks and, for this reason, infrastructure in coastal areas sometimes requires repair or reconstruction due to the corrosion of reinforcing steel bars.

Recent standard specifications, for example, the JSCE (Japan Society of Civil Engineer) standard, present simple methods for the durable design of marine environment structures. However, the proposed method has been formulated based on limited number of measured data and requires improvement for reasonable durability designs. Therefore, a reliable prediction model to calculate airborne chloride penetration into concrete structures is necessary to evaluate the service life of concrete structures and to realize rational maintenance.

Under airborne chloride environment, chloride concentration on the surface of concrete structure depends on the amount of airborne chloride supply, which varies due to wind direction, wind speed, wave height, obstacles, distance from the seashore, etc [3]. The concentration of airborne chloride at specific times and locations differs. Moreover, when a structure is exposed to airborne chloride, chloride and water ingression do not occur uniformly on the concrete surface. Consequently, the boundary condition used in the calculation of chloride penetration under conditions with airborne chloride is more complex compared to structures submerged in seawater.

Furthermore, under actual weathering conditions, chloride concentration on the concrete surface can be affected by rainfall. Pure water can wash chloride from the concrete surface [4, 5] and chloride inside the structure can gradually diffuse out [6]. As a result, the total amount of chloride in the concrete structure is reduced [6].

Due to complex environmental conditions, existing models to predict chloride ingress into concrete for the direct exposure case, such as submerged condition or cyclic wetting and drying conditions, cannot be used to predict chloride penetration in case of airborne chloride attacks. Therefore, a new model to predict chloride ingress into concrete structure in airborne chloride environments is necessary.

Moreover, in reality, the recorded of airborne chloride intensity data are limited. Although a numerical model to predict airborne chloride ingression is available, it may not be sufficient to evaluate the service life of infrastructure. Thus, in such a case, it is also necessary to have a system, which can predict chloride ingression without recorded airborne chloride data.

1.3. Objective of the study

The primary objective of this research is to develop a time-dependent, computational model to predict the amount of airborne chloride penetration into concrete under actual environmental conditions. To obtain a valid prediction of chloride penetration, the washout effects of rainfall are taken into account for calculations. The results from the model prediction will be verified through comparisons with laboratory experimental data and on-site measurement data.

Since the past recorded data of airborne chloride are limited, the main objective of this research is to develop a comprehensive system that can predict chloride ingression into concrete structures without recorded airborne chloride data. This comprehensive system can be used to determine the amount of airborne chloride generated by breaking waves, transported by wind flow, and ingression through the concrete surface at specified positions. The proposed framework is verified through onsite measurements to confirm its validity.

1.4. Outline

As noted, the main objective of this research is the development of a comprehensive computational system to predict the amount of airborne chloride penetration under actual environmental conditions without previously recorded data.

The structure of the dissertation is outlined below.

Chapter 2 This chapter presents general reviews of previous studies on airborne chloride penetration and the effect of rainfall on airborne chloride penetration. Moreover, the experimental methodology to simulate airborne chloride penetration in the laboratory is reviewed.

Chapter 3 This chapter presents the proposed comprehensive system and relevant models used in the system. Relevant models in the comprehensive system are as follows:

1) Modeling of generation and transportation of airborne chloride;
2) Modeling of moisture and chloride flux at concrete surface;
3) Modeling of chloride transport in cementitious materials.

Furthermore, verifications and limitations of each model are discussed.

Chapter 4 In this chapter, a modification of the airborne chloride surface flux model is discussed. To verify the modified model, a comprehensive series of

experiment were conducted under controlled conditions. Moreover, airborne chloride and chloride penetration data under actual environmental conditions were collected and used to verify the proposed model.

Chapter 5 This chapter presents the verification of the airborne chloride generation and transportation model throughout on-site measurement data in various locations in Japan.

Chapter 6 A verification of the proposed comprehensive system with onsite measurement data at Okawa Bridge is presented.

Chapter 7 The final chapter includes a conclusion of the current study and recommendations for future research.

A characterization of the current study is presented in Figure 1-2.

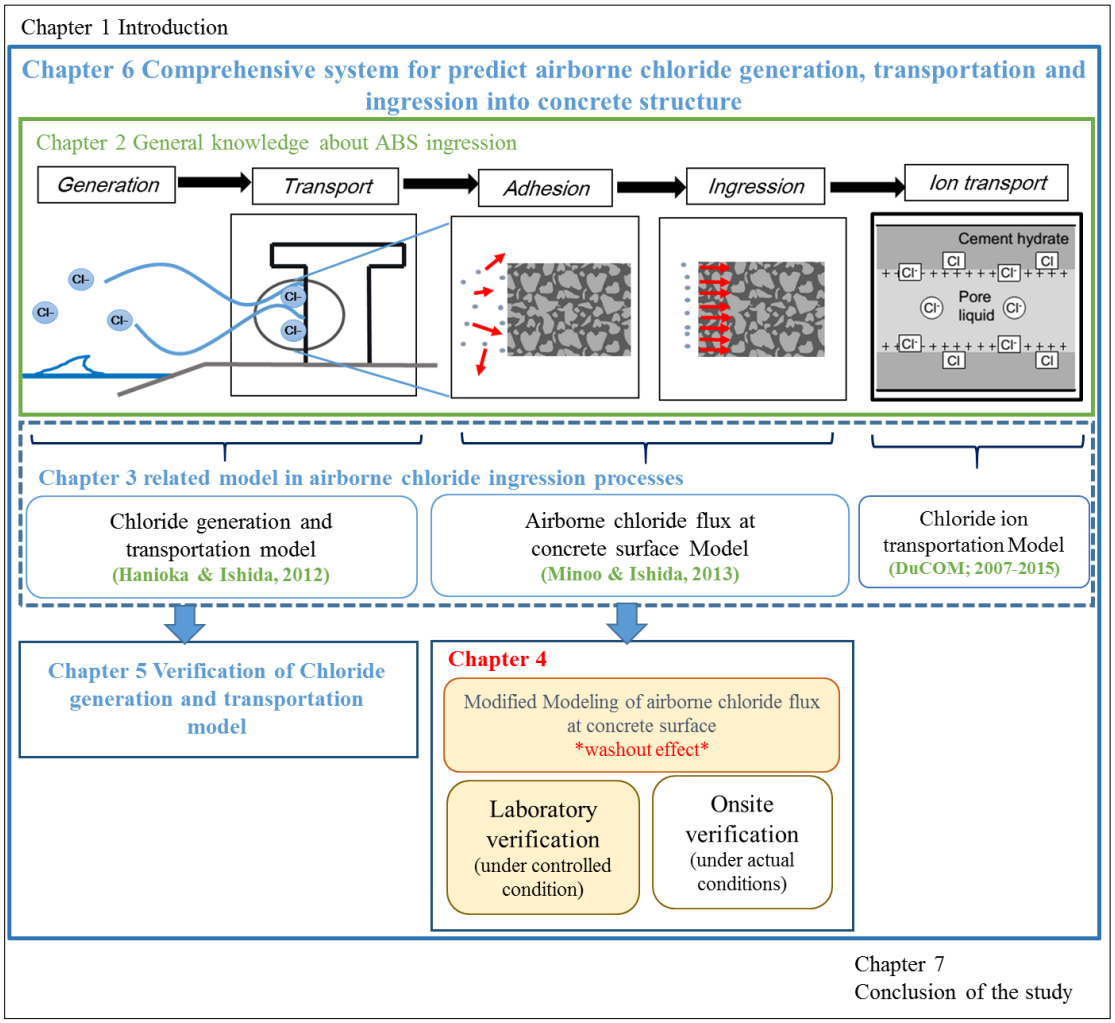

Figure 1-2 General scope of research.

1.5. Reference

[1] P. Mehta and P. J.M. Monteiro, Concrete ; Microstructure, Properties , and Materials, 3rd ed., New York: McGraw-Hill, 2006, pp. 121 - 124.

[2] P. Mehta, Concrete in the Marine Environment, Taylor & Francis Books, Inc, 2003.

[3] N. Bongochgetsakul, S. Kokubo and S. Nasu, "Measurement of Airborne Chloride Particle Sizes Distribution for Infrastructures Maintenance," in *IESL-SSMS Joint Symposium*, Colombo, Srilanka, 2011.

[4] H. Yamashita, T. Shimomura and F. Yamada, "Study of chloride concentration on concrete surface affected by Airborne Chloride.," in *Japan Concrete Institute Annual Conference*, Japan, 2007. (In Japanese)

[5] T. Yasuda, Y. Kishimoto, T. Tsutsumi, Y. Hama and M. Zakaria, "Fundamental Study on Influence of Rain and Wind on Durability of Building Wall," in *Repairing and Maintenance of Concrete Structures*, 2013. (In Japanese)

[6] K. Hong and E. Hooton, "Effects of fresh water exposure on chloride contaminated concrete," *Cement and Concrete Research*, vol. 30, pp. 1199-1207, 2000.

Chapter 2
Overview about Airborne Chloride Ingression

2.1. Introduction

Reinforced concrete has become the most commonly used material to build marine structures. There can be a number of reasons for this, such as excellent water resistance, structural flexibility which enables concrete elements to be formed into a variety of shapes and sizes, and the low cost and ready availability of concrete-making materials globally [1].

Concrete infrastructure which exposed to marine environment may deteriorate as a result of combined effects of chemical action of seawater constituents on cement hydration products, crystallization pressure of salts within concrete when subject to wetting and drying conditions, freezing and thawing in cold climates, corrosion of embedded steel in reinforced or pre-stressed concrete section, and physical erosion due to wave action [2]. Figure 2-1 diagrams the deterioration of concrete structures in marine environments [1].

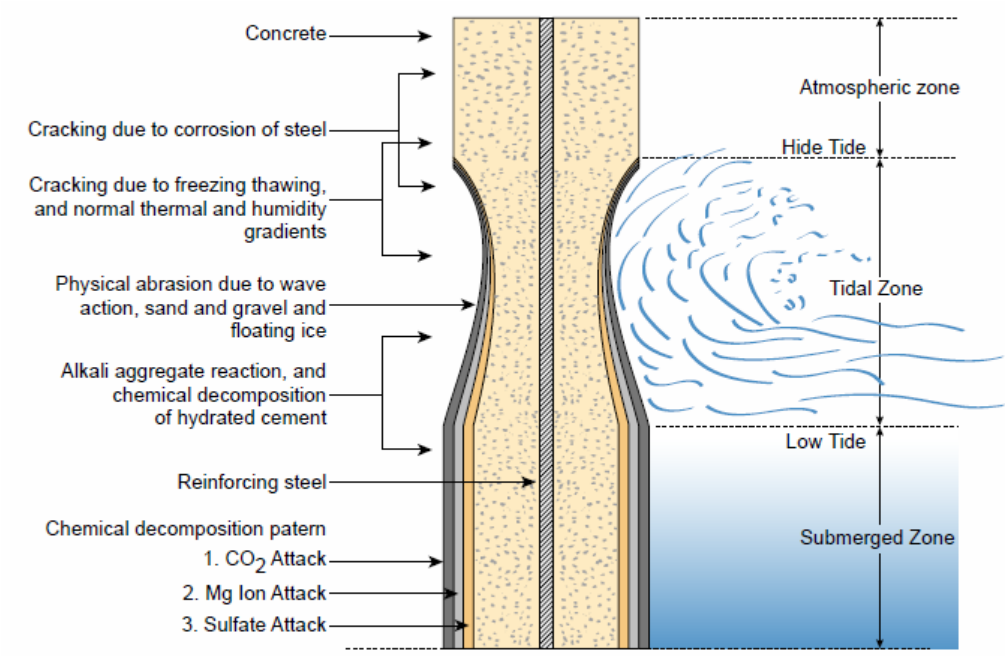

Figure 2-1 The possible deterioration of concrete structures in marine environments [1].

Even though reinforced concrete under marine environment has a number of causes for the decline in quality of the structure but corrosion of embedded steel is, generally, the major cause of concrete deterioration in reinforced and pre-stressed concrete (PC) structures exposed to seawater [2]. Corrosion of reinforcement in concrete not only reduces the reinforcement bar diameter but also causes damage to the covering concrete.

Concrete structures in marine environments can be divided into two main categories of exposure, direct and indirect. Direct exposure includes structures that are partially or fully submerged in sea water. Indirect exposure includes structures which do not directly contact the seawater but interact with airborne chloride (sea salt aerosol), such as bridge structures or buildings near the coast, among others [2, 3, 4]. The classification of concrete structures in marine environments is shown in Table 2-1.

Table 2-1 Classification of marine exposure.

Exposure zones	***Type of exposure***	
Submerged zone	*Direct exposure*	Constantly submerged under sea water
Tidal zone		The zone between low and high tidal elevations. Wetting and drying is controlled by the rise and fall of tide. Concrete surfaces in tidal zones re cyclical exposed to sea water
Splash zone		The splash zone is limited by the extent of splash from breaking waves above the tidal zone. Structures in this zone are randomly exposed to sea water.
Atmospheric zone	*Indirect exposure*	The area where chloride particles from breaking waves are carried by wind flow and attached to concrete structures. The surface of a concrete structure in this zone is randomly exposed to airborne chloride.

Several studies have examined the mechanism of chloride penetration into concrete under conditions of direct exposure. During direct exposure, the chloride concentration on the concrete surface is uniform, unlike indirect exposure conditions. For this reason, the amount of chloride penetration can be easily predicted.

Under indirect exposure conditions or in the atmospheric zone, difficulties arise in predicting chloride ingression into concrete structures from airborne chloride. This is because the chloride concentration on the concrete surface varies due to the wind direction, wind speed, wave height, obstacles, and distance from the seashore, among other factors [5].

To characterize the mechanism of chloride penetration under airborne chloride conditions, this chapter presents general knowledge about airborne chloride and presents factors that affect airborne chloride penetration into concrete.

2.2. The deterioration of concrete structures in airborne chloride environments

Most seawater from different locations is fairly uniform in its chemical composition, characterized by the presence of 3.0–3.5% soluble salts by mass. The ionic concentrations of Na^+ and Cl^- are the highest, typically 11,000 and 20,000 mg/l, respectively [2].

Airborne chloride (Sea salt aerosol or airborne salt) is chloride particles generated by the breaking wave and transported in the atmosphere by the wind flow. The airborne chloride particles contain around 3% salt, similar to the sea water concentration [6].

Airborne chloride or sea salt aerosol contributes to the deterioration of concrete structures. The chloride from airborne chloride accumulates on a surface of infrastructure and diffuses into concrete materials. The chloride from the airborne chloride can initiate and accelerate the corrosion process of embedded steel bars. Figure 2-2 shows damage to a concrete structure after a lengthy exposure to airborne salt in Alexandria, Egypt.

Figure 2-2 Existing RC residential structures suffering from heavy corrosion caused by airborne chloride attacks from the Mediterranean Sea in Alexandria, Egypt (2013) [7].

Airborne chloride ingression into concrete structures can be described by the following processes: i) airborne chloride generation; ii) transportation; iii) surface adsorption, iv) ingress through concrete surface, and v) chloride ion transportation inside cementitious materials [5], as shown in Figure 2-3

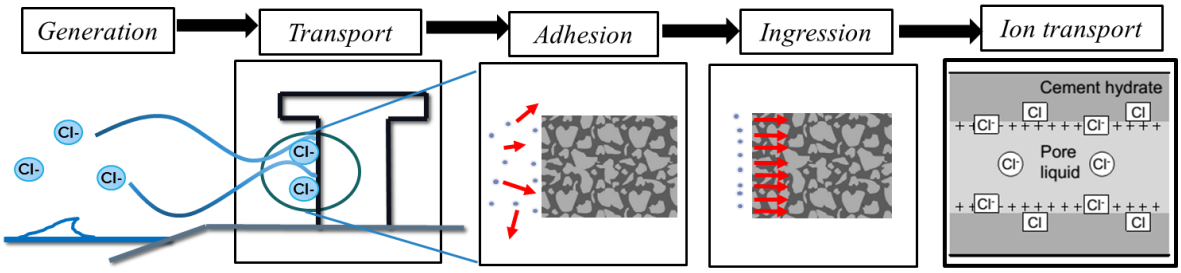

Figure 2-3 Airborne chloride ingress process in concrete structures.

2.2.1. Airborne Chloride Generation and Transportation

Airborne chloride particles are generated when sea waves reach the seashore or an obstacle [8]. The size of airborne chloride particles (seawater aerosol) mainly depends on weather, wave conditions, and coastal topology [5]. It has been reported that obstacles such as wave breakers or cliffs contribute to a higher amount of airborne chloride of a larger size [8]. Larger particles of airborne chloride rapidly drop vertically due to the force of gravity. However, smaller particles can be transported by the wind across long distances [5].

Additionally, the amount of airborne chloride at each position is changed due to wind direction, wind speed, obstacles, and distance from the seashore [5, 8]. Faster wind speeds can carry more salt longer distances and airborne chloride levels is trended to be higher within the same distance [9]. Figure 2-4 shows airborne chloride levels around Japan and Figure 2-5 shows the airborne chloride concentration over 1 year in Shinanokawa, Niigata, Japan.

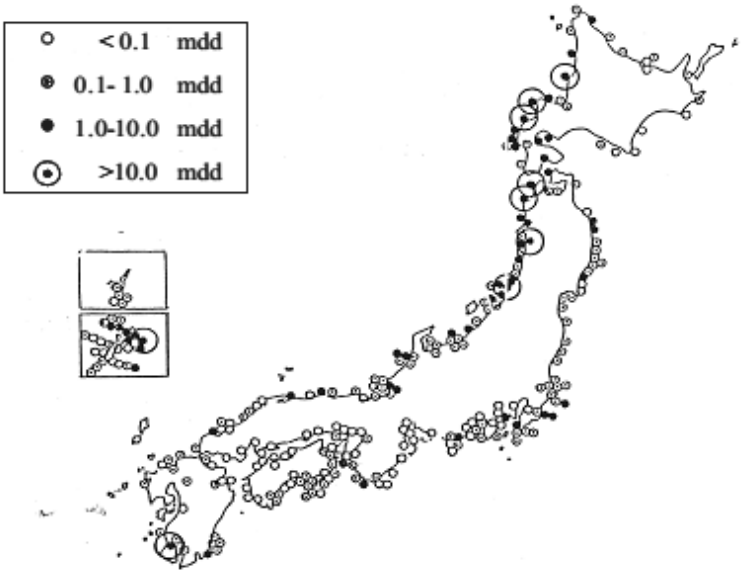

Figure 2-4 Airborne chlorides in Japan, as investigated by the Public Work Research Institute (PWRI) [10].

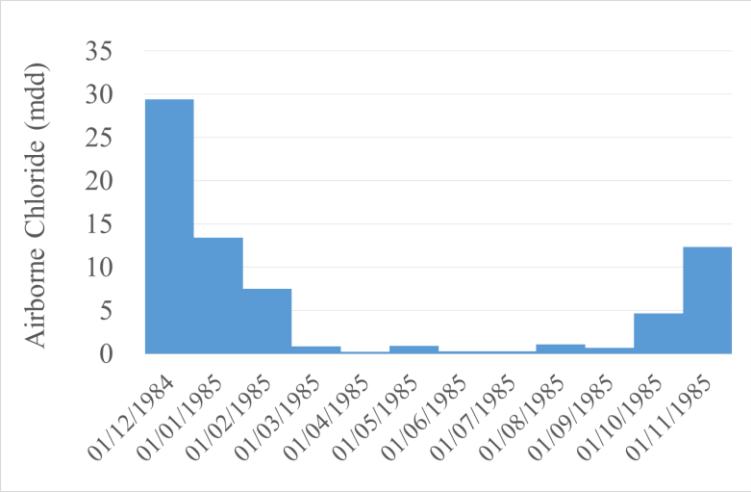

Figure 2-5 Airborne chloride concentrations from October 1985–November 1986, Shinanokawa, Niigata, Japan (reported by PWRI) [10].

2.2.2. Airborne Chloride Absorption and Ingression

Airborne chloride particles consist of two components, chloride ions and water. When airborne chloride particles attach to the concrete surface, both water and chloride ions penetrate the material. Therefore, to examine the mechanism of airborne chloride ingression, water and chloride ingression behavior should be studied.

1) Chloride ion transport mechanism

The chloride ion transport mechanism through a porous cement network can be describe as follows [11, 12]:

- **Diffusion**

Diffusion is the movement of chloride ions in a concentration gradient. For this to occur, the concrete must have a continuous liquid phase and there must be a chloride ion concentration gradient.

- **Capillary absorption**

Absorption of water containing chloride into concrete that is not saturated (capillary sorption). This is typical in bridge decks and parking slabs exposed to deicing salts where the concrete cover is likely to be partially-saturated, and in the tidal and splash zones of marine structures.

- **Permeation**

Chloride ingress that is driven by pressure gradients. If there is an applied hydraulic head on one face of the concrete, chlorides may permeate the structure. However, situations where a hydraulic head is consistently applied to concrete structures are rare.

These mechanisms can bring chlorides into the concrete and initiate the corrosion of steel bars.

2) Moisture transmission into concrete in marine environments

In a marine environment, moisture transmission plays a vital role for chloride movement in concrete. Wet environments can be classified into three types, depending on the mechanism by which moisture transportation takes place [4].

- **Humid environment**

An environment where the relative humidity is close to 100% and moisture diffuses into pores through a concentration gradient.

- **Submerged environment**

The condition when concrete is immersed in water. The main transport is the capillary suction of liquid water. Surface tension is the primary cause of liquid to rise in capillaries. In this condition, water can also penetrate concrete under water pressure.

- **Rainfall environment**

Finally, in actual environmental condition, there is also the water supplies from precipitation, such as rainfall or snow. When rainfall reaches the concrete surface, moisture can be transported into the concrete by capillary actions. This is similar to concrete in a submerged condition but without external water pressure on the concrete surface.

2.3. Airborne Chloride Collection Methods

There are several methods to measure the amount of airborne chloride at a specified position. To develop a computational model for predicting airborne chloride penetration, it is necessary to study the differences between each method.

2.3.1. Wet Candle

The wet candle method is one of the common methods for checking the concentration of airborne chloride in the atmosphere. This method follows the standards ASTM G140 and ISO 9225 [13, 14].

The wet candle device is composed of a wick inserted into a 500 mL Erlenmeyer flask containing deionized water or 40% glycol. The chloride particles are trapped by the wet wick which is wrapped by gauze. The end of the gauze is immersed in the solution inside the flask. The wet candle device is shown in Figure 2-6 and Figure 2-7.

After exposure, liquid samples from the testing set are collected and titrated with 0.05 M silver nitrate ($AgNO_3$) solution or others chemical methods are used to determine the amount of chloride.

The device should be installed 1.5 meters above ground level and away from walls which could inhibit the free circulation of air. The candle should be exposed to the sea or other sources of chloride. It should be noted that in conditions with relatively low humidity or under dry conditions, the device may not capture salt particles. Thus, at intervals, the sample and water level inside the flask need to be carefully checked [9].

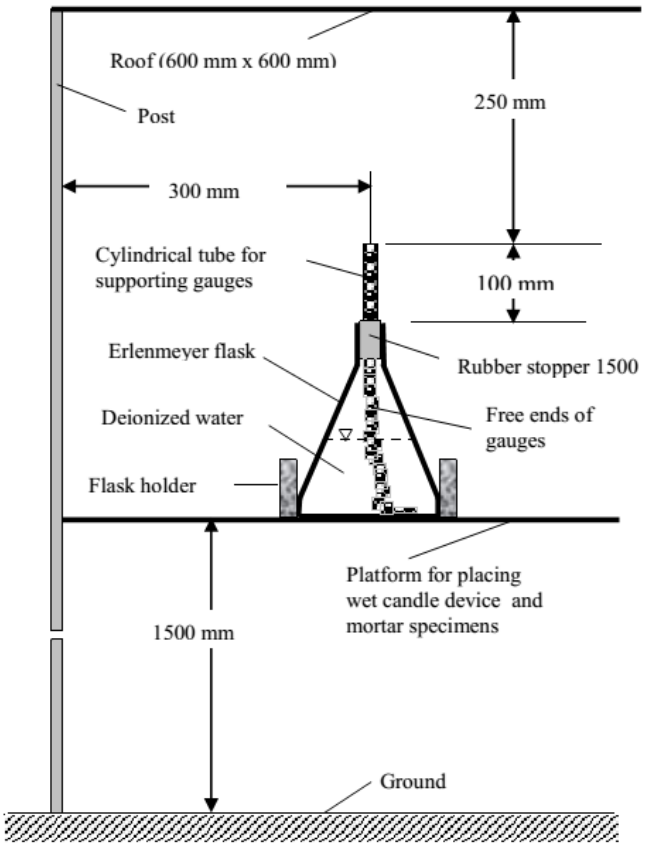

Figure 2-6 Typical wet candle device [14].

Figure 2-7 Example of wet candle device setup [15, 16].

2.3.2. Dry Gauze

The dry gauze method is specified by the Japanese standard JIS Z 2382 [17]. The device consists of 10 x 10 cm gauze attached to a frame to capture airborne chloride.

This method can capture chloride on a concrete surface by attached the device to the structure. However, the amount of airborne chloride that can be captured by the gauze is limited by the capacity of gauze itself. To avoid errors, frequent sampling is necessary [18]. The dry gauze set up device is shown in Figure 2-8.

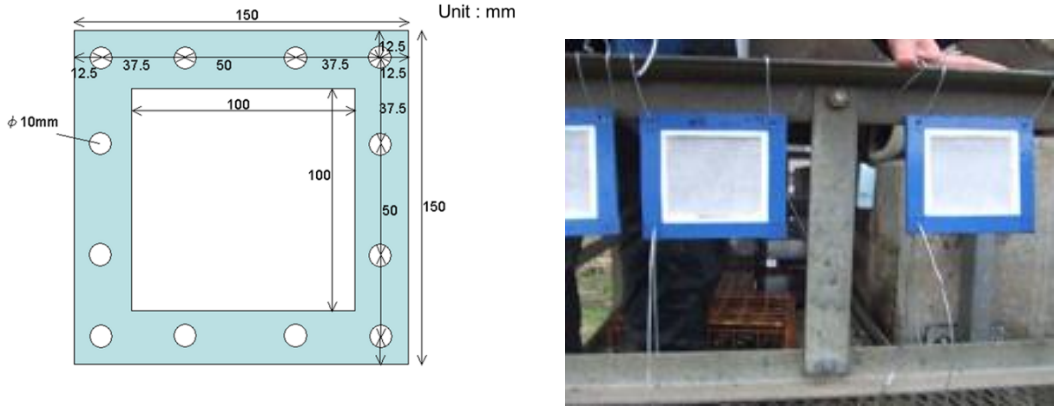

Figure 2-8 Example of dry gauze device setup [18].

2.3.3. Tank sample

The airborne chloride capture method was developed by the Public Work Research Institute (PWRI), Japan [10]. Airborne chloride is deposited in a stainless steel capture board (size 10 x 10 cm^2) connected with a plastic tube to a plastic container.

Airborne chloride on the capture board is washed off with pure water collected in the plastic container. After the test, the water inside the plastic container is titrated with silver nitrate solution ($AgNO_3$) to determine the amount of airborne chloride. The equipment used for these methods is shown in Figure 2-9 and Figure 2-10 [19].

This method can be used to determine levels of airborne chloride over long periods and cannot capture small amounts of chloride in short periods.

Figure 2-9 Airborne chloride capture tank and plastic container inside [19].

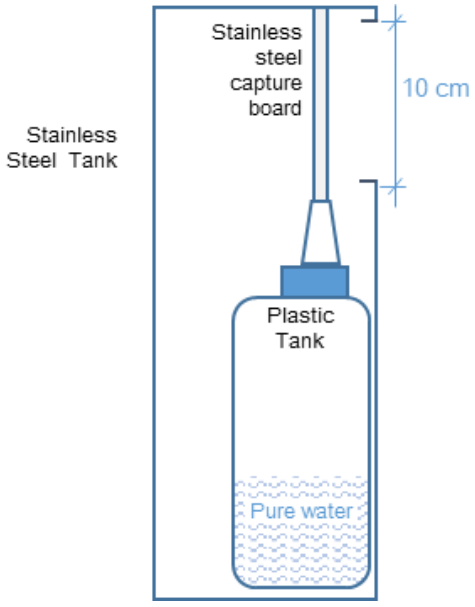

Figure 2-10 Diagram of airborne chloride capture tank.

2.3.4. Mortar chip

Many past researches used small cement paste or mortar specimens to determine the amount of chloride in the atmosphere [18, 20]. This method can determine the amount of aerosol at a specific position because the specimen size is small compared to tank equipment. However, with this type of specimen, chloride capture capacity is effected by the properties of cement paste, such as the water-to-cement ratio (W/C) or

thickness. Additionally, the specimen can be washed by rainfall, reducing the concentration of chloride on the specimen surface.

Figure 2-11 Plastic container inside the stainless steel tank [19, 20].

2.4. Comparison of Techniques for the Measurement of Airborne Chloride

The airborne chloride collection methods described can determine the relative amount of chloride at specific locations and times. However, each method provides different values of airborne chloride [10, 21]. A comparison between methods is presented in table 2-2.

Table 2-2 Summary of techniques for airborne chloride capture.

Method	Test duration	Notes
Wet candle	1–3 months	- Cannot measure chloride at precise positions - Wind direction attached to sample and device may not be the same
Tank capture	1–3 months	- Cannot measure chloride at precise positions
Dry gauze	2 hrs	- Cannot be used for long term exposure
Mortar chip	1–3 months	- Can be effected by rainfall and proportions of mortar mix

2.5. Washout Effect

In actual environmental conditions, chloride concentration on concrete structures is influenced by the climate, location, and weather [22]. Water particles from rainfall or melted snow can wash chloride from the concrete surfaces [6, 23, 24]. This is called the washout effect and its mechanism is shown in Figure 2-12.

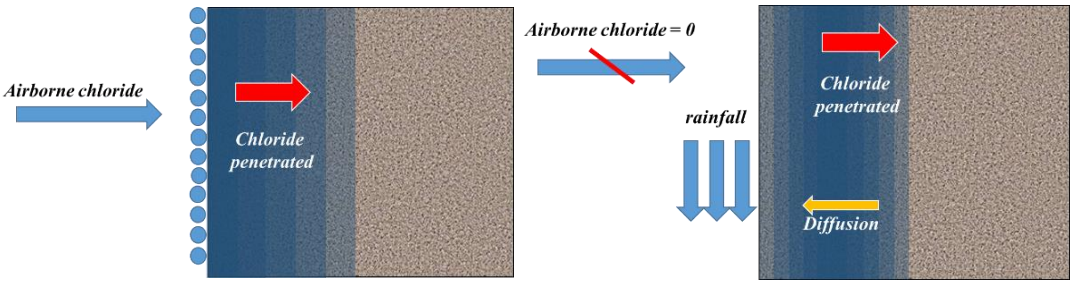

Figure 2-12 Airborne chloride washout mechanism schematic.

This phenomena is confirmed by [23]. From past research, the experiment was conducted by using mortar specimens. Specimens were exposed to airborne chloride and the surface was washed by pure water after the exposure. A summary of the experiment is presented in *Figure 2-13*.

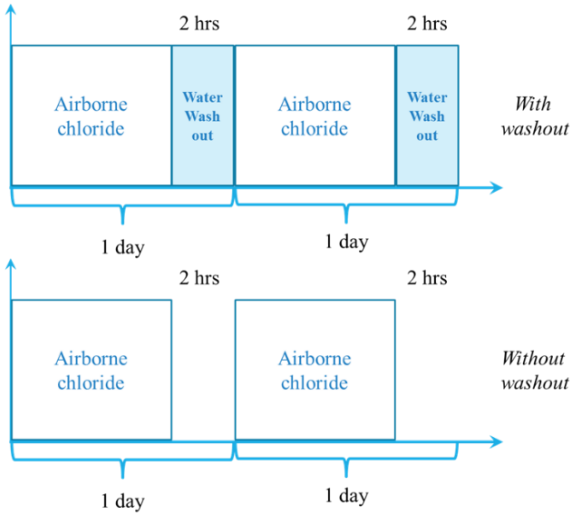

Figure 2-13 Washout experiment summary (Modified figure from the reference) [23].

After exposure, chloride on the surface (~1 cm depth) was determined with titration method. The experimental results show that chloride on the surface is reduced when the surface is washed with pure water. The results of the experiment are shown in Figure 2-14.

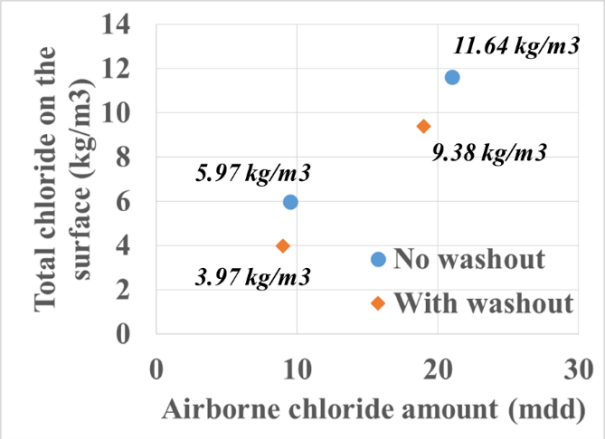

Figure 2-14 Total chloride with and without washout (Modified figure from reference) [23].

Moreover, a field survey suggests that the concentration of chloride on concrete structures dramatically decreases due to rain [6]. The concentration was determined by collecting cement paste powder from the concrete surface and titrating the powder sample. The concrete powder was collected by rubbing sand paper against the concrete surface. The change of chloride concentrations on the surface is shown in Figure 2-15 [6].

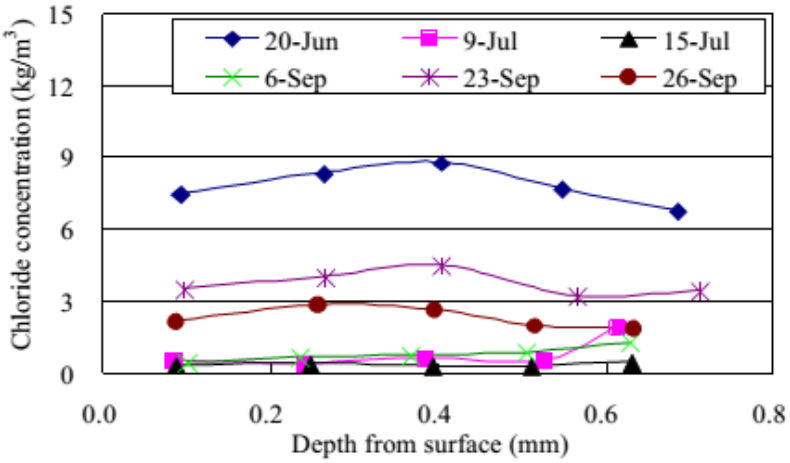

Figure 2-15 Survey results from Maehama, Kochi Prefecture (30 m from seashore) [6].

Figure 2-15 shows the results of 6 samples taken between June 20, 2003 and September 26, 2003 during the rainy season. The data shows that the chloride concentration on the structure's surface changes due to the washout effect from rainfall after the initial sampling date.

The washout effect can also reduce the amount of chloride further inside concrete materials, not only on the surface. It has been reported that when a specimen is exposed to chloride and then pure water, the total amount of chloride inside the specimen is reduced [25].

To determine this, four specimens were submerged in a solution of Sodium Chloride (NaCl), concentration 1 mol/L, for 120 days. After submersion, specimens were placed into distilled water for either 0, 30, 60, or 120 days.

When the specimens were placed in distilled water, chloride inside the specimens gradually diffused out. Submersion in pure water over longer periods of time results in a significant difference in the chloride concentration, as shown in Figure 2-16 [25].

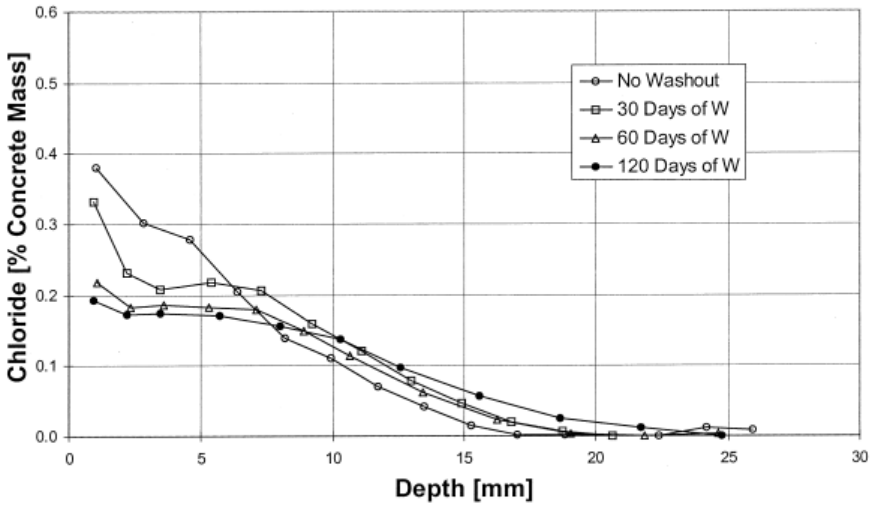

Figure 2-16 Chloride concentration reduces after submersion in distilled water [25].

The results of this experiment demonstrate a clear decrease in the concentration of chloride near the surface and deeper in the concrete after submersion in pure water for 120 days.

2.6. Airborne Chloride Ingression using Wind Tunnels

To simulate environmental conditions for airborne chloride in the laboratory, a wind tunnel can be used. In 2007, Nagaoka University developed a prototype wind tunnel to study chloride penetration in mortar specimens in addition to the washout effect [22, 23, 26]. The wind tunnel prototype is shown in following figure.

Figure 2-17 Wind tunnel prototype to simulate airborne chloride environmental conditions [23].

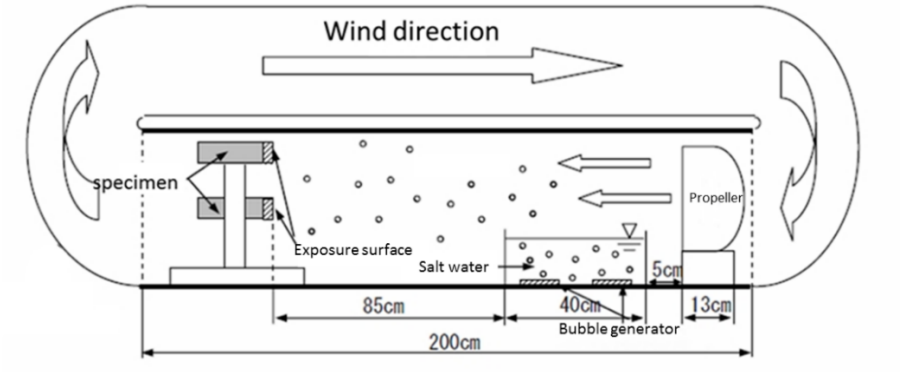

Figure 2-18 Diagram of wind tunnel prototype (Modified figure from the reference) [23].

To determine the amount of airborne salt inside the chamber, dry gauze specimens were installed at various positions. After 4 hrs, the gauze at each position was removed from the frame and submerged in pure water. The amount of chloride the gauze contained was determined by titration. Dry gauze specimen sizes and installation positions are shown in Figure 2-19.

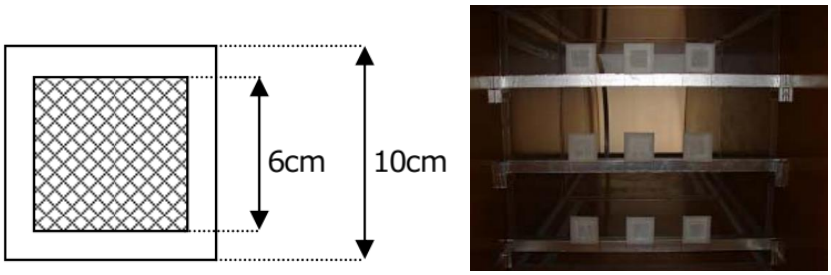

Figure 2-19 Dry gauze specimen and installation positions [26].

In 2008, the University of Tokyo used the same concept to develop a wind tunnel [27, 28, 29] . Figure 2-20 shows a diagram of the wind tunnel developed by Concrete Laboratory, University of Tokyo.

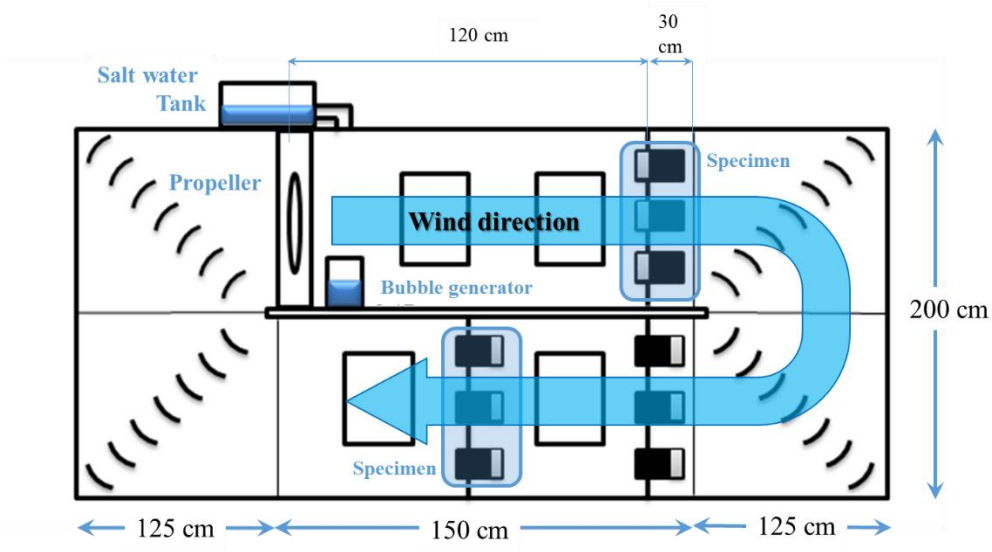

Figure 2-20 Diagram of wind tunnel by the University of Tokyo.

A general overview of using the wind tunnel to simulate airborne chloride environmental conditions in the laboratory is shown in Figure 2-21.

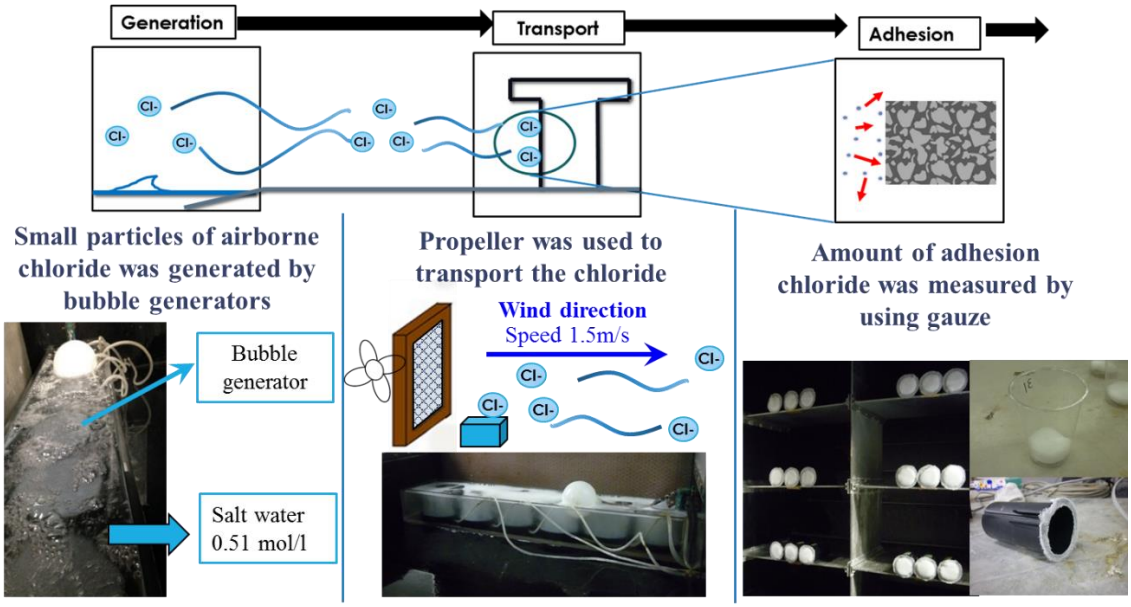

Figure 2-21 Using a wind tunnel to simulate an environment with airborne chloride.

For the experiments, a salt bath and bubble generator were first installed inside the wind tunnel. The salt bath was filled with Sodium Chloride (NaCl) solution with a concentration of 3% (0.51 mol/l), the same concentration of NaCl in sea water. The bubble generator was placed inside the salt water bath to generate small salt particles, Figure 2-22.

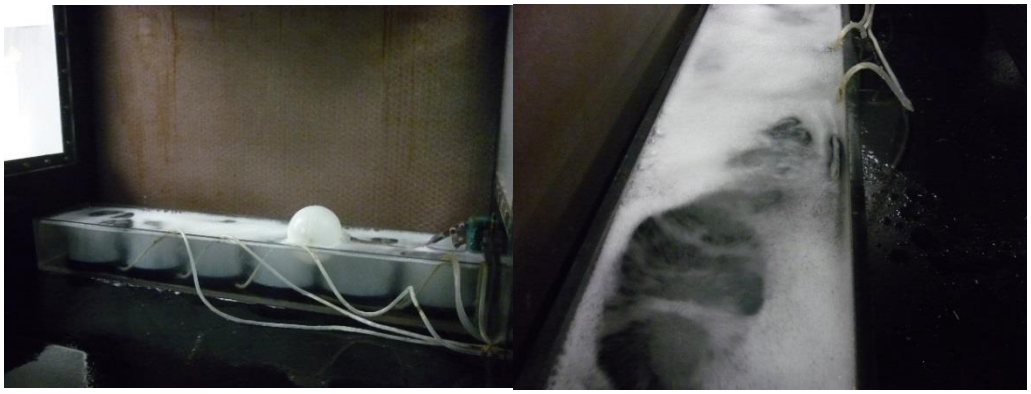

Figure 2-22 Salt bath and bubble generator inside the wind tunnel [29].

Behind the salt bath, a propeller was installed. The propeller was used to generate air flow inside the chamber. The air flow transports the airborne chloride particles inside the wind tunnel, as shown in Figure 2-23 [27]. The average wind speed in this test was ~1.5 m/s.

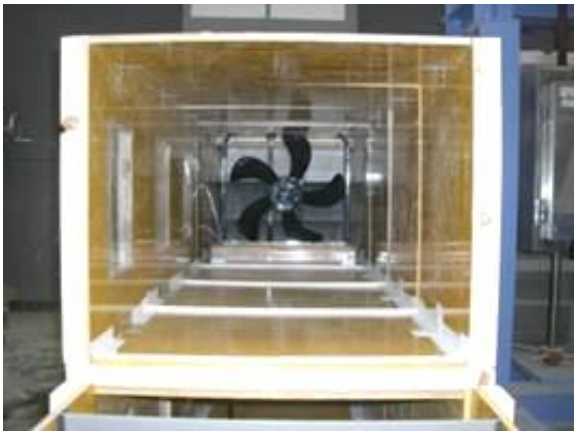

Figure 2-23 Propeller to generate wind flow inside the chamber.

To determine the amount of airborne chloride that adhered inside the chamber, in this case instead of dry gauze, gauze and cotton specimens were installed at various positions.

Dry gauze specimen is a free end specimen, thus, the wind can flow through the gauze, Figure 2-24. However, under actual conditions, wind flow is blocked by the structure and the wind speed decreases in front of the concrete surface.

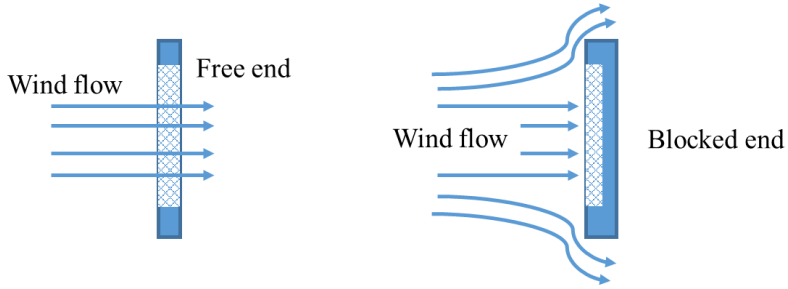

Figure 2-24 Difference between free end and blocked ended specimens.

For this reason, the amount of chloride captured by dry gauze differs from actual exposure conditions. Thus, a blocked end specimen was made using a plastic mold filled with cotton and covered with gauze, as shown in Figure 2-25.

Figure 2-25 Gauze and cotton specimens.

After exposure (4–8 hrs), gauze and cotton samples at each position were submerged in pure water and titrated to determine the amount of chloride at each position [29].

To determine the amount of chloride ingression, mortar specimens were installed at each position. Specimens used in the test were coated with epoxy with the exception of the exposure surface. Specimen and the exposure positions are shown in Figure 2-26 and Figure 2-27 [29]. After the test, each specimen was ground to powder and titrated to determine the chloride penetration.

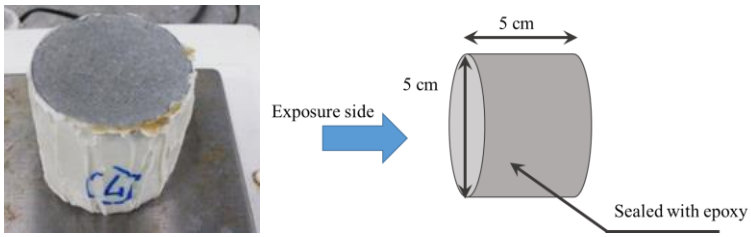

Figure 2-26 Mortar specimen in exposure test.

Figure 2-27 Mortar specimen installation position.

2.7. Reference

[1] P. Mehta and P. J.M. Monteiro, Concrete ; Microstructure, Properties , and Materials, 3rd ed., New York: McGraw-Hill, 2006, pp. 121 - 124.

[2] P. Mehta, Concrete in the Marine Environment, Taylor & Francis Books, Inc, 2003.

[3] Ervin Poulsen and Leif Mejlbro, Diffusion of Chloride in Concrete: Theory and Application, Taylor & Francis Inc., 2006, pp. 10-11.

[4] P. O. Iqbal, "Chloride Transport Coupled with Moisture Migration in Non-Saturated Concrete Exposed to Marine Environment and Application to Cracked Concrete," The University of Tokyo, Tokyo, 2008.

[5] N. Bongochgetsakul, S. Kokubo and S. Nasu, "Measurement of Airborne Chloride Particle Sizes Distribution for Infrastructures Maintenance," in *IESL-SSMS Joint Symposium*, Colombo, Srilanka, 2011.

[6] S. Swatekititham, "Computational Model for Chloride Concentration at Surface of Concrete Under Actual Environmental Condition," The dissertation submitted to Kochi University of Technology, Kochi, Japan, 2004.

[7] A. M. Y. Mohammed, A. Ahmed and K. Maekawa, "Seismic Evaluation of Coastal RC Building Vulnerable to an Airborne," in *Proceedings of the International Conference on Ageing of Materials & Structures*, Delft, Netherlands, 2014.

[8] S. Kokubo and H. Okamura, "Calculation Model for Airborne Chloride Ion based on Seawater Particle Generation," *JSCE journal of hydraulic, coastal and environmental engineering*, vol. 65, pp. 259-268, 2009.

[9] Y.-S. Chen, H.-J. Chiu, Y.-W. Chan, Y.-C. Chang and C.-C. Yang, "The Correlation between Air-Borne Salt and Chlorides Cumulated on Concrete Surface in the Marine Atmosphere Zone in North Taiwan," *Journal of Marine Science and Technology*, vol. 21, pp. 24-34, 2013.

[10] Public Work Research Institute, "Report on Investigation of Airborne Chloride in Japan (III), PWRI report No.2687," 1988. (In Japanese)

[11] K.D. Stanish, R.D. Hooton and M.D.A. Thomas, "Testing the Chloride Penetration Resistance of Concrete: A Literature Review," Federal Highway Administration.

[12] B. Martin-Perez, "Service Life Modelling of R.C. Highway Structures Exposed to Chlorides," University of Toronto, Toronto , 1999.

[13] American Society for Testing Materials, "ASTM G-140-02 Standard test method for determining atmospheric chloride deposition rate by wet candle method," 2002.

[14] K. M. Hossain and S. M. Easa, "Spatial Distribution of Marine Salts in Coastal Region Using Wet Candle Sensor," *International Journal of Research and Reviews in Applied Sciences*, vol. 7, no. 3, pp. 228-235, 2011.

[15] G.R. Meira, M.C. Andrade, I.J. Padaratz, M.C. Alonso and J.C. Borba Jr., "Measurements and modelling of marine salt transportation and deposition in a tropical region in Brazil," *Atmospheric Environment*, vol. 40, p. 5596–5607, 28 April 2006.

[16] K. Suzuki and R. Ian N., "Atmospheric Chloride Deposition Rate for Corrosion Prediction on Oahu," 2011.

[17] Japanese Standards Association, "JSA JIS Z 2382 Determination of pollution for evaluation of corrosivity of atmospheres," 1998. (In Japanese)

[18] T. Ishida, A. Kita, S. Hanioka, L. A. Ho Thi and Y. Matsuda, "A study on Mechanism of airborne chloride transport and migration into mortar based on onsite measurement," in *Proceedings of the Concrete Structure Scenarios*, 2012. (In Japanese)

[19] K. Koyanagi, "Combined Effects of Binders and Curing Conditions on Ingress of Chloride Ions into Cementitious Materials," The Univ ersity of Tokyo, Tokyo, Japan, 2014. (In Japanese)

[20] T. Saeki, M. Takeda, K. Sasaki and T. Shima, "Study on Quantittive Estimation of Aerosol Chlorides Condition," *JSCE,* vol. 66, no. 1, pp. 1-20, 2010. (In Japanese)

[21] S. Hanioka, "Varification and enchancement of Airborne Chloride Generation and Transportation Model Based on Field Measurement," The University of Tokyo, Tokyo, Japan, 2011. (In Japanese)

[22] D. Nuralinah, "Laboratory test and Numerical Analysis of Chloride Ingress into Concrete Subjected to Airborne Salt," Nagaoka University of Technology, Niigata, Japan, 2012.

[23] H. Yamashita, T. Shimomura and F. Yamada, "Study of chloride concentration on concrete surface affected by Airborne Chloride.," in *Japan Concrete Institute Annual Conference*, Japan, 2007. (In Japanese)

[24] M. I. El-Desouky and T. Tsubaki, "Durability Improvement of Concrete Structures by Wash-away of Chloride," *Society for Social Management Systems Internet Journal,* May 2012.

[25] K. Hong and E. Hooton, "Effects of fresh water exposure on chloride contaminated concrete," *Cement and Concrete Research,* vol. 30, pp. 1199-1207, 2000.

[26] Y. Aoki, K. Kamiura, T. Fukuchi and T. Shimomura, "Study on Surface Chloride and Chloride Ingress into Mortar Subjected to Airborne Salt by Wind Tunnel," *Proceeding of the Japan Concrete Institute,* vol. 32, no. 1, pp. 821-826, July 2010. (In Japanese)

[27] K. Horikiri, "Measurement of airborne salinity by a new method and study on the penetration behavior into concrete," The University of Tokyo, Toyko, 2009. (In Japanese)

[28] A. Kita, "Quantification of airborne chloride penetration based on wind tunnel and field measurement," The University of Tokyo, Tokyo, Japan, 2009. (In Japanese)

[29] T. Ishikawa, "Modeling of airborne chloride penetration flux into concrete," The University of Tokyo, Tokyo, Japan, 2010. (In Japanese)

Chapter 3
Proposed Comprehensive System to Simulate Airborne Chloride Ingression and Overview of Relevant Computational Model

3.1. Introduction

In marine environments, the deterioration of RC structures is caused by airborne chloride attacks. For this reason, infrastructure used in coastal areas often requires repair or reconstruction due to the corrosion of reinforcing steel bars.

In the atmospheric zone, airborne chloride is generated by breaking waves, transported by wind flow, and attached to the surface of concrete structures. After airborne chloride is attached to the surface, adsorption takes place and chloride ions begin to ingress into the concrete through the surface, migrating into cementitious materials. The process of airborne chloride ingression is shown in Figure 3-1.

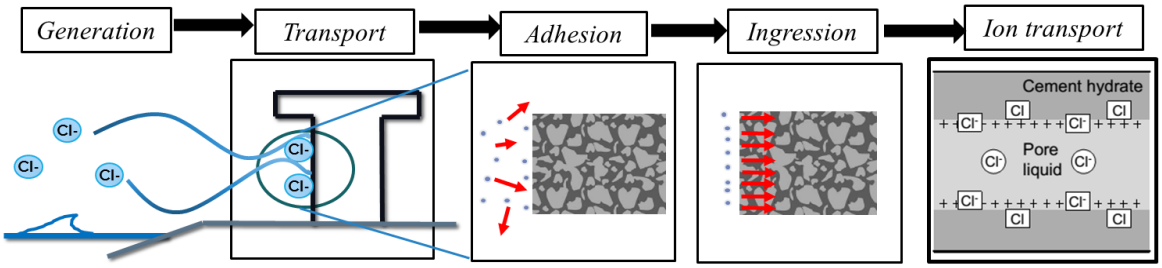

Figure 3-1 Airborne chloride ingression into concrete [1].

In general, in environments with airborne chloride, the chloride concentration in concrete increases with an increase in the amount of airborne chloride on the concrete's surface. Recent JSCE standards (2012) [2] present a simple method to determine the concentration of chloride in concrete under airborne chloride environmental condition, as shown in the following equation:

$$C_d = C_0(1 - erf\frac{x}{2\sqrt{Dt}}), \quad (3\text{-}1)$$

where C_0 is the chloride ion concentration on the concrete surface (kg/m^3), x is the concrete cover thickness (mm), D is the diffusion coefficient of chloride ions in concrete (cm^2/year), and t is the design life time for chloride attacks (year).

The chloride ion concentration on the concrete surface (C_o) can be determined according to the distance of the target structure from the coastline, as shown in Table 3-1.

Table 3-1 Chloride ion concentration on concrete surface, C_o (kg/m^3).

Area	**Splash zone**	**Distance from the coastline（km）**				
		Near shore line	*0.10*	*0.25*	*0.50*	*1.0*
Hokkaido, Tohoku, Hokuriku, Okinawa	13.0	9.0	4.5	3.0	2.0	1.5
Other		4.5	2.5	2.0	1.5	1.0

However, under actual environmental conditions, the amount of airborne chloride on concrete surfaces is also affected by wind speed, wind direction, and rainfall, among other factors [3, 4]. Moreover, observational data from the PWRI [33] propose the concentration of chloride on the concrete surface also changes when the concrete mix proportion is changed, as shown in Figure 3-2.

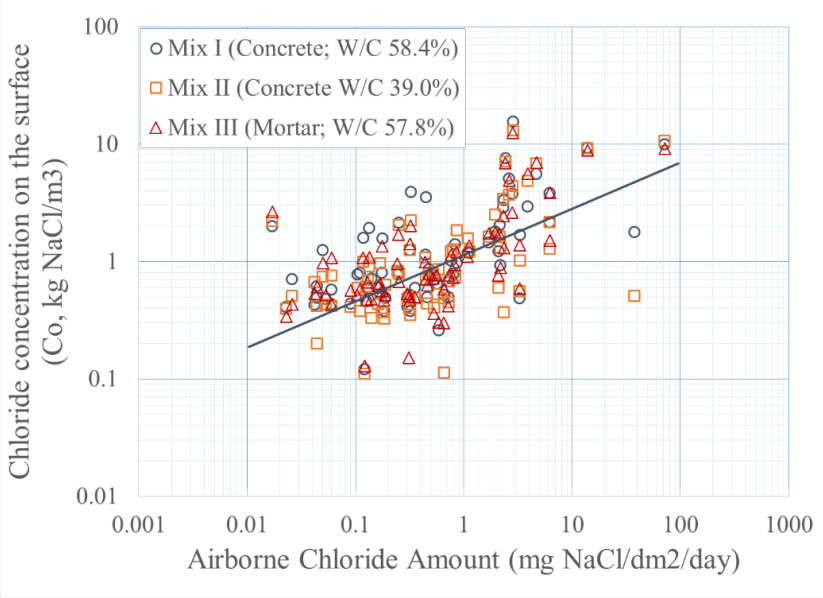

Figure 3-2 The relationship between the amount of airborne chloride and chloride ion concentration on concrete surfaces [33].

For this reason, the method proposed by recent standards may not be appropriate to evaluate the service life of concrete structures. Therefore, a reliable computational model to calculate airborne chloride penetration into concrete structures is necessary.

In 2013, modeling methods for moisture and chloride flux at on concrete surfaces was developed [6]. To calculate chloride concentration in concrete, the amount of airborne chloride, determined by observation, is necessary as the input for calculations. However, in some cases, airborne chloride data from onsite observations are not adequate.

In such cases, while a numerical model to predict airborne chloride ingression is available, it may not be sufficient; and so it is necessary to have a system which can predict chloride ingression without recorded airborne chloride data.

This chapter introduces a comprehensive system to predict chloride generation, transportation, and ingression into concrete structures. The chapter also reviews relevant models for the system and verifies each model.

3.2. The Proposed Comprehensive System and Relevant Models

As discussed, in reality, the data of airborne chloride intensity is not always available. For this reason, this study introduces a comprehensive system to calculate airborne chloride ingression.

A comprehensive system is a system which can determine the amount of airborne chloride generated by breaking waves, transported by wind flow, and calculate its ingression into concrete.

As previous presented, airborne chloride penetration into concrete can be viewed as the following processes: i) airborne chloride generation, ii) transportation, iii) surface adsorption, iv) ingress through concrete surface, and v) chloride ion transportation inside cementitious materials [1, 3]. To determine the amount of airborne chloride ingression, calculations can be divided into three stages:

1) calculate the amount of chloride generation and transportation at a specified position;
2) calculate the water and chloride surface flux on the concrete surface;
3) calculate the amount of chloride ingression inside cementitious material.

Each step can be conducted by using existing calculation models developed in past research. The relevant calculation models are shown in Figure 3-3

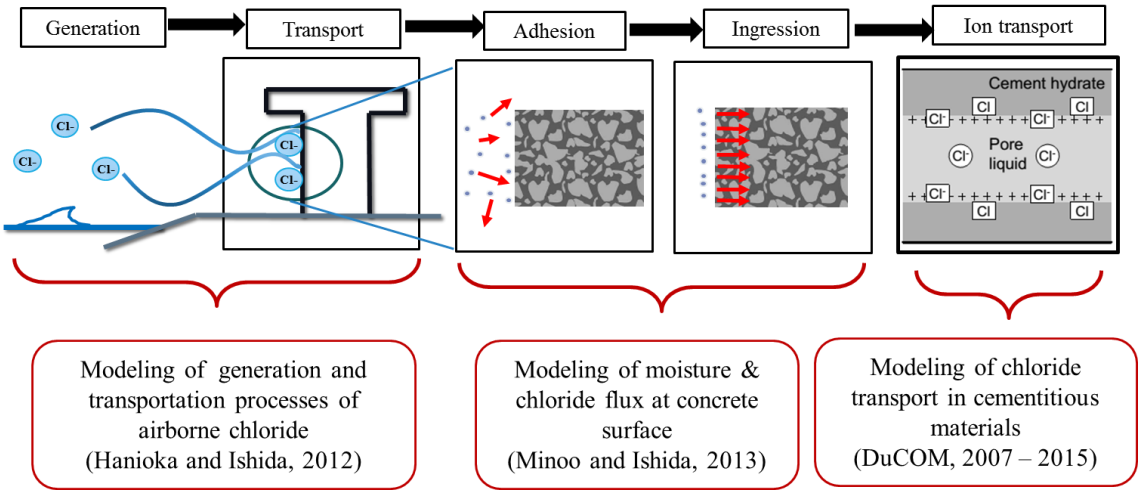

Figure 3-3 Airborne chloride ingression process and relevant calculation models.

If each calculation model is connected to each other, the system can determine the amount of the chloride ingression from the beginning of the generation processes. First, the

amount of airborne chloride at a specified position can be calculated using the airborne chloride generation and transportation model [4, 7]. After the airborne chloride amount is calculated, this data will be given the input for the airborne chloride surface flux model [6]. By using this concept, it is possible to determine the amount of chloride ingression without recorded airborne chloride data.

To complete the comprehensive system, each calculation model is studied and verified to ensure its validity. The following section presents each concept, calculation method, and verification.

3.3. Modeling of Chloride Transport in Cementitious Materials (DuCOM; 2007-2015)

The durability computation model *Durability Concrete Model* (DuCOM) (Durability COncrete Model) is used in the analysis. DuCOM is a composite, multipurpose model that predicts the properties of concrete from the beginning of hydration. This computational system is capable of evaluating the early stage development of cementitious materials and the deterioration process of hydrated products under long-term environmental actions [8, 9]. In this analysis system, mix proportions, environmental conditions, curing conditions, and other data are used as inputs.

DuCOM consists of several sub-models which work together and exchange data in real time. In this model, the development of micro-pore structures at early stages is obtained based on the degree of cement hydration computed from the mix proportions. In moisture transport, both vapor and liquid phases of mass transport are considered. The moisture distribution and micro-pore structure information are inputs for the chloride transport model. A schematic representation of each module of DuCOM for chloride penetration is shown in Figure 3-4.

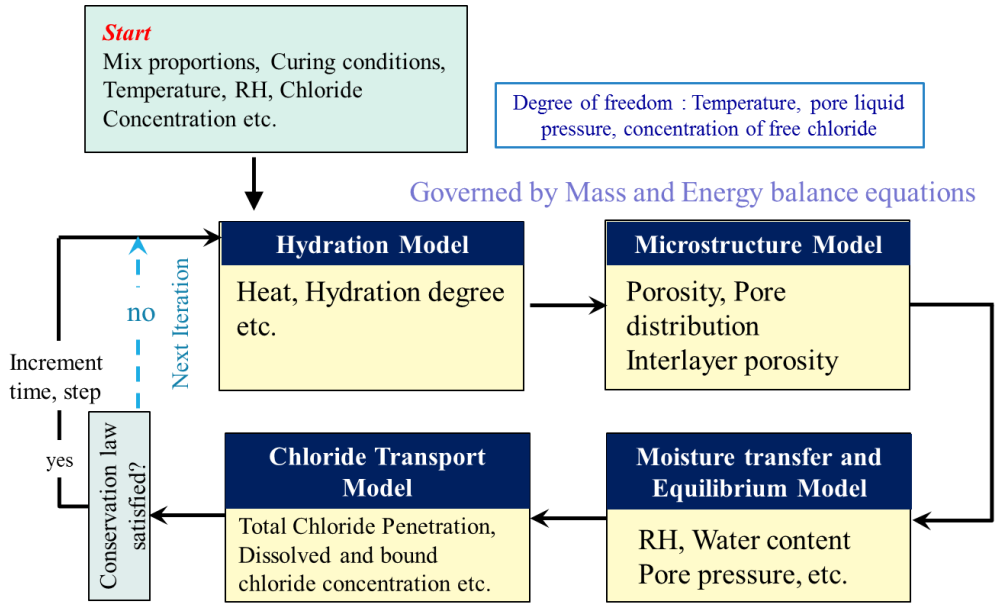

Figure 3-4 Framework of DuCOM system for chloride penetration calculation.

The main transport mechanisms for chloride ingression into concrete are capillary suction and diffusion. Thus, to determine the amount of chloride that has penetrated into concrete, the model of moisture transfer and the model of chloride transportation should be discussed.

3.3.1. DuCOM Moisture Transfer and Equilibrium Model

Moisture transport in concrete materials plays an important role in the deterioration of infrastructure. Water which penetrates the material can also be the path for deleterious materials, including chloride ions. Thus, to predict chloride ingression, water movement inside micro-pore structure is considered [10].

In DuCOM, the moisture transport model for cementitious materials considers the quasi-equilibrium of liquid and gas phases. The contributions of the diffusion, as well as bulk movements of moisture, are combined in the model. The total porosity of the cementitious material is divided into interlayer, gel, and capillary porosity. The moisture model considers the contributions of each of these components from a thermodynamic viewpoint. The macroscopic moisture transport characteristics of flow, such as conductivity, are obtained directly from the microstructure of the porous media. This is achieved by considering the mass conservation of moisture capacity, conductivity, pore structure development, and hydration loss [8, 9, 10].

The moisture capacity is obtained from pore structures, the summation of gel, capillary, and interlayer porosity. Moisture conductivity comprises the liquid and vapor phases computed from the pore structure. Pore structure development is based on cement particle expansion and the average degree of hydration. Finally, moisture loss due to hydration is directly obtained from hydration model of DuCOM [11].

To determine the water movement inside porous materials, pore size and distribution should be considered. In the DuCOM analytical system [8, 9], each of the capillary and gel porosity distributions is represented by a simplistic Raleigh-Ritz distribution function:

$$V(r) = 1 - exp(-Br), dV(r) = Br\, exp(-Br)\, d\, in(r), \tag{3-2}$$

where $V(r)$ is the fractional pore volume of the distribution up to pore radius r (m), and B is the porosity distribution parameter (1/m), representing the peak of porosity distribution on a logarithmic scale.

If the pore shape is assumed to be a perfect cylindrical shape, the pore radius with which the equilibrated interface of liquid and vapor is determined, r_c (m), can be calculated as follows:

$$r_c = C \cdot r_s = -\frac{2C \cdot \gamma \cdot M}{\rho \cdot RT} \frac{1}{\ln h}, C = 2.15, \tag{3-3}$$

where C is the coefficient for considering the equivalent thickness of adsorbed water, γ is the surface tension of the liquid (N/m), M is the molecular mass of the liquid (kg/mol), ρ is the density of liquid water (kg/m^3), R is the universal gas constant (J/mol·K), T is the absolute temperature (K), and h is the relative humidity (RH).

Assuming that all pore of radii smaller than r_c are filled with water, by integrating the pore volume that below pore radius r_c in a porosity distribution, we can obtain the expression of saturation degree S_c, given by:

$$S_c = 1 - \exp(-Br_c). \tag{3-4}$$

In DuCOM system, the flux of liquid water in micro-pore structures q_l (kg/m^2.s) is expressed through equation 3-2 by integrating the water flux in pores smaller than radius r_c at a porosity distribution $V(r)$. The flux of liquid water q_1 [kg/m^2.s] can be calculated using the following model based on Darcy's Law [9, 11]:

$$q_l = -\frac{\rho\phi^2}{50\eta}\left(\int_0^{r_c} r dV\right)^2 \nabla P = -K_l \nabla P\,, \tag{3-5}$$

where ϕ is the porosity inside the material, ρ is is the density of liquid water (kg/m^3), η is the viscosity of the fluid (Pa.s), K_l is the water permeability coefficient (kg/Pa.m.s), and P is the pore pressure (Pa). The unsaturated state in porous media is considered in the model with the integration process in the preceding equation.

After penetration, liquid water penetration is suggested to stop at a certain depth in dense materials [12]. The equilibrium between friction force and water pressure is expressed with equation 3-6 by assuming that pores inside the material are a cylindrical shape [1, 13].

$$\tau_{yield} = \frac{r_{\lim}}{2} \cdot \nabla P\,, \tag{3-6}$$

where τ_{yield} is the constant for the friction at the pore surface (N/m^2), r_{lim} is the limit of the pore radius (m), and P is the water pressure in pores (N/m^2). When τ_{yield} is fixed, it limits pore radius r_{lim} which is effective for water movement and can be calculated under certain gradients of pore pressure. r_{lim} is considered with the water permeability coefficient (K_l) as the lower limit of integration in equation 3-7 and Figure 3-5 [13].

$$\begin{cases} K_l = \dfrac{\rho\phi^2}{50\eta}\left(\displaystyle\int_{r_{\lim}}^{r_c} r dV\right)^2 & \left(r_c \geq r_{\lim}\right) \\ K_l = 0 & \left(r_c < r_{\lim}\right) \end{cases} \tag{3-7}$$

Equation 3-7 considers that water in pores whose radii are smaller than r_{lim} does not move despite the pore water pressure. When liquid water permeates into unsaturated concrete materials, water pressure gradients are formed along the depth from the surface and, generally, the gradient decreases with depth. This leads to an increase in r_{lim}, and, at certain depths, r_{lim} reaches to r_c, meaning that the stagnation of water saturation can be achieved with the proposed model. The τ_{yield} value for OPC is set as 4.0 (N/m^2) [12].

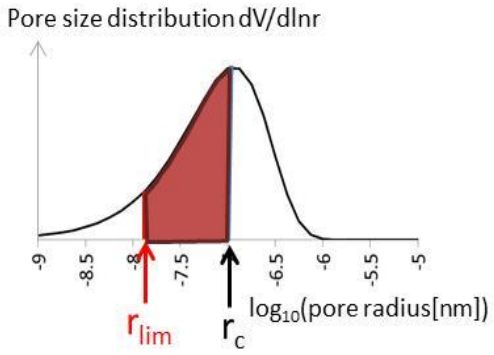

Figure 3-5 Water content related to the permeability coefficient [13].

3.3.2. DuCOM Chloride Ingression Model

The general model for predicting chloride ion ingress is based on Fick's diffusive law, but it has been suggested that a simple diffusive law may not directly be applicable to concrete with long term exposure because the depth of chloride ion ingress is strongly related to the degree of saturation [13]. Thus, mechanisms other than the traditional advection-diffusion law need to be considered to predict chloride movement.

In the proposed model, the volume of entrapped water in ink-bottle-shaped pores is also considered and the equivalent degree of saturation is expressed with S_{ink}, with which arbitrary temperatures and relative humidity (RH) history can be considered [14]. Accordingly, the total degree of saturation S_{tot} is given as the summation of S_c, S_{ink}, and S_{ads}, representing the adsorbed water content:

$$S_{tot} = S_c + S_{ink} + S_{ads}. \tag{3-8}$$

The total water content in the unit cement paste volume W (m^3/m^3) is expressed as:

$$W = \emptyset \cdot S_{tot}, \tag{3-9}$$

where $\emptyset$ is the summation value of the total capillary porosity and gel porosity in cement matrix.

The study [15] determined that chloride ions cannot penetrate through pores whose radii are smaller than specific sizes because of the electrical interaction between

ions and pore walls. Thus, the threshold value for chloride ion movement in pore water, r_{thre} (m), is considered [13].

It is assumed that chloride ions are unable to pass through pores which are smaller than r_{thre}, even if pores are saturated with water. The water in extremely small pores is not thought to be active in chloride ion movement. The threshold radius r_{thre} is considered in chloride ion transport models as the water content available for chloride movement [13], as shown in Figure 3-6.

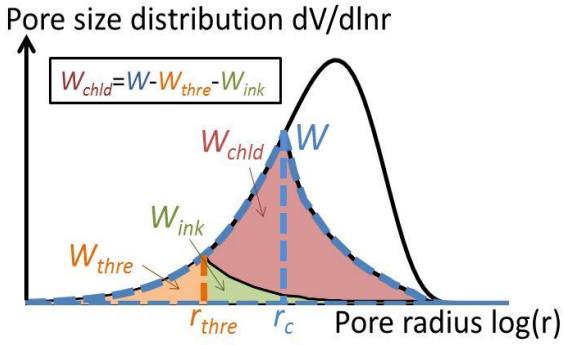

Figure 3-6 Water content and pore size [13].

The water volume in pores whose radii are smaller than r_{thre} (expressed as W_{thre} (m^3/m^3)) is formulated:

$$W_{thre} = \phi \cdot S_{thre} = \phi \cdot \int_0^{r_{thre}} dV = \phi \cdot \{1 - \exp(-Br_{thre})\} \ , \tag{3-10}$$

where S_{thre} is the equivalent degree of saturation for the W_{thre}. The water volume existing in the ink-bottle pores which are connected to these pores can be formulated as follows, referring to a study by Ishida *et al.* (2005):

$$W_{ink} = \phi \cdot S_{ink} = \phi \cdot (-S_{thre} \cdot \ln S_{thre}), \tag{3-11}$$

where W_{ink} is the water content in ink-bottle shaped pores connected to the pores for W_{thre}. As a result, the total water content available for chloride ion movement, W_{chld}, is expressed as

$$\begin{cases} W_{chld} = W - W_{thre} - W_{ink} & (r_c \geq r_{thre}) \\ W_{chld} = 0 & (r_c < r_{thre}) \end{cases}. \tag{3-12}$$

The suggested value of r_{thre} for Ordinary Portland Cement (OPC) is 10 nm [13]. However, it should be noted that in cases when r_{thre} is 10 nm, the corresponding RH is ~80%. Therefore, chloride ions cannot move in the pores when the RH is under 80% in the analysis.

Using the modified water content W_{chld} which consider the threshold radius for chloride ion movement, the total chloride ion flux in a cement matrix can be expressed as

$$J_{ion} = -\left(W_{chld} \cdot \delta \cdot D_{ion}\right) \cdot \nabla C_{ion} + W_{chld} \cdot \mathbf{u} \cdot C_{ion}, \tag{3-13}$$

where J_{ion} is the flux of the chloride ions (mol/m^2.s), δ is the constrictivity, D_{ion} is the diffusion coefficient (m^2/s), C_{ion} is the molar concentration of chloride ions in the liquid phase (mol/m^3), and **u** is the velocity vector of a solution flow in pores (m/s). The first term represents the flux of chloride ions due to diffusion from the concentration gradient and the second term represents the advection constituent in chloride ion flux.

The constrictivity (δ) is the effect of interactions between pore structures and ion transports. The contrictivity value can be expressed as

$$\delta = m\delta_1\delta_2 \qquad (\text{m} = 6.38, \text{ if } \delta \geq 1.0, \delta = 1.0), \tag{3-14}$$

where δ_1 is the reduction parameter for dimensional change and connectivity of the pores and δ_2 is the reduction parameter for electrical interaction.

If the cross section of a pore space segment is straight, then constrictivity becomes unity, whereas if segments are restricted at certain points, the value of constrictivity is less than unity [16, 17], as shown in Figure 3-7.

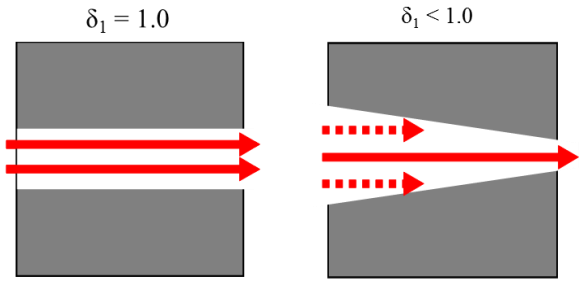

Figure 3-7 Relation between constrictivity and porosity of pore structure [16].

With this assumption, the value of δ_1 is introduced in the proposed model. If the cross section of a pore space segment is straight, then constrictivity (δ_1) = 1. If the segments are restricted at certain points, then the value of constrictivity (δ_1)is less than 1. The value of δ_1 can be calculated as:

$$\delta_1 = 0.495 \tanh\{4.0(\log(r^{peak}) + 6.2)\} + 0.505, \quad (3\text{-}15)$$

where r^{peak} is the maximum radius of the pore.

Another factor which effects chloride penetration is the amount of bound chloride. Nakarai K. (2006) proposes a model for the constrictivity for Ca2+ (positive ion) [18]. On the basis of this model, a constrictivity model for Cl^- (negative ion) can be proposed in which the effect of ion and pore wall interactions and effect of bound chloride on the movement of chloride are expressed, as shown in Figure 3-8.

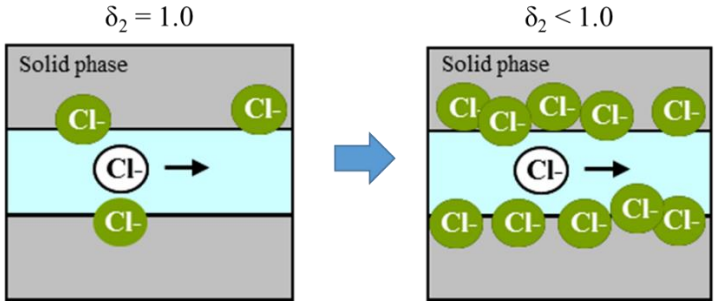

Figure 3-8 Effect of bound chloride on pore radius [17].

When bound chloride content increases, interactions between free chlorides with bound chlorides increase. This slows diffusion and reduces the diffusion coefficient. At certain points, if chloride ions are restricted by bound chloride, it may delay other chlorides from moving deeper into the concrete [16, 17]. The reduction parameter for electrical interaction, represented by parameter δ_2, can be expressed as

$$\delta_2 = 1.0 - 0.627C_b + 0.107C_b^2, \quad (3\text{-}16)$$

where C_b is the bound chloride concentration (kg Cl/kg cement).

3.3.3. Experimental Verification of Chloride Ion Transportation Model

For the verification of chloride ion transportation model, the experiment and the analysis were conducted by Takahashi Y. (2012) [13]. The test method and the results are shown as following

1) Test method and boundary conditions.

The experiment was conducted using mortar specimens with a size of 40× 40×160 mm^3. Each specimen used 100% OPC and W/C was between 20–50%.

All specimens were cured with water for 28 days. After curing, specimens were coated with epoxy on 5 surfaces, except on exposure side. Then, each specimen was submerged in a solution of 3% NaCl for 1 year before chloride ion amounts were measured through titration with $AgNO_3$.

Figure 3-9 Test specimen.

2) Experimental results and model verification

The experiment and analysis results are shown in Figure 3-10. The experimental results show that the chloride ion distributions are significantly influenced by W/C. It can be concluded that the depth of chloride ion ingress is reduced when W/C decreases [13].

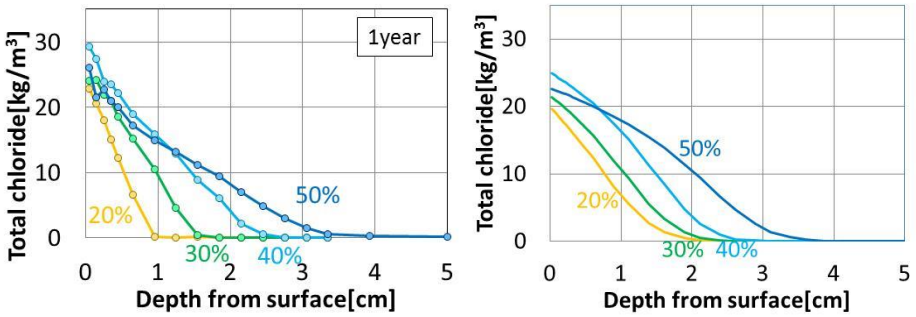

Figure 3-10 Total chloride ion distribution from experiment (left) and analysis results with proposed model (right).

By comparing simulated results to the experimental data, it can be concluded that the proposed analytical system can potentially be applied to each W/C for chloride ingression.

3.4. Modeling Moisture and Chloride Flux at Concrete Surfaces

The boundary conditions for chloride penetration in concrete structures for sea water immersion and airborne chloride differ. For sea water immersion, the moisture flux and chloride concentration on concrete surfaces is uniform. Meanwhile, the concentration of chloride on concrete surfaces in conditions with airborne chloride condition is not constant. Under actual environmental conditions, the intensity of airborne chloride changes in all seasons due to wind direction, wind speed, wave height, obstacles, and distance from the seashore [3]. Moreover, when the structure is exposed to airborne chloride, only some parts of the structure are wet and others dry, as shown in Figure 3-11.

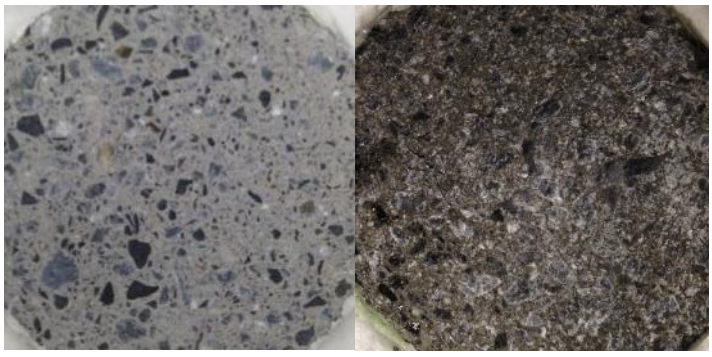

Figure 3-11 Specimen surface before exposure to airborne chloride (left) and after exposure to airborne chloride (right).

Due this reason, chloride and water ingression do not occur uniformly on concrete surfaces. Therefore, the boundary condition used in the calculation of chloride penetration under airborne chloride condition should be changed [1, 6].

To provide more reliable calculations, the calculation of chloride and moisture flux on the concrete surfaces is introduced into DuCOM system [6]. Figure 3-12 shows the framework of DuCOM system included surface flux model to calculate airborne chloride penetration. The amount of airborne chloride amount, temperature, relative humidity, and precipitation data are needed as the input for the calculation.

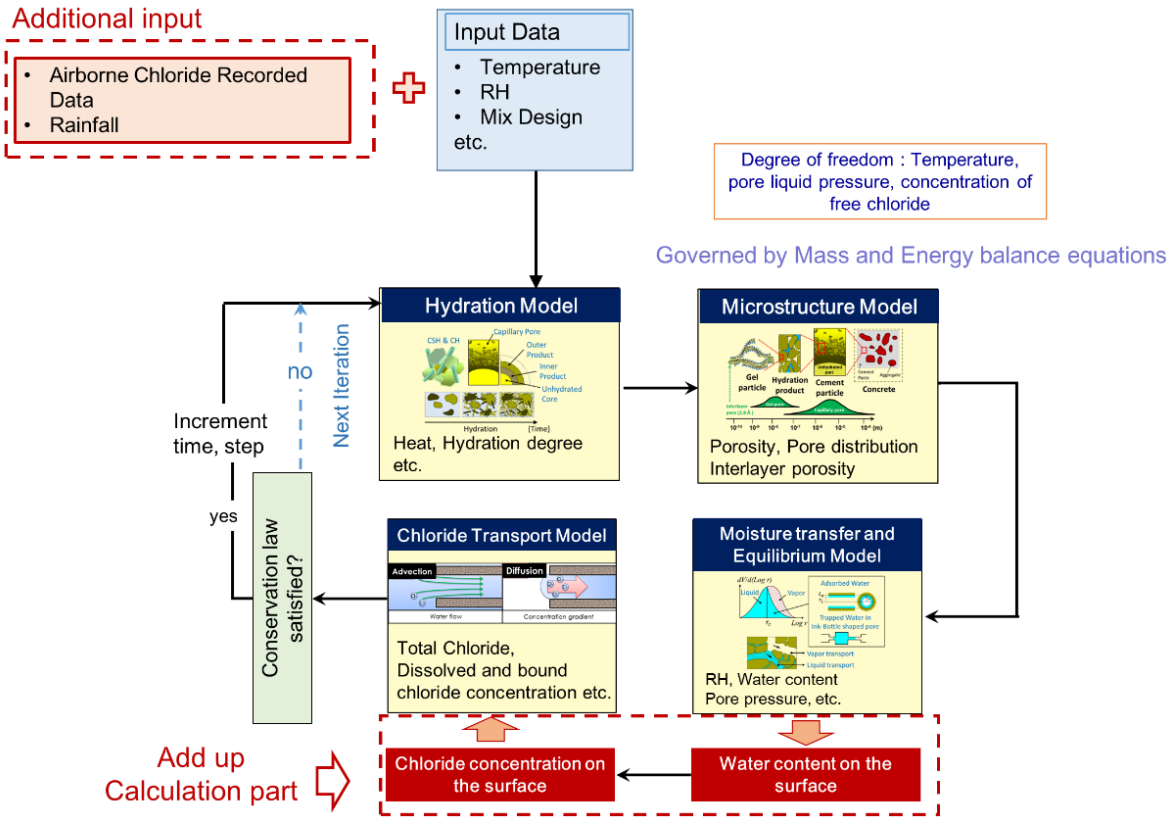

Figure 3-12 Framework of DuCOM system including surface flux calculation (for chloride penetration under airborne chloride conditions).

3.4.1. Model Assumptions and Influential Parameters in the Calculation

As mention in the previous section, when airborne chloride attaches to concrete surfaces, some parts of the concrete surface become wet and some part remain dry.

Therefore, to simulate the mechanism of airborne chloride ingression on concrete surfaces, wet and dry sections of the concrete surface have been assumed [6, 19].

To calculate the amount of the water which can contain on a concrete surface, it is assumed that there is a thin layer on the concrete surface. This thin layer represents temporary storage for water and chloride [6]. The previous study reported that some amount of water can remain on the concrete surface with a maximum thickness of 0.1 mm [20]. Consequently, the calculation the thin layer to be 0.1 mm thick. A concept of the thin water layer is shown in Figure 3-13.

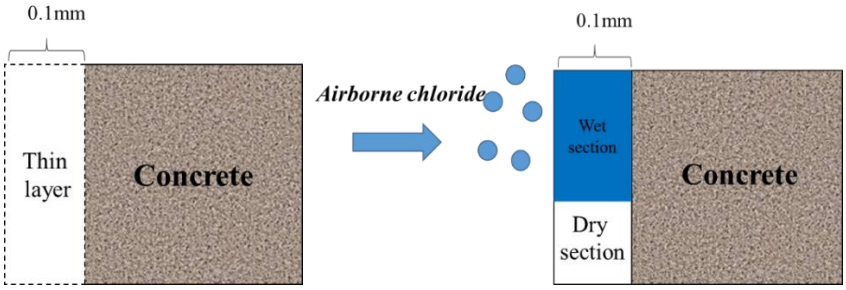

Figure 3-13 Concept of thin layer, wetting, and drying section assumptions.

Airborne chloride particles consist of two component which are water and chloride ions. The concentration of chloride ions in the particle is equal to 0.51 mol/L , equal to the chloride concentration in sea water (3% by mass) [3, 7]. After airborne chloride accumulates inside the thin layer, water and chloride ions from airborne chloride particle will begin to penetrate through the concrete surface. The mechanism of the moisture and chloride behavior in the thin layer is shown in Figure 3-14.

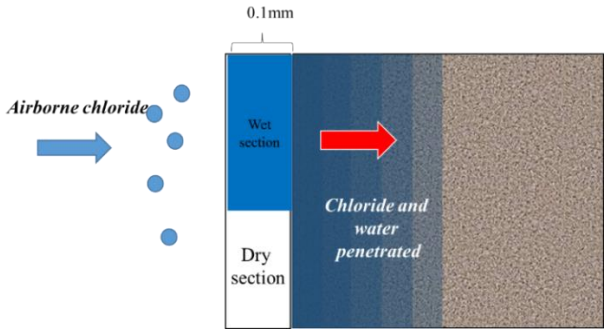

Figure 3-14 The mechanism of moisture and chloride behavior in a thin layer.

The flux of water on a concrete surface is calculated from the amount of water from airborne chloride particles. The water flux from airborne chloride is represented by the parameter Q_{air_water}, given as an input for analysis. The volume of water that penetrates the concrete from the thin layer is Q_{in_water} (kg/m^2.s).

In the model, the ratio of water that can remain on the concrete surface or the ratio of the wet section are represented by the parameter S_{wet}. The mechanism of moisture transmission behavior in the thin layer is shown in Figure 3-15.

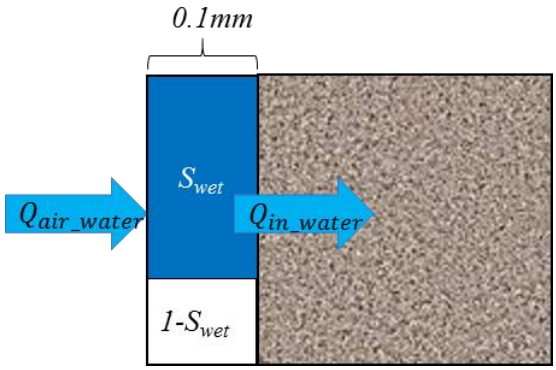

Figure 3-15 Moisture transmission behavior in the thin layer.

On the other hand, the flux of chloride on concrete surfaces is calculated from the amount of chloride ions in airborne chloride particles. The chloride ion flux from airborne chloride is represented by the parameter Q_{air_cl} and the amount of chloride ions that have penetrated into the concrete is Q_{in_cl} (mol/m^2.s). The behavior of the chloride penetration through the thin layer is shown in Figure 3-16.

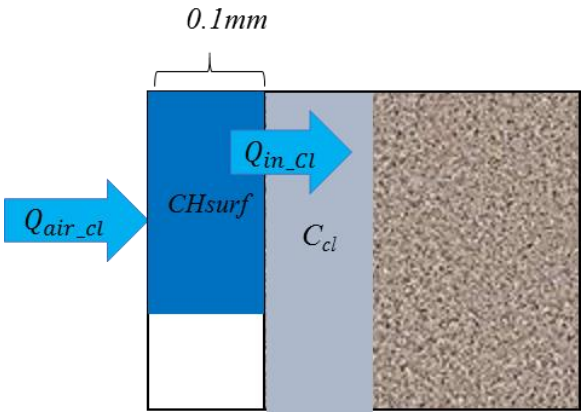

Figure 3-16 Chloride ion penetration through the thin layer.

Parameter CH_{surf} in Figure 3-16 is the concentration of chloride on the concrete surface inside the thin water layer (mol/m^2).

Chloride ions from the thin water layer penetrate into the concrete through advection and diffusion mechanisms, as shown in the Figure 3-17 [9, 6]. Advection describes the mechanism which chloride ingresses into concrete along with the movement of water in the material. Diffusion describes the mechanism by which chloride ions are transported due to different gradients of chloride concentrations inside the water layer and material.

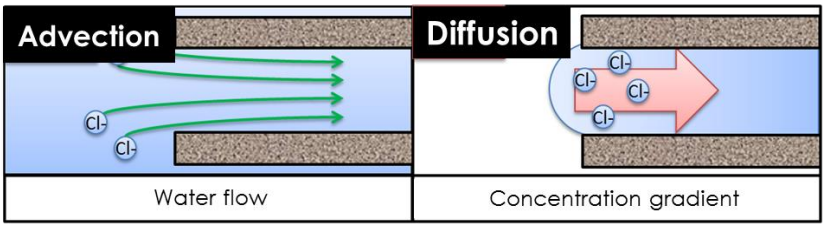

Figure 3-17 Chloride ion penetration mechanisms.

With these mechanisms, it can be inferred that water ingression or moisture movement effects the degree of chloride penetration. Thus, in the calculation, the degree of water penetration is first calculated. Then, the degree of water penetration is considered in the chloride ingression calculation.

3.4.2. Inputs for Calculation

From the previous section, to calculate the amount of chloride ingression into concrete, a determination of the amount of airborne chloride is necessary.

The amount of airborne chloride can be a value from observations or tests. However, for the analysis, the amount of the airborne chloride must be converted to the water flux (Q_{air_water}), given as an input for the analysis.

Q_{air_water} can be calculated from the amount of airborne chloride from airborne chloride capture equipment with the following equation:

$$Q_{air\_water} = \frac{ABS \times \rho_w}{M_{cl} \times 0.51 \times 1000}, \quad (3\text{-}17)$$

where ρ_w is the density of water (kg/m^3), M_{cl} is the molecular weight of chloride, 35.45 × 10^{-3} (kg/mol), 0.51 is the concentration of chloride in the water particle (mol/l), and ABS is the amount of airborne chloride (kg/m^2.s).

3.4.3. Calculating Surface Moisture Penetration

With this model, the water flux and the amount of water penetration are calculated. Then, the water flux on the concrete surface and water penetration amount will be given as the input to the chloride penetration model to calculate chloride penetration, as shown in Figure 3-12.

From Figure 3-15, the ratio of the wet part of the concrete surface, S_{wet}, can be calculated by considering the mass balance equation between the flux of water attached to the concrete surface (Q_{air_water}) and water penetration into the concrete (Q_{in_water}). S_{wet} can be calculated as

$$\frac{S_{wet}}{dt} \times T \times \rho_w = Q_{air\_water} + Q_{in\_water}, \quad (3\text{-}18)$$

where T is the thickness of the thin layer (assumed to be 0.1 mm) and ρ_w is the density of water (kg/m^3). Q_{in_water} is calculated based on the water penetration driven by the gradient potential between the inside of the concrete and water on the surface. Water penetration occurs only from the wet part of the thin layer. As the RH of the wet part can be considered to be the same as water, equal to 1.0, the quantity of water that has penetrated, Q_{in_water}, can be calculated as

$$Q_{in\_water} = S_{wet} \times K_{water} (RH_{bound} - 1.0), \quad (3\text{-}19)$$

where K_{water} is the moisture transfer coefficient = 5.0×10^{-5} (kg / m^2.s), and RH_{bound} is the relative humidity inside the concrete surface, which is internally calculated in the finite element method (FEM) computation.

In DuCOM system, the degree of hydration and pore size distribution of the materials are also taken into account in the calculation. Thus, S_{wet} and Q_{in_water} change if the quality of the concrete and/or the amount of airborne chloride change. Figure 3-18 shows the behavior of S_{wet} when the amount of airborne chloride changes and Figure 3-19 shows the calculation results of S_{wet} and water penetration with different amounts of airborne chloride.

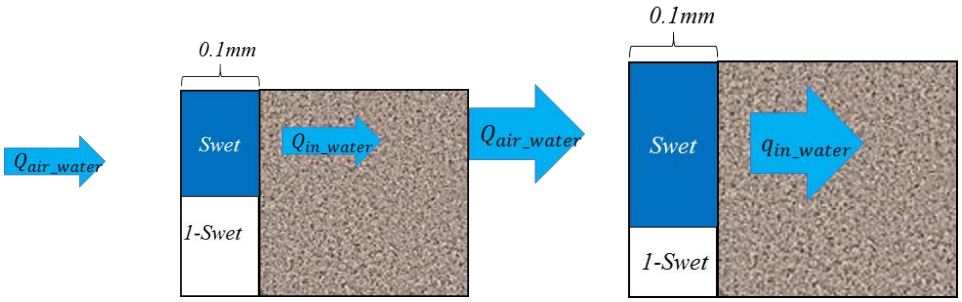

Figure 3-18 S_{wet} changes due to different amounts of airborne chloride.

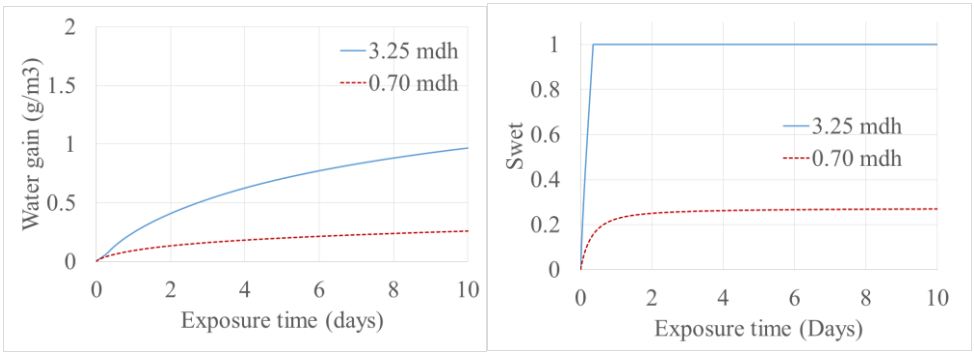

Figure 3-19 S_{wet} and water increase with different amounts of airborne chloride (W/C 0.30).

Furthermore, when the concrete has a low W/C, the concrete will become dense, Q_{in_water} will reduce, and S_{wet} will be higher when compared with high W/C concrete, as shown in Figure 3-20 and Figure 3-21.

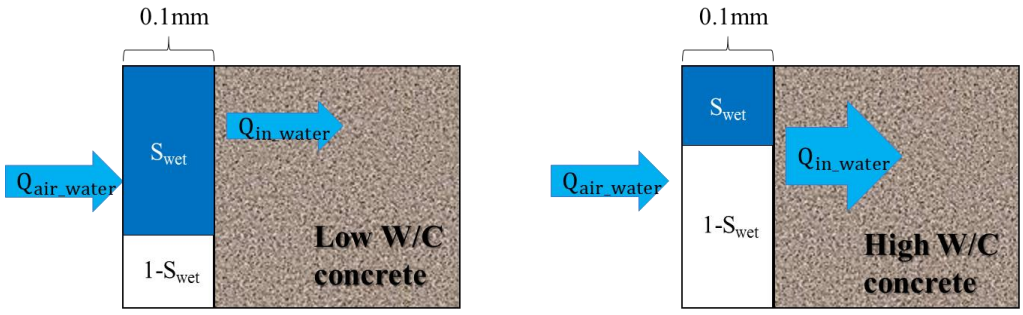

Figure 3-20 S_{wet} and Q_{in_water} with different W/C.

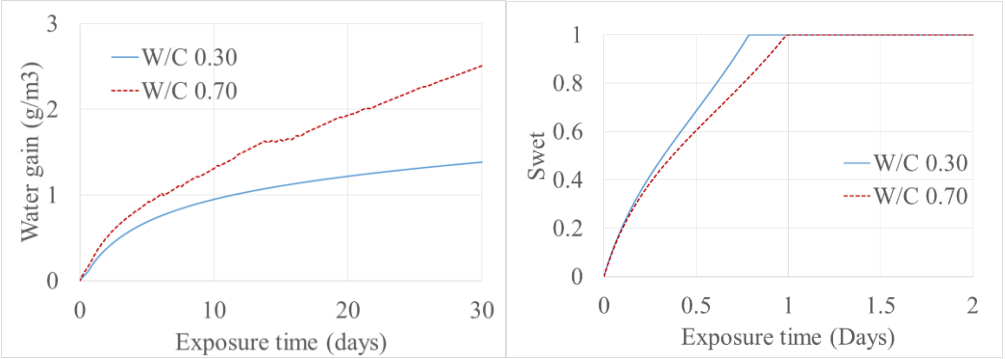

Figure 3-21 S_{wet} and water increase with different W/C (airborne chloride 3.25 mdh).

From Figure 3-21, when W/C = 0.70, S_{wet} is lower than W/C 0.30 at the beginning of the calculation but more water can penetrate the specimen.

3.4.4. Calculation of Airborne Chloride Penetrations

The amount of chloride penetration from the concrete surface is calculated by considering the chloride concentration on the concrete surface as a thin layer.

From Figure 3-16 shows Q_{air_cl} (mol/m^2.s), the airborne chloride flux on the concrete surface and Q_{in_cl} (mol/m^2.s), the number of chloride ions that have penetrated the concrete structure, CH_{surf} (mol/m^2), the concentration of chloride on the concrete surface inside the thin water layer, and C_{cl}, the chloride ion concentration inside the concrete surface (mol/l).

For the computation, Q_{air_cl} can be calculated by considering the chloride concentration in the water flux on the concrete surface (Q_{air_water}), determined by Equation 3-20.

$$Q_{air\_cl} = \frac{Q_{air\_water} \times 0.51 \times 1000}{\rho_w}, \qquad (3\text{-}20)$$

where Q_{air_water} (kg/m^2.s) is the flux of water containing airborne chloride particles attached to the concrete surface, given as an input of the analysis, 0.51 represents the concentration of chloride in the water particles (mol/l), and ρ_w is the density of water (kg/m^3).

In order to calculate the amount of chloride penetration into concrete, the diffusion and advection mechanisms are taken into account in the model. The model assumes that chloride penetration only occurs through wet part in the thin layer.

The total amount of chloride penetration can be considered as the sum of advection and diffusion of chloride into the concrete. Q_{in_cl} can be expressed by

$$Q_{in\_cl} = Q_{adv} + Q_{diff}, \quad (3\text{-}21)$$

where Q_{adv} is the chloride ion penetration from advection from the thin water layer into concrete (kg/m^2.s). Q_{adv} can be determined by:

$$Q_{adv} = \frac{Q_{in\_water} \times CH_{surf} \times 1000}{\rho_w}, \quad (3\text{-}22)$$

Q_{diff} in Equation 3-21 is the amount of chloride penetration through diffusion, caused by the gradient potential between the thin water layer and the concrete surface (kg/m^2.s). Q_{diff} can be calculated as

$$Q_{diff} = S_{wet} \times K_{cl} \times (C_{Cl} - CH_{surf}), \quad (3\text{-}23)$$

where K_{cl} is the chloride transmission coefficient = 1.0×10^{-3} (m/s). C_{Cl} is the concentration of chloride ions at the exposure surface (mol/l), calculated in the DuCOM based on the amount of chloride penetration on the concrete surface.

CH_{surf} can be determined by solving the mass conservation equation for the chloride ion content in the thin water layer, formulated as

$$\frac{d(CH_{surf})}{dt} \times 1000 \times T \times S_{wet} = Q_{air\_cl} + Q_{in\_cl}, \quad (3\text{-}24)$$

where S_{wet} is the value computed by Equation 3-18 and T is the thickness of the thin layer, equal to 0.1 mm.

3.4.5. Experimental Verification of Moisture and Chloride Surface Flux Model under Controlled Conditions

For the verification, experimental results were taken from previous research by Ishikawa T. (2012) [19] and completed by Minoo H. (2013) [6]. The objective of this experiment is to determine chloride penetration under various airborne chloride intensities.

The overall process of the experiment is shown in Figure 3-22.

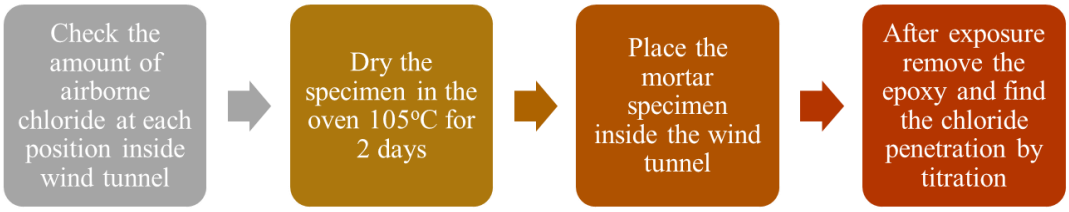

Figure 3-22 Total chloride penetration experiment process.

1) Test methods and environmental conditions

To determine the amount of chloride ingression, mortar specimens with a W/C 50% were installed inside a wind tunnel. The mortar specimen used in the test is shown in Figure 3-23.

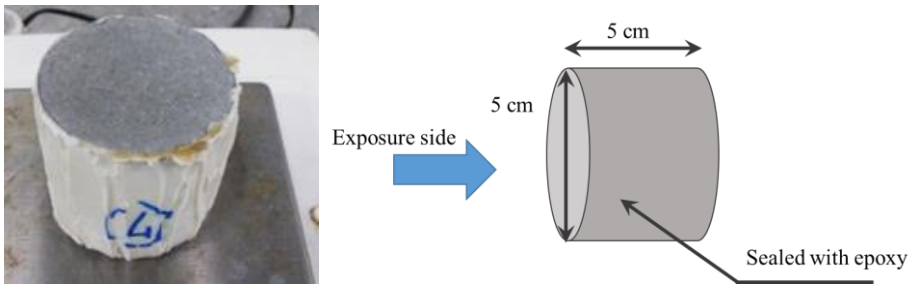

Figure 3-23 Mortar specimen in exposure test.

Specimens were cured under sealed conditions for 20 days and then dried in an oven at 105 ^{o}C for 2 days to reduce surface moisture and accelerate the chloride penetration rate.

After the exposure test, each specimen was removed from the wind tunnel, removed the epoxy (Figure 3-24), and crushed into powder. The powder sample was titrated with a silver nitrate solution to determine the total amount of chloride.

Figure 3-24 Removing epoxy coating from mortar specimen.

2) Experimental results and model verification

In the experiment, the flux of airborne salt inside the wind tunnel was between 0.055–1.170 mdh (mg/dm^2/hr), depending on the position [6, 19]. In the calculations, the RH inside the wind tunnel was assumed to be 90%. The experimental and analytical results of the total chloride penetration are shown in Figure 3-25.

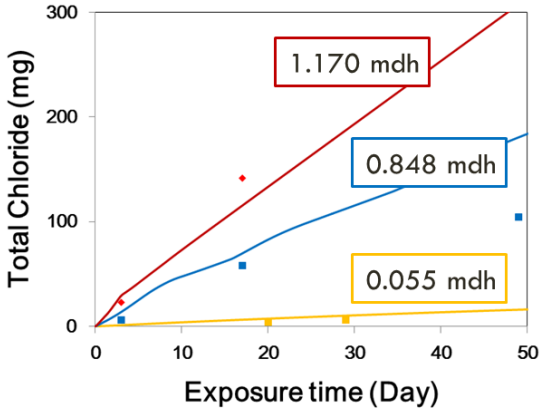

Figure 3-25 Airborne chloride penetration results from the experiment and the analysis [6].

The calculation with the proposed model shows different amounts of chloride penetration when the amount of airborne chloride is changed. However, for 0.848

mdh, the results from the proposed model overestimated the total chloride penetration after 17 days.

3.4.6. Experimental Verification of Moisture and Chloride Surface Flux Model Under Actual Environmental Conditions

With the proposed model, verification through onsite measurement data was conducted. Data for the verification was taken from PWRI Report [21]. The experiment was conducted between December 10, 1984 and December 9, 1987 in Japan to investigate the amount of airborne chloride and chloride penetration.

1) Test methods and environmental conditions

To determine the amount of airborne chloride, the tank sample method was used. The airborne chloride was checked every month during the testing period. Examples of amounts of airborne chloride are shown in Figure 3-26.

Figure 3-26 PWRI airborne chloride capture equipment.

To investigate the amount of chloride penetration, mortar with a W/C of 57.8% was used to make test specimens measuring 10×10×10 cm^3. Each specimen was placed near the tank.

For the verification, data was picked up from an exposure site in Niigata prefecture, near Shinanokawa River.

2) Experimental results and model verification

For the calculation, the air temperature, relative humidity received from the Automated Meteorological Data Acquisition System (AMEDAS) from the Japan

Meteorological Agency at Niigata station. The results of the analysis are shown in Figure 3-27.

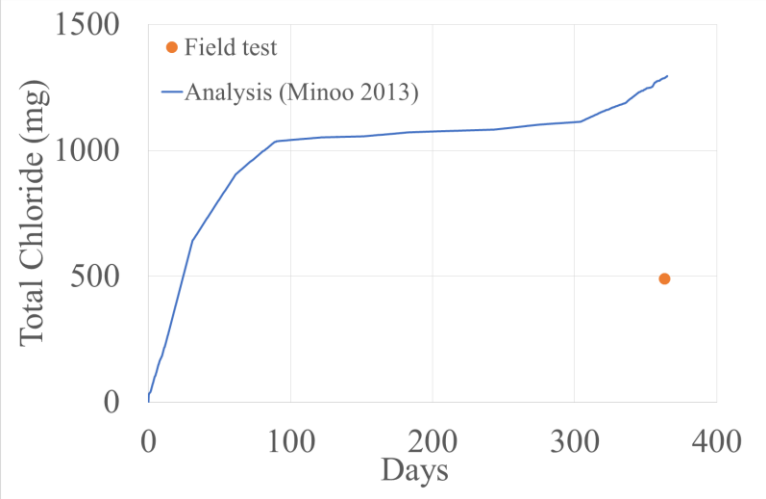

Figure 3-27 Verification result with proposed model [6].

The verification by the proposed model shows an overestimation of results when compared to experimental data. This may be because assumptions in the proposed model are not appropriate or because conditions in the model do not match with actual environmental concditions.

3.5. Modeling of Generation and Transportation of Airborne Chloride [3, 7, 22]

The amount of airborne chloride at specific locations changes due to wind direction, wind speed, obstacles, and distance from the seashore [3, 4]. Thus, the amount of airborne chloride for each region and season are different. To calculate airborne chloride generation and transportation, environmental data and exposure conditions are important to determine.

3.5.1. Kokubo and Okamura Model [4, 22]

In 2009, modeling for airborne chloride generation and transportation was developed [11, 46]. This model can be used to predict the amount of airborne chloride from generation and after transportation at each position.

The model assumes that the wave breaking point is the initiation point of chloride production and airborne chloride is assume to distributes vertically along a

vertical line passing through the initial point of the breaking wave. The total amount of airborne chloride (θ_{total}) is assume to be a function of the height of breaking wave:

$$\theta_{total} = \delta \cdot \theta_0 \cdot f(H_b) \cdot \frac{1}{T}, \tag{3-25}$$

where θ_{total} is the total airborne chloride produced (particle number/m^3/sec), θ_0 is the referent number of the seawater aerosol produced equal to $2.0x10^4$ particle number/m^3/sec, δ is the coefficient on the place of airborne chloride production, T is the wave period (sec), and $f(H_b)$ is a function of the breaking wave height. In this case, $f(H_b) = C \cdot H_b$, where C is a constant equal to 1.0.

The size of airborne chloride particles, produced at the same time, is non-uniform. The airborne chloride particle size at the initial point is assumed to follow an exponential function:

$$f(d) = \frac{1}{d_a}\exp(-\frac{d}{d_a}), \tag{3-26}$$

where d is the diameter of airborne chloride (m), d_a is the average diameter of airborne chloride (m), and the total number of airborne chloride diameter d_i (particle number/m^3/sec) can be calculated by integrating the density function in the range of $\triangle$ d:

$$\theta_{d_i-total} = \theta_{total} \cdot \int_{d=d_i-\frac{\Delta d}{z}}^{d=d_i+\frac{\Delta d}{z}} \frac{1}{d_a}\exp(-\frac{1}{d_a} \cdot d)dd. \tag{3-27}$$

It is assumed that the airborne chloride produced at the initial point is vertically distributed. The distribution function of airborne chloride is

$$f(z) = \frac{1}{Z_a}\exp(-\frac{Z}{Z_a}), \tag{3-28}$$

where Z_a is the average height of the vertical distribution of airborne chloride (m),and Z is the height from the initial (m).

The vertical distribution of airborne chloride, it is assumed that when the wave height is higher, the vertical distribution distance will be higher. Z_a can be expressed as a function of breaking wave height:

$$Z_a = \varepsilon \cdot H, \tag{3-29}$$

where ε is the coefficient for the vertical airborne chloride distribution and H is the wave height, which is equal to observed significant wave heights for the open sea conditions and the height of breaking waves for seashore conditions.

The amount of airborne chloride with diameter d_i at height Z_j can be found with:

$$\theta_{d_i Z_j} = \theta_{d_i - total} \cdot \int_{z=z_i-\frac{\Delta z}{2}}^{z=z_i+\frac{\Delta z}{2}} \frac{1}{Z_a} \exp\left(-\frac{Z}{Z_a}\right) dz. \quad (3\text{-}30)$$

In the original Kokubo and Okamura model, it is assumed that the airborne chloride transportation is the process of moving the airborne chloride to a target point by the wind. Airborne chloride particles fall because of the force of gravity. The vertical distribution of the wind is assumed to be constant during the transportation.

The total chloride at a specific position after the generation and transportation of airborne chloride can be calculated as:

$$\theta_{d_i Z_j, x} = \theta_{d_i - total} \cdot \int_{z=z_i-\frac{\Delta z}{2}}^{z=z_i+\frac{\Delta z}{2}} \frac{1}{Z_a} \exp\left(-\frac{1}{Z_a}\left\{z_j + W_{d_i}\left(\frac{x}{U}\right)\right\}\right) dz, \quad (3\text{-}31)$$

where x is the distance from the initial point to the target point, U is the wind velocity, W_{d_i} is the falling velocity of airborne chloride particle size di, calculated as:

$$W_{d_i} = \left\{\frac{4 g d_i}{3 C_D} \cdot \frac{(\rho_p - \rho_{air})}{\rho_{air}}\right\}^{\frac{1}{2}}, \quad (3\text{-}32)$$

where g is the acceleration of gravity (m/sec^2), d_i is the airborne chloride diameter (m), ρ_p is the density of sea water (kg/m^3), ρ_{air} is density of air (kg/m^3), and C_D is the drag coefficient, calculated as:

$$C_D = \begin{cases} \frac{24}{Re} & when\ Re < 1 \\ \left(0.55 + \frac{4.8}{\sqrt{RE}}\right)^2 & when\ 1 < Re < 10^4 \end{cases} . \quad (3\text{-}33)$$

Re is the Reynolds number and can be determined as

$$Re = \frac{(W_{d_i} \cdot d_i)}{\left(\frac{\mu}{\rho_{air}}\right)}, \quad (3\text{-}34)$$

where μ is the dynamic viscosity of air (kg/m/sec).

The coefficient and constant of the proposed model are shown in Table 3-1.

Table 3-2 Coefficients and constants for the proposed model.

		On shore		On open sea
		Obstacle	**Beach**	
δ		1	40	400
θ_0		2×10^4		
da		350	20	8
ε	d≧da	2	2.5	40
	d＜da	10		

From equation 3-31, the total number of airborne chloride particles with diameter d_i at each position is calculated. The chloride ion intensity ($M_{d_i Z_j,x}$; kg/m^3/sec) can be calculated from the total number of chloride particle as

$$F_{d_i Z_j,x} = \theta_{d_i Z_j,x} \cdot \frac{4}{3}\pi\left(\frac{d_i}{2}\right)^3 \cdot \rho_p \cdot \frac{Cl}{100} \cdot U, \quad (3\text{-}35)$$

where ρ_p is the density of sea water (kg/m^3), U is the wind velocity (m/sec), and Cl is the concentration of chloride ions in the sea water, equal to 1.9% by weight.

Then, the total amount of chloride can then be determined through the summation of the total airborne chloride particles with diameter d_i, as shown in equation 3-36.

$$F_{Z_j,x} = \sum \theta_{d_i Z_j,x} \cdot \frac{4}{3}\pi\left(\frac{d_i}{2}\right)^3 \cdot \rho_p \cdot \frac{Cl}{100} \cdot U. \quad (3\text{-}36)$$

However, the amount of chloride at each position is dependent on the wind direction. Equation 3-37 shows the amount of airborne chloride when the wind direction is normal to the concrete surface. When the wind deviates from this direction, the total chloride intensity can be calculated as

$$F_{Z_j,x\_adjust} = F_{Z_j,x} \cdot \cos\theta\,, \quad (3\text{-}37)$$

where θ is the deviated wind direction from the normal surface. Moreover, the proposed model assumes that the airborne chloride can attach to the concrete surface when the wind direction is ± 67.5 degree from the normal direction (Figure 3-22).

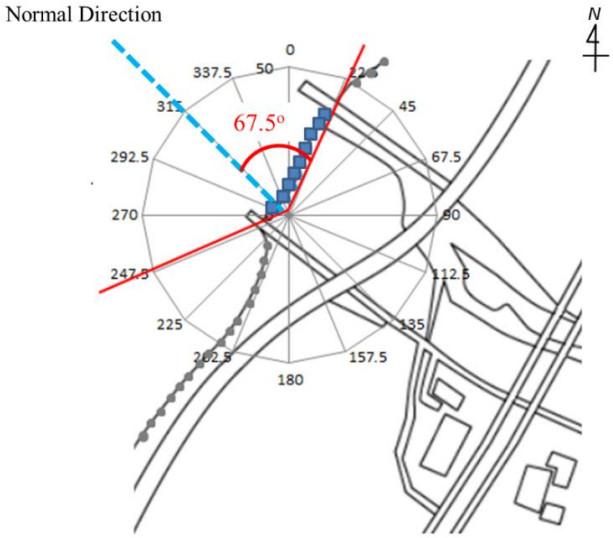

Figure 3-28 Directions from which airborne chloride can attach to structure.

3.5.2. Modified Kokubo and Okamura Model by Hanioka (2011)

Hanioka S. (2011) has proposed a modified model, changing the wind velocity distribution in the vertical direction and the average size of airborne chloride [7, 23].

1) Wind velocity distribution

Observation results [7] suggests wind velocity is not consistent and the wind velocity at the different heights is not identical. Thus, a power law is introduced. The wind velocity at the target position can be calculated as

$$U = U_0 \left(\frac{z}{z_o}\right)^{\frac{1}{n}}, \tag{3-38}$$

where U_0 is the reference wind speed (from the AMEDAS database), z_0 is a reference height equal to 6 m from the experiment, z is the measurement position height, and n is the power law constant (in this case, 7; Figure 3-29).

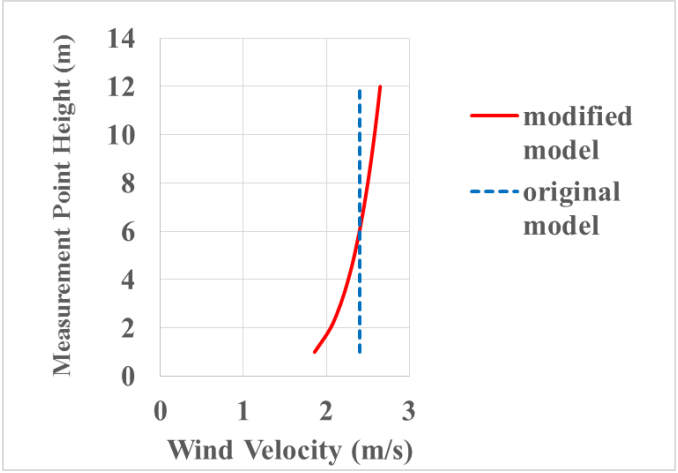

Figure 3-29 Wind velocity distribution.

2) Average Airborne chloride particle [7]

In the original Kokubo and Okamura model, the average airborne chloride particle size was assumed to be constant depending on the exposure condition. However, when the breaking wave height is higher, the average particle size of the airborne chloride particles should be larger (Figure 3-30).

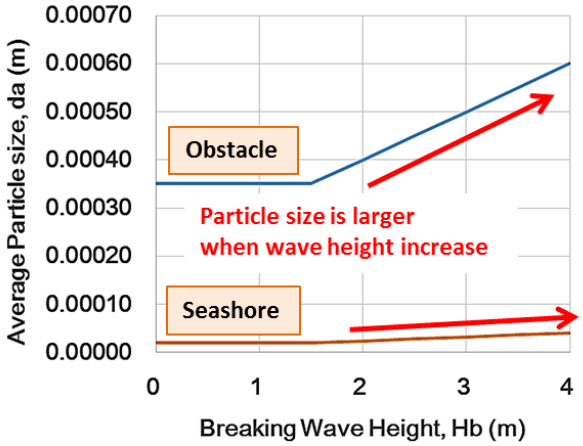

Figure 3-30 Average particle size of airborne chloride.

The average airborne chloride particle size can be calculated with Table 3-3.

Table 3-3 Average airborne chloride particle size.

Breaking wave height	Obstacle (μm)	Beach/ seashore (μm)
Lower than 1.5 m	$d_a = 350$	$d_a = 20$
Higher than 1.5 m	$d_a = 100 \times H_b + 200$	$d_a = 8 \times H_b + 8$

3.5.3. Experimental Verification of Airborne Chloride Generation and Transportation Model with Dry Gauze

To verify the proposed model, an experiment was conducted by Hanioka S. (2011) [7] near Okawa Bridge in Niigata prefecture, Japan (Figure 3-31).

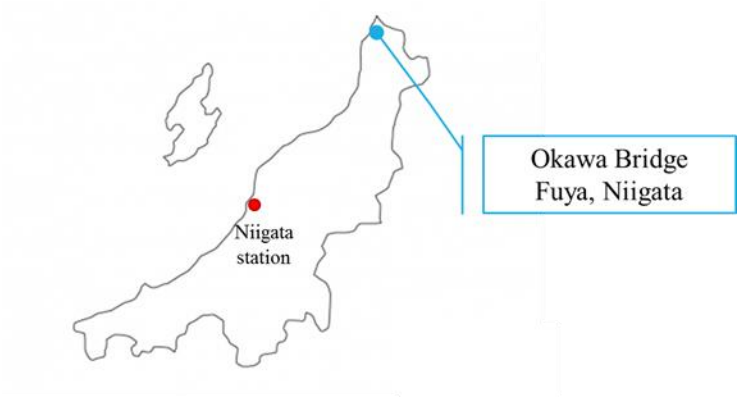

Figure 3-31 Exposure site near Okawa Bridge.

In the experiment, the dry gauze method was used [24] to collect airborne chloride. Dry gauze samples were attached on a tripod at 2, 4, and 6 m (Figure 3-32). The distance from the measurement position to the coastline was 100 m (Figure 3-33).

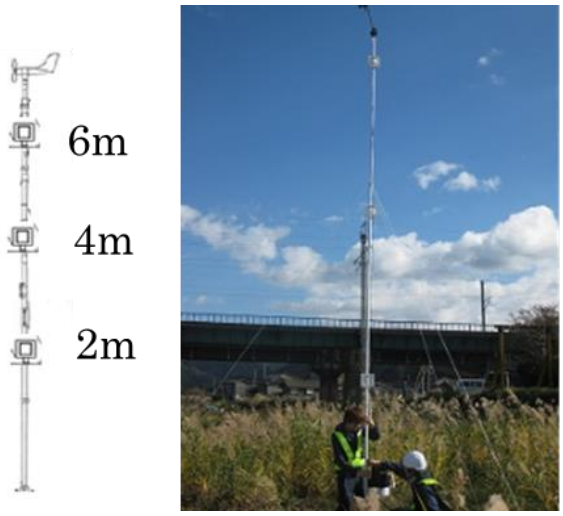

Figure 3-32 Dry gauze on tripod [7].

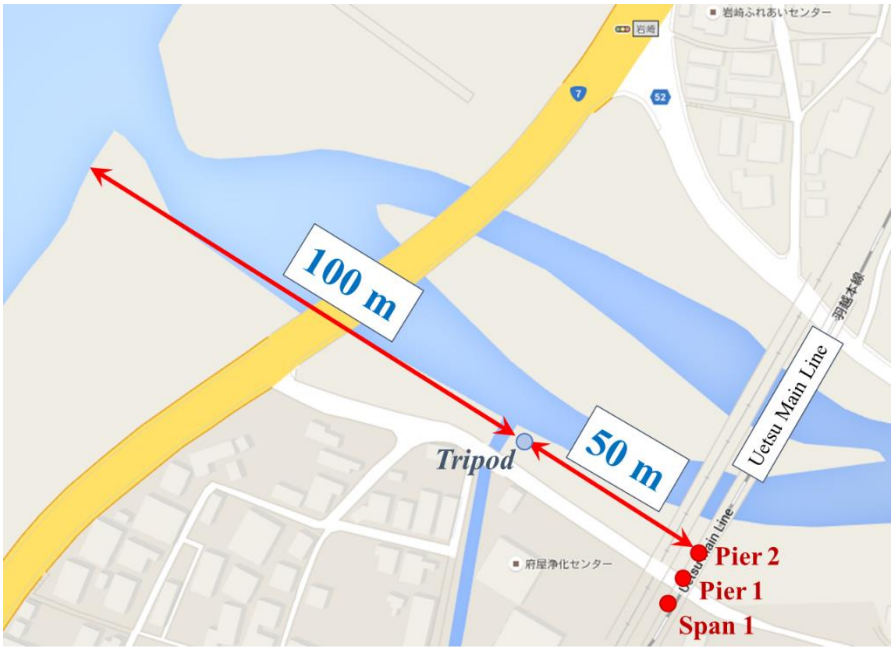

Figure 3-33 Tripod position near exposure site.

1) Exposure condition

The exposure condition was checked by onsite observations and from a bird's-eye view [7, 23]. There were obstacles in front of the exposure site (Figure 3-34; Figure 3-35).

Figure 3-34 Environmental condition near exposure site.

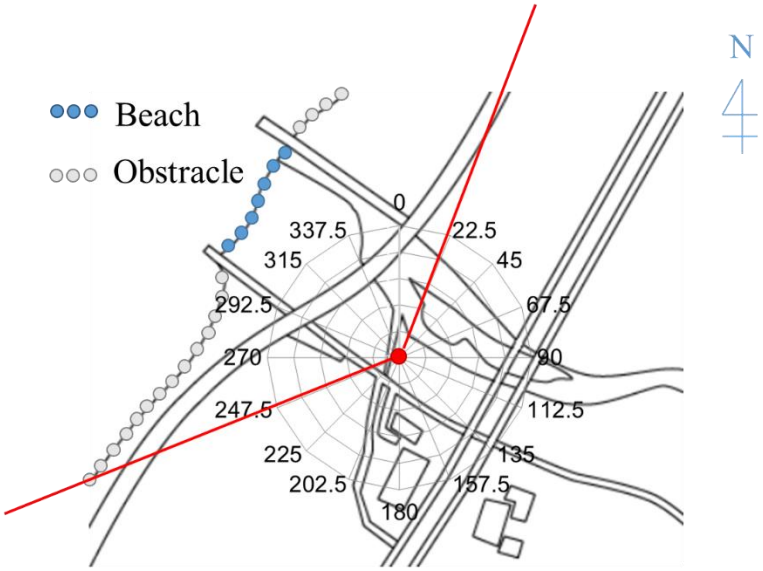

Figure 3-35 Exposure conditions near exposure site and obstacle positions (100 m from the seashore).

2) Environmental input data for calculation

- Wave height, tidal cycle, and water depth data from the Nationwide Ocean Wave information network for Ports and Harbours (NowPhas) Database at Sakata station.
- Wind speed and direction from AMEDAS Database from Nezugaseki station.

3) Verification

The results of the analysis are shown in Figure 3-36 and Figure 3-37. For the tripod, with the original Kokubo and Okamura Model, the value from the

calculation shows a different distribution trend when compared with the experimental results (Figure 3-37). This is due to the power law for wind velocity distribution applied in the calculation.

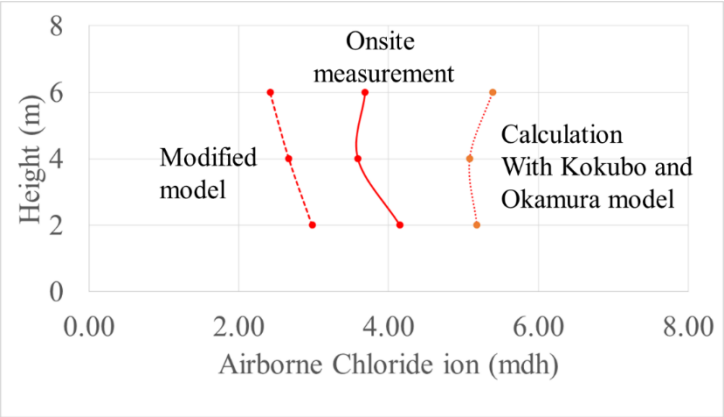

Figure 3-36 Experiment with tripod and analysis results (6 January 2011).

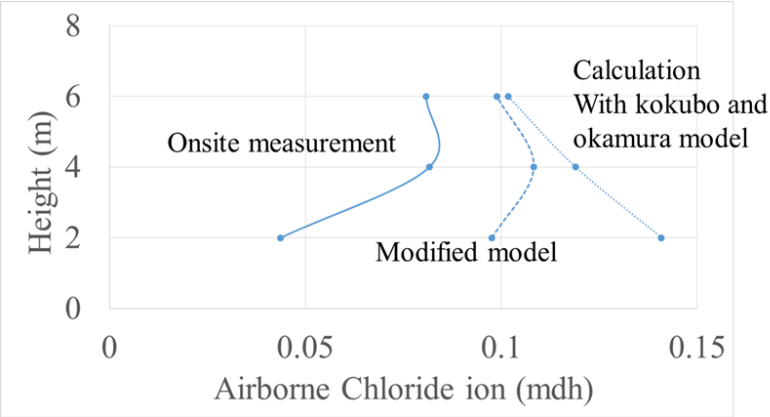

Figure 3-37 Experiment with tripod and analysis results (10 August 2011).

For the verification results, the modified model can calculate the change in airborne chloride at different heights. As seen in Figure 3-37, the calculation results from the model by Kokubo and Okamura has different trends when compared with onsite measurement data. Therefore, the modified model is used in the comprehensive system.

3.6. Summary

In marine environments, the deterioration of reinforced concrete structures is caused by airborne chloride attack and therefore infrastructure in coastal areas sometimes requires repairs or reconstruction due to the corrosion of reinforcing steel bars. Therefore, a reliable computational model to calculate airborne chloride penetration into concrete structures is necessary to evaluate the service life of concrete structures and to perform maintenance. However, in reality, airborne chloride data is limited. Thus, it is also necessary to develop a comprehensive system to determine the amount of airborne chloride ingression without recorded airborne chloride data.

This chapter presented a concept for a comprehensive system. This comprehensive system considers the amount of chloride generation, transportation, and ingression by connecting three calculation models. The concept of each model was discussed and a verification of each model was reviewed or conducted.

From the verifications, the concrete surface model overestimates chloride ingression from the moisture and chloride flux. This may be due to inappropriate assumptions in the analysis or because conditions during analysis did not match with actual environmental conditions. Therefore, a modification of the model should be considered.

Furthermore, the verification of the generation and transportation model is limited. To use the airborne chloride generation and transportation model in the comprehensive system, additional verifications are necessary.

3.7. Reference

[1] T. Ishida, Y. Takahashi and R. Wattanapornprom, "Numerical simulation of chloride migration in concrete structure under harsh environmental conditions," in *International Conference on the Regeneration and Conservation of Concrete Structures*, Nagasaki, Japan, 2015.

[2] JSCE Comittee, "Standard Specification for Concrete Structure," Japan Society of Civil Engineers, 2012. (in Japanese)

[3] N. Bongochgetsakul, S. Kokubo and S. Nasu, "Measurement of Airborne Chloride Particle Sizes Distribution for Infrastructures Maintenance," in *IESL-SSMS Joint Symposium*, Colombo, Srilanka, 2011.

[4] S. Kokubo and H. Okamura, "Calculation Model for Airborne Chloride Ion based on Seawater Particle Generation," *JSCE journal of hydraulic, coastal and environmental engineering,* vol. 65, pp. 259-268, 2009.

[5] Public Work Research Institute, "Report on Investigation of Airborne Chloride in Japan (IV), PWRI report No. 3175, Public Work Research Institute, 1993. (in Japanese)

[6] H. Minoo, T. Ishida and T. Ishikawa, "Chloride Ion Ingress Model on the Concrete Surface Under Airborne Chloride Action," in *Japan Concrete Institute Annual Conference*, Japan, 2014. (in Japanese)

[7] S. Hanioka, "Verification and enhancement of airborne chloride generation and transportation model based on field measurement," The university of Tokyo, 2011. (in Japanese)

[8] K. Maekawa , R. Chaube and T. Kishi, Modeling of concrete performance, 1st ed., New York: E&FN Spon, 1999.

[9] K. Maekawa, T. Ishida and T. Kishi, Multi-Scale Modelling of Structural Concrete, Taylor and Francis, 2008.

[10] O. I. Prince and T. Ishida, "Modeling of chloride transport coupled with enhanced moisture conductivity in concrete exposed to marine environment," *Cement and Concrete Research,* vol. 39, pp. 329-339, April 2009.

[11] T. Ishida, K. Maekawa and T. Kishi, "Enhanced Modeling of Moisture Equilibrium and Transport in Cementitious Materials under Arbitrary Temperature and Relative Humidity History," *Cement and Concrete Research* , vol. 37, pp. 565-578, 2007.

[12] S. Okazaki and T. Kishi, "Simulation of dead slow permeation of dead slow water into concrete based on non-Newtonian clued mechanics," in *EASEC-10,* 2006.

[13] Y. Takahashi and T. Ishida, "Modeling of chloride ion ingress and liquid water movement in mortars and concretes with low water-to-cement ratio," in *International Conference on Sustainable Construction Materials and Technologies 3*, Kyoto, Japan, 2013.

[14] T. Ishida, K. Maekawa, T. Kishi, G. Iwata and C. Kusuhara, "Enchanced Modelling of Moisture Equilibrium and Transport in Cementitious Materials under Arbitrary Temperature and Relative Humidity History," *Journal of JSCE,* vol. 68, no. 795, pp. 39-53, 2005.

[15] S. Goto, K. Shigeru, T. Takagi and M. Daimon, "Pore Size Distributions and Ion Diffusion in cement hydrates," *Proceedings of Cement and Concrete,* vol. 36, pp. 49-52, 1982.

[16] T. Ishida, O. I. Prince and Ho Thi Lan Anh, "Modeling of chloride diffusivity coupled with non-linear binding capacity in sound and cracked concrete," *Cement and Concrete Research,* vol. 39, pp. 913-923, October 2009.

[17] O. I. Prince, "Chloride Transport Coupled with Moisture Migration in Non-Saturated Concrete Exposed to Marine Environment and Application to Cracked Concrete," The University of Tokyo, Tokyo, 2008.

[18] K. Nakarai, T. Ishida and M. Koichi, "Multi-scale physiochemical modeling of soil–cementitious material interaction," *Soils and Foundation,* vol. 46, no. 5, pp. 653-664, 2006.

[19] T. Ishikawa, "Modeling of airborne chloride penetration flux into concrete," The University of Tokyo, Tokyo, Japan, 2010.

[20] T. Yasuda, Y. Kishimoto, T. Tsutsumi, Y. Hama and M. Zakaria, "Fundamental Study on Influence of Rain and Wind on Durability of Building Wall," in *Repairing and Maintenance of Concrete Structures*, 2013.

[21] Public Work Research Institute, "Report on Investigation of Airborne Chloride in Japan (III), PWRI report No.2687," 1988. (in Japanese)

[22] S.Kokubo, "Calculation model for airborne chloride ion based on seawater aerosol production," Kochi University of Technology, Kochi, 2009. (in Japanese)

[23] T. Ishida, A. Kita, S. Hanioka, L. A. Ho Thi and Y. Matsuda, "A study on Mechanism of airborne chloride transport and migration into mortar based on onsite measurement," in *Proceedings of the Concrete Structure Scenarios*, 2012. (in Japanese)

[24] Japanese Standards Association, "JSA JIS Z 2382 Determination of pollution for evaluation of corrosivity of atmospheres," 1998. (in Japanese)

Chapter 4
Airborne Chloride Surface Flux Model Modification and Verification

4.1. Introduction

The previous chapter presented the concept and calculation method of existing airborne chloride surface flux models [1]. The verification results suggest the chloride ingression from the model overestimated experimental results in some cases. This may be due to the impropriate assumptions in the model or because conditions in the analysis do not match actual environmental conditions. Therefore, in order to obtain the reliable calculations, a modification of the model should be considered.

This chapter, the modification and additional assumptions used in the model will be explained. Moreover, results from the calculation are verified through comparisons with experimental laboratory data and on-site measurements.

4.2. Model Modification

As mentioned in the previous section, the existing model was verified by using experimental results and on-site measurement data. Still, from the calculation, in both cases, the total chloride ingression amount were relatively high compared to experimental results. Thus, this section considers a modification of the airborne chloride surface flux model.

4.2.1. Chloride Concentration on the Surface

Using the existing model concept with the same environmental conditions and concrete properties, when the amount of the airborne chloride is higher, more water can remain in the thin layer and the wet section (S_{wet}) will become larger. The mechanism of the moisture and chloride behavior in the thin layer are shown in Figure 4-1.

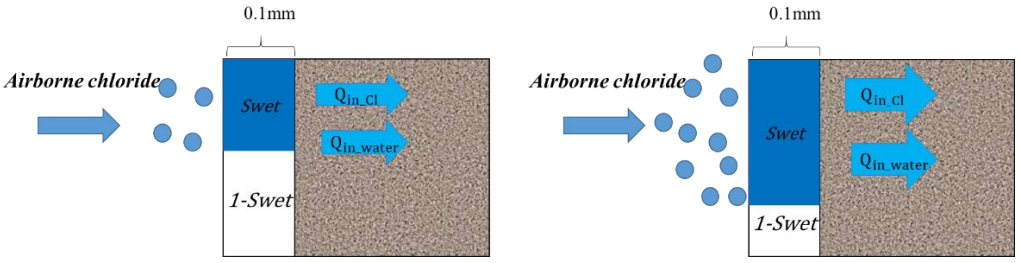

Figure 4-1 Mechanism of the moisture and chloride behavior in thin layer with different amounts of airborne chloride.

On the other hand, if the amount of airborne chloride is the same, when the RH of the surrounding environment is higher, the wet section (S_{wet}) will increase and larger amounts of chloride can penetrate the concrete, as shown in Figure 4-2.

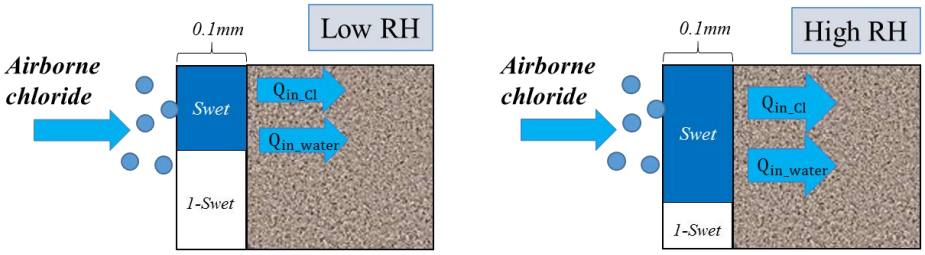

Figure 4-2 Wet section in thin layer with low RH and High RH.

Sensitivity analysis was conducted to check the assumption by analyzing chloride penetration under different relative humidity levels. It was assumed that airborne chloride (chloride ion) in the environment condition is equal to 1.20 mdh and the W/C of the concrete is equal to 50%. With the existing model, the total chloride penetration can be calculate (Figure 4-3).

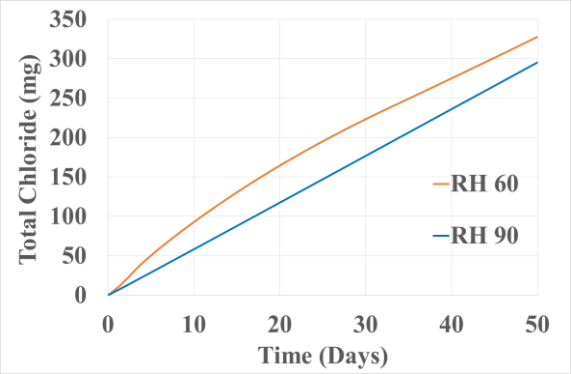

Figure 4-3 Total chloride penetration with different relative humidity levels.

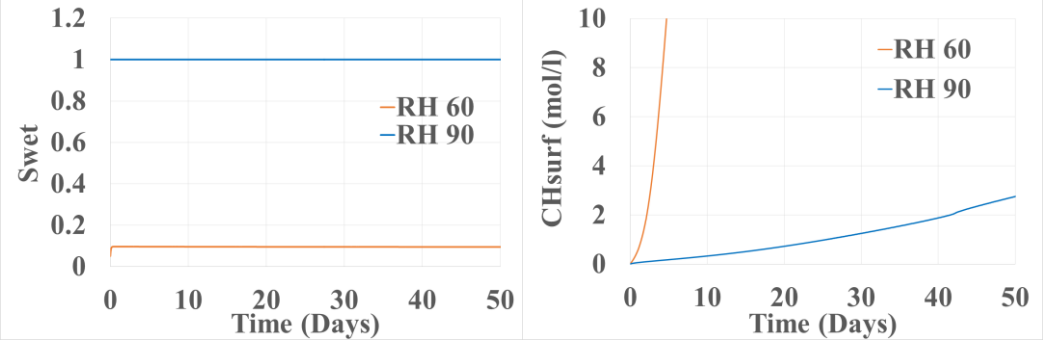

Figure 4-4. S_{wet} and CH_{surf} parameters from the calculation.

From the analysis with the existing model, when the RH is low, the wet section, S_{wet}, is reduced. However, the total chloride amount is greater than cases with high RH due to higher chloride concentration on concrete surfaces.

From the past research, under natural conditions, the amount of dissolved sodium chloride in the solution is limited. The maximum concentration of the saturated solution of sodium chloride in pure water is ~5.4 mol/l [2]. Hence, in the modified model, the chloride concentration on the surface (CH_{surf}) is limited to 5.4 mol/m^2.

Figure 4-5 and Figure 4-6 show the analysis results after limiting the chloride concentration on the surface.

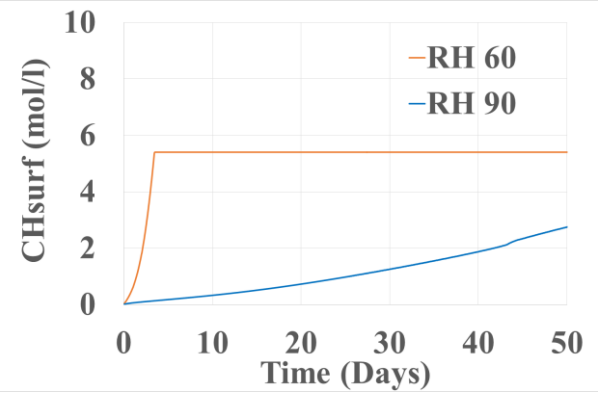

Figure 4-5 CH_{surf} parameter from the calculation after limited chloride concentration on the surface.

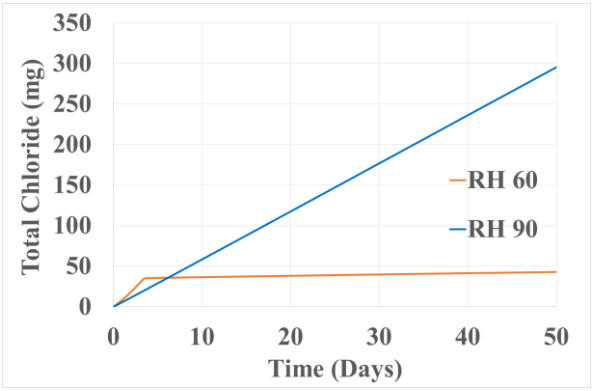

Figure 4-6 Total chloride penetration under different relative humidity levels.

To verify the modified model, after the chloride concentration on the surface was limited, data from previous research (Ishikawa T., 2012) was used [3]. Figure 4-7 shows the verification results with the original model and modified model. In the calculation, the relative humidity inside the wind tunnel is assumed to be 90%. In comparison with experimental results [3], the analysis after limiting the CH_{surf} value shows a better match.

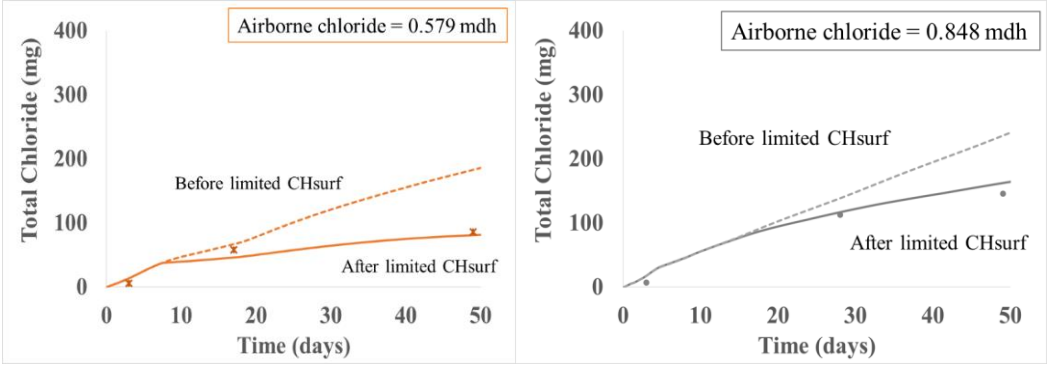

**Experiment by Ishikawa T. (2011)* [30]

Figure 4-7 Experiment and model results with original and modified model.

Additionally, a verification with different airborne chloride intensities was conducted. The experimental and analytical results of the total chloride penetration are shown in Figure 3-25.

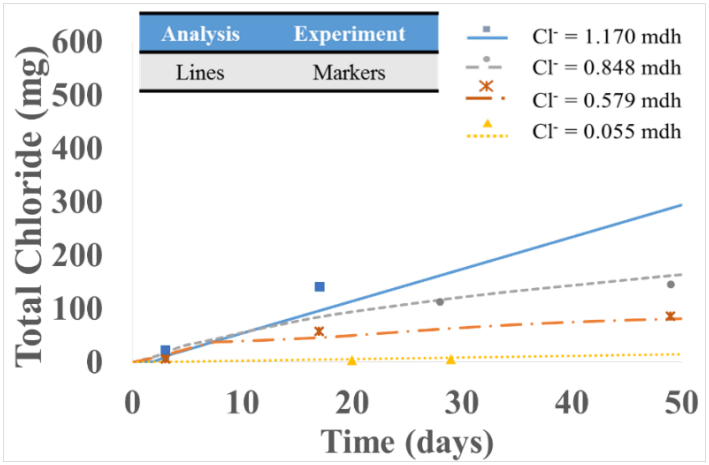

Figure 4-8 Total chloride penetration with different airborne chloride intensities.

From the results, the modified model can be used to calculate the total chloride penetration with different airborne chloride conditions.

4.2.2. Chloride Washout Calculation

As discussed in section 3.4.6, the original model by Minoo H. (2013) overestimates onsite measurement data. This may be because assumptions in the calculation do not matched actual environmental conditions.

Under actual environmental conditions, chloride concentration on the concrete structure is influenced by the climate, location, and weather [4]. Water particles from rainfall can wash chloride from concrete surfaces [5, 6]. This effect, as discussed, is called the *washout effect*. The washout effect mechanism is shown in Figure 4-9.

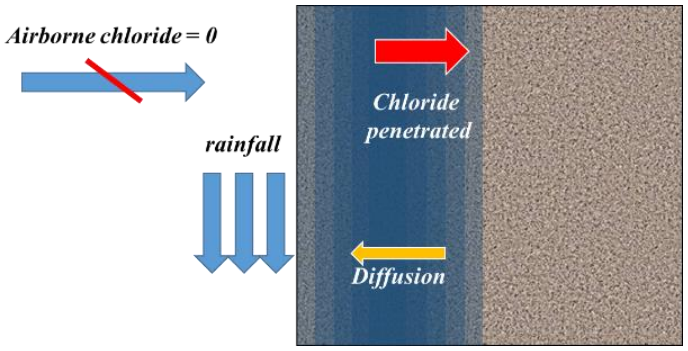

Figure 4-9 Airborne chloride washout mechanism.

Previous research reports that the chloride concentration on concrete structures decreases due to rainfall [5]. However, the effect of the rainfall is not included in the existing model. Therefore, to obtain a valid prediction of chloride penetration into concrete structures under actual environmental conditions, the washout effect should be considered.

In the modification, it is assumed that the washout effect occurs when the concrete is subjected to rainfall and the amount of the water is large enough to wash the concrete surface. During this stage, the concrete surface is wet and without dry areas. This condition can be represented when the value of S_{wet} becomes 1.0, as shown in Figure 4-10

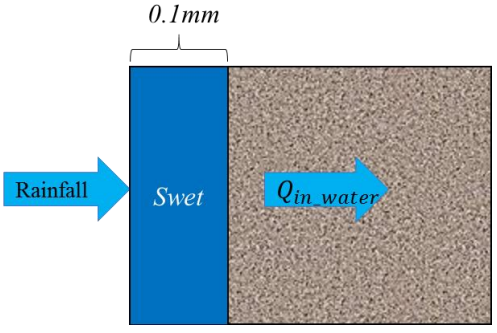

Figure 4-10 Saturation of concrete surface with water from rainfall.

The chloride concentration on the concrete surface (CH_{surf}) becomes 0 when subject to the heavy rainfall (the intensity of heavy rainfall will be described in section 4.4.2) and the washout effect occurs. At this stage, the chloride inside the concrete gradually diffuses from inside the concrete to the outside, as shown in Figure 4-11.

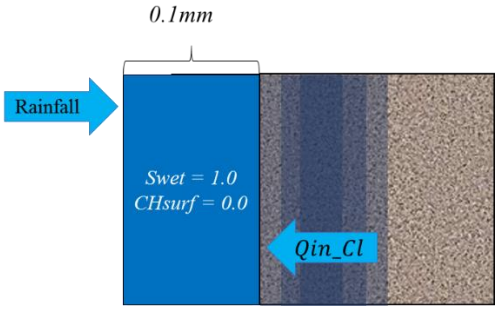

Figure 4-11 Washout effect of rainfall on concrete surface.

Therefore, the chloride ion penetration from advection becomes 0 and the amount of chloride reduction from diffusion can be calculated as:

$$Q_{diff} = 1.0 \times K_{cl} \times (C_{Cl} - 0.0). \quad (4\text{-}1)$$

With the proposed calculation method, if the washout effect occurs, chloride concentration on the concrete surface is reduced and the total chloride inside the specimen is also reduced, as shown in Figure 4-12.

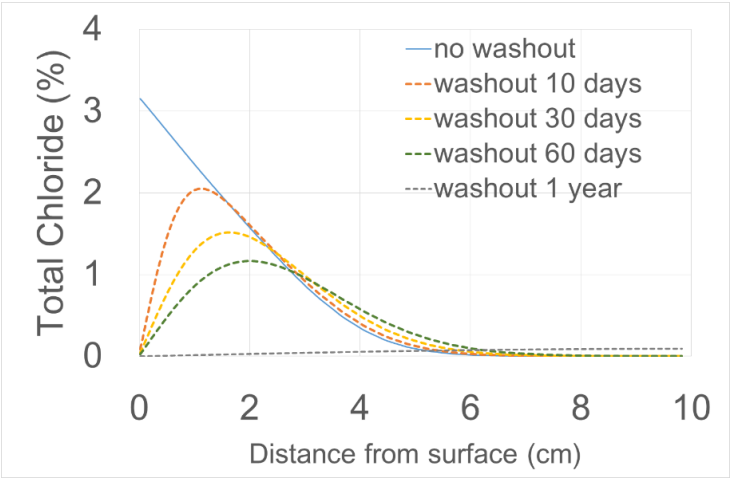

Figure 4-12 Analytical results when washout effect is continuous (sensitivity analysis with W/C 0.55).

4.2.3. Surface Moisture Penetration under Rainfall Conditions

Under actual environmental conditions, wetting environments can be classified into two forms depending on the mechanism by which the moisture transport takes place [7]:

- Humid environment

  An environment where the relative humidity is close to 100% and moisture diffuses into pores through the concentration gradient.

- Submerged environment

  An underwater environment where the main transport is due to the capillary suction of liquid water. Surface tension is the primary cause of liquid rising in capillaries. It is known from experiments and theory that the sorption flux is high at the beginning for a few hours and then reduces sharply, depending on the porosity and connectivity of porous network [8]. In submerged environments, the hydraulic pressure acts on the exposed surface and moisture moves under the positive pore pressure head.

In the actual environmental condition, structures near the coast can be exposed to both conditions. When concrete is exposed to airborne chloride condition, the boundary condition is closer to a humid environment. However, when the structure is subject to rainfall and water from precipitation covers the concrete surface, the boundary condition is closer to a submerged condition.

In the existing model, the water ingression mechanism for airborne chloride and under rainfall are the same. Thus, moisture transmission under rainfall conditions should be modified.

In DuCOM system, distinguishing submerged conditions from unsaturated humid environments is proposed by applying hydraulic water pressure. There are two options to define the boundary conditions in the analytical system. For water submergence, positive pore pressure equal to the hydraulic head of water is applied to the exposed surface. For an unsaturated environment, the negative pore pressure computed with Kelvin's equation is used [7, 9, 10].

In a completely saturated condition, the calculation can be reproduced by applying hydraulic pressure at the surface node of the elements so that the sorption flux of liquid water can be simulated more realistically [7].

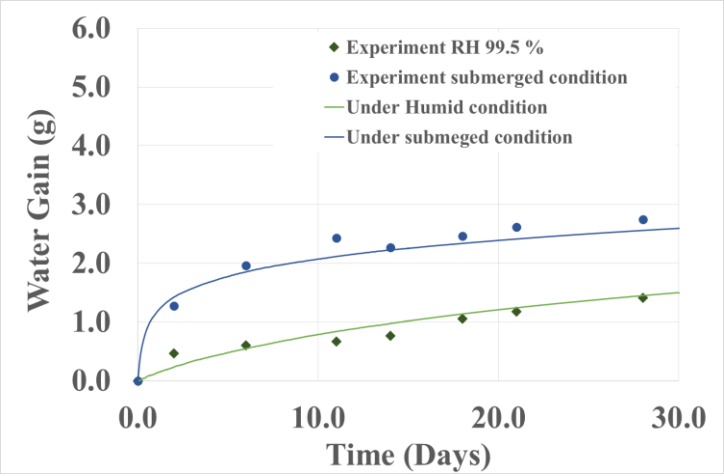

Figure 4-13 Experiment and analysis for wetting at 99.5% RH and submerged environment (W/C 0.35) [7].

On the other hand, under rainfall conditions, calculating water immersion by applying hydraulic pressure to the surface is somewhat difficult. To calculate water penetration by applying hydraulic pressure, the calculation needs to be restarted each time the concrete is submerged in water.

In reality, rainfall does not continue for a long time and rainfall intensity is not constant. According to the AMEDAS database, rainfall mostly occurs for a few hrs, as shown in Table 4-1.

Table 4-1 Frequency of rainfall from December 10, 1984–December 10, 1985 (in Niigata Prefecture, Japan).

Rainfall duration (hour)	Frequency
1	215
2	65
3	36
4	28
5	19
6	17
7	5
8	5
9	4
10	2
Over 10 hrs	13

As mentioned above, the amount of airborne chloride, rainfall intensity, and rainfall duration are not constant. Therefore, calculating moisture penetration under these conditions with applied hydraulic pressure in the original model is difficult and time consuming.

To calculate water penetration under rainfall conditions in this study, an equivalent method is introduced. To increase the water absorption capacity when the concrete surface is exposed to rainfall in a short time, the moisture transfer coefficient is enlarged by a magnified factor (MF). The proposed model assumes that when the concrete is exposed to heavy rainfall, the volume of water penetrated the concrete from the rainfall can be calculated as:

$$Q_{in\_water} = S_{wet} \times MF \times K_{water} (RH_{bound} - 1.0), \qquad (4\text{-}2)$$

where K_{water} is the moisture transfer coefficient = 5.0×10^{-5} (kg / m^2.s) and RH_{bound} is the relative humidity inside the concrete surface. To define the heavy rainfall value, a sensitivity analysis was conducted, explained in detail in section 4.4.2.

The value of MF is assumed from the sensitivity analysis. Figure 4-14 and Figure 4-15 show the results from sensitivity analysis using different values of MF.

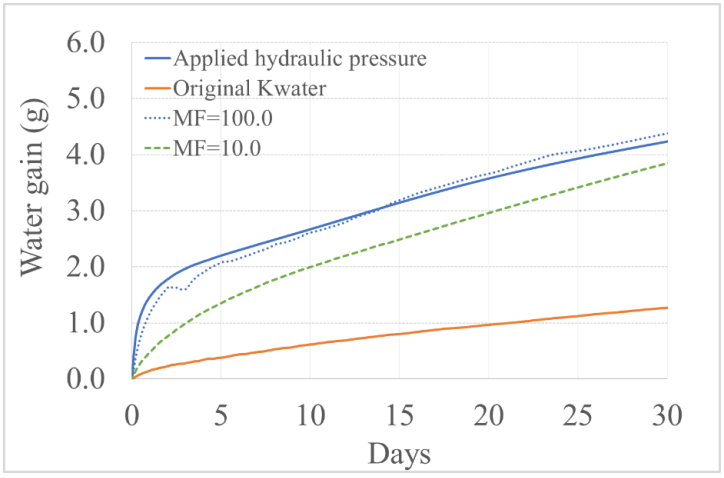

Figure 4-14 Sensitivity analysis when MF is applied (W/C 0.50).

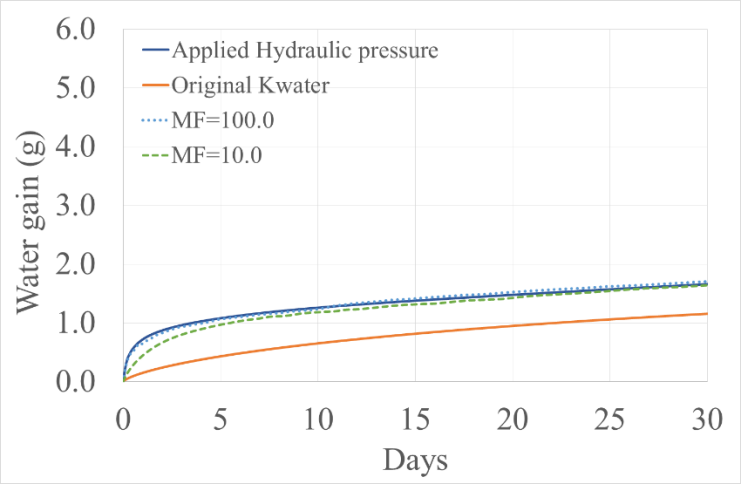

Figure 4-15 Sensitivity analysis when MF is applied (W/C 0.40).

The results show when MF = 100.0, the penetrated water (water gain) value is close to applied hydraulic pressure conditions. Therefore, under heavy rainfall, MF = 100.0 can be used to predict water ingression.

4.3. Experimental Verification of Moisture and Chloride Surface Flux Model Under Controlled Conditions

The previous section presented modifications of the existing model. In order to verify the new proposed model, a comprehensive experimental series was conducted under controlled conditions in the laboratory. Each experiment represents phenomena which influence chloride penetration under airborne chloride conditions. Figure 4-16 shows a general schema of the experimental series for the verification.

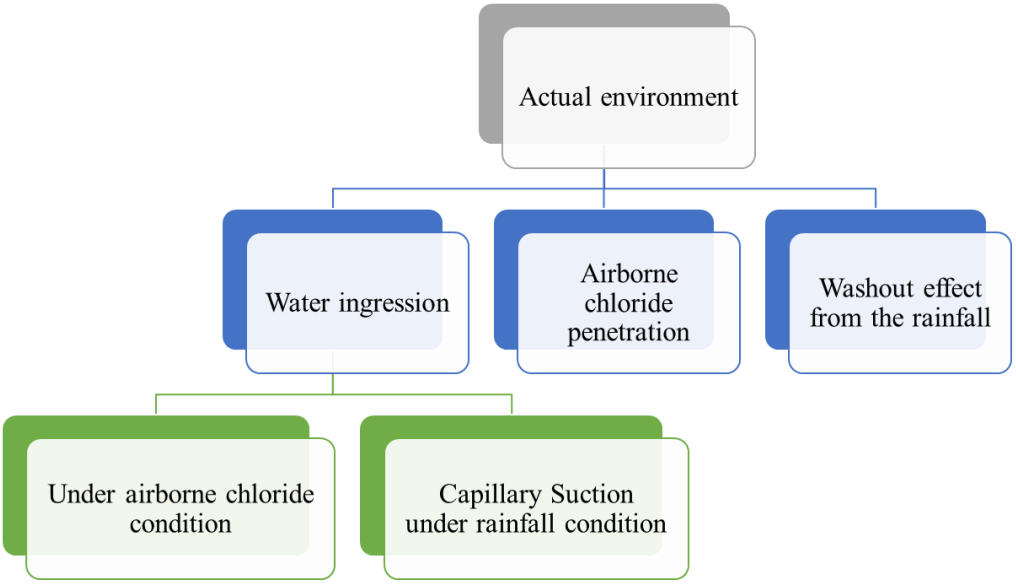

Figure 4-16 Experimental series for model verification.

4.3.1. Water Ingression

As discussed in section 4.2.3., water ingression under actual environment conditions can considered through two mechanisms [7].

In humid environments, the airborne chloride particle attach to the structure. For the ingression from capillary suction mechanism, the structure is subject to rainfall and water from the precipitation covers the concrete surface. Therefore, to verify the water ingression mechanism, two experiments were conducted.

4.3.1.1. Water Ingression Under Airborne Chloride Conditions

To simulate airborne chloride conditions in the laboratory, a wind tunnel was used [1, 3, 10, 11]. Inside the wind tunnel, a salt bath was filled with NaCl solution with a concentration of 3%. Bubble generators were installed in the salt bath to generate small salt particles, transported inside the tunnel by the air flow generated by a propeller. Inside the wind tunnel, specimens were installed to examine water ingression.

A diagram of the wind tunnel used in the experiment is shown in Figure 4-17.

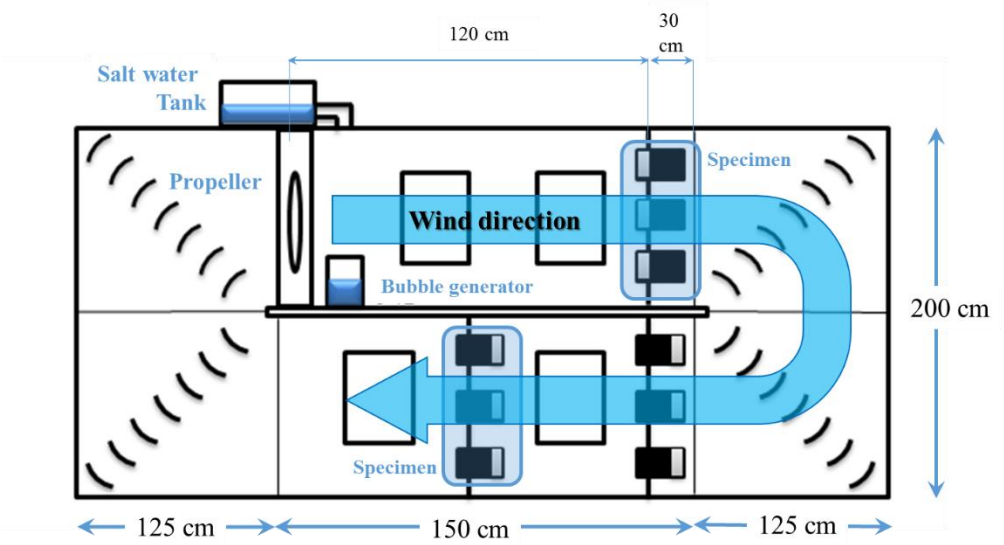

Figure 4-17 Wind tunnel equipment used to simulate airborne chloride conditions.

The objective of this experiment as to determine water ingression into the specimen under airborne chloride conditions. Specimens with W/C of 40% under seal and water curing conditions were used in the test.

1) <u>Experimental methodology</u>

The experimental methodology is described in detail in the following sections.

Figure 4-18 Steps for checking water ingression under airborne chloride conditions.

- <u>Measurement of airborne chloride</u>

To find the amount of airborne salt inside the wind tunnel, in this step, the gauze and cotton specimens were installed. The specimens were prepared

using a cylindrical plastic mold (Ø 5 x 10 cm) filled with cotton and the surface covered with gauze, as shown Figure 4-19.

Figure 4-19 Cotton and gauze specimen for measuring amount of airborne chloride.

After an exposure period of 1 day, the gauze and cotton were removed and submerged in pure water to wash the chloride from the gauze and cotton. Then, the amount of chloride in the water was determined by titration.

- Mortar specimen preparation

In this experiment, cylindrical mortar specimens with a diameter of 5 x 10 cm and a W/C of 40% were prepared. The mix proportion is shown in Table 4-2. After casting, specimens were cured under water and seal condition for 30 days. After curing, each specimen was dried in an environmental control room (temperature = 20 ^{o}C, RH = 60%) for 60 days.

Table 4-2 Mix proportion for wind tunnel experiment.

W/C	Cement (kg/m^3)	Sand (kg/m^3)	Water (kg/m^3)
0.40	675	1340	270

After drying, the exposure surface was grinded out around 1-2 mm by with a surface grinding machine to control the quality of the surface and decrease the bleeding effect on the surface. Before exposure, each specimen was coated with epoxy with the exception of the surface to be exposed and weighed. An exposure specimen is shown in Figure 4-20.

Figure 4-20 Specimen for water ingression test.

- Measuring the amount of water ingression

For the test, the weight of each specimen was taken regularly with an electronic scale sensitive to three decimal places.

Figure 4-21 Measuring water ingression.

2) Experimental results and model verification

The experimental and analysis results for the water ingression are shown in Figure 4-22 and Figure 4-23.

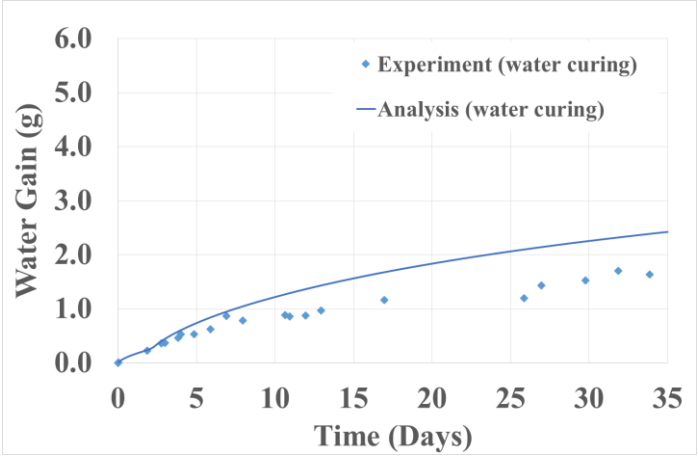

Figure 4-22 Experiment and analysis for water ingression OPC W/C 40% (water curing; chloride flux 1.01 mdh, RH 90.0).

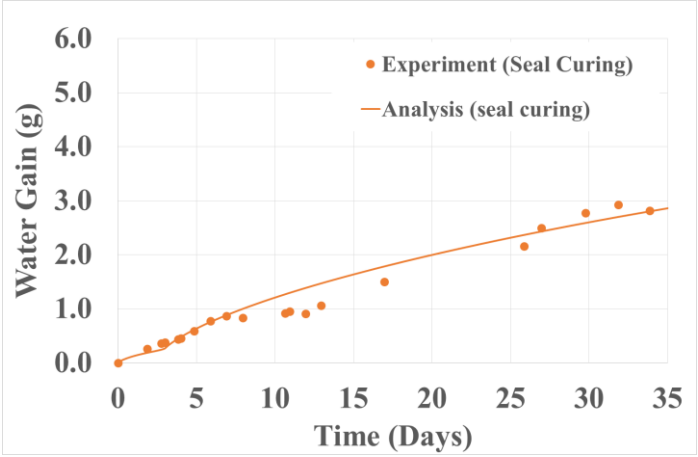

Figure 4-23 Experiment and analysis for water ingression OPC W/C 40 % (Seal curing; chloride flux 1.19 mdh, RH90.0)

In the analysis, the RH is assumed to be 90%. The figures, show that with similar amounts of airborne chloride, the experimental and model results show different amounts of water ingression when the curing condition is changed. It can be concluded that the proposed concept can be used to calculate water ingression under controlled conditions.

The results of the proposed model showed a good result for seal curing with a slight overestimation in water curing after 10 days of exposure. The overestimation may be due to inconsistencies in the airborne chloride flux

during the experiment. In the wind tunnel, wind speed at each position can be changed due to the obstacle. Furthermore, if the level of the salt water is changed, the amount of airborne chloride at each position is also changed [11]. Because of these factors, the amount of airborne chloride at each position inside the wind tunnel is not constant during the test (explained in detail in Appendix I).

4.3.1.2. Water ingression by capillary suction

When rainfall attached on the dry concrete surface, the water rapidly absorbs into the concrete by capillary action. To verify water ingression under rainfall conditions, a water absorption experiment was conducted.

In the experiment, it was assumed that the water absorption under rainfall is not effected by gravity or water pressure; only water absorption from capillary action was considered.

1) <u>Methodology</u>

In this experiment prism, specimens of 4x4x16 cm size were prepared and OCP Type I was used. The mix proportions are shown in Table 4-3.

Table 4-3 Mix proportion for water ingression test.

Mix	W/C (%)	Cement (kg/m^3)	Sand (kg/m^3)	Water (kg/m^3)
N40	40	840	1000	336
N50	50	737	1000	369

All specimens were cured through submersion in water for 30 days at 20 ^{o}C. After curing, all specimens were placed inside an environment control room at RH 60% and 20 ^{o}C for 30 days to reduce the moisture content inside the specimens. Then, samples were coated with epoxy except for the exposure side, as shown in Figure 4-24.

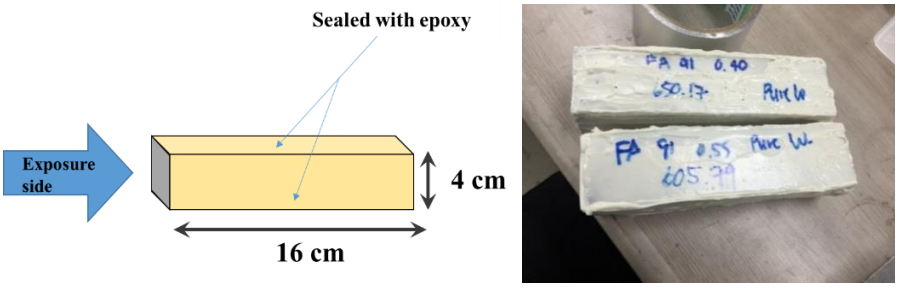

Figure 4-24 Specimen coated with epoxy before immersion.

The absorption test was conducted following the ASTMC1585-04 Standard Test Method for Measurement of Rate of Absorption of Water by Hydraulic-Cement Concretes [12].

Before specimens were exposed to pure water, the exposure surface was grinded to control the consistency of the surface as shown in Figure 4-25.

Figure 4-25 Surface grinding before submersion.

For the test, specimens were submerged in water with a control depth of 3–5 mm and weight change was recorded regularly with an electronic scale sensitive to two decimal places. Figure 4-26 show the testing method of this experiment.

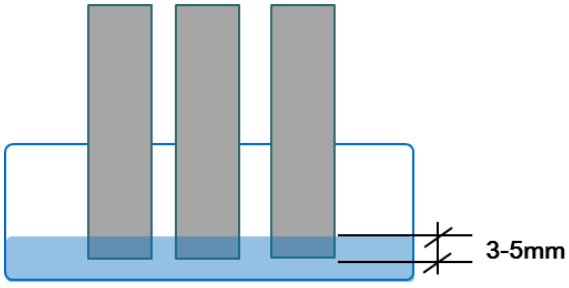

Figure 4-26 Testing method for verified water ingression.

2) Experimental results and model verification

Figure 4-27 and Figure 4-28 show the experimental and analysis result for the water ingression test.

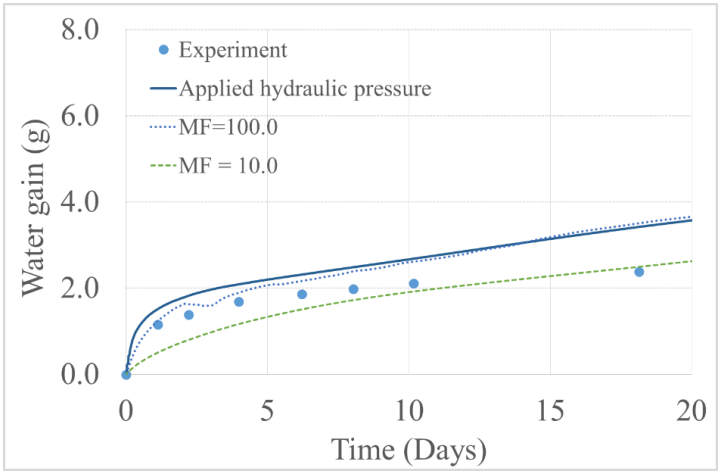

Figure 4-27 Experiment and analysis for water ingression (OPC W/C 50%).

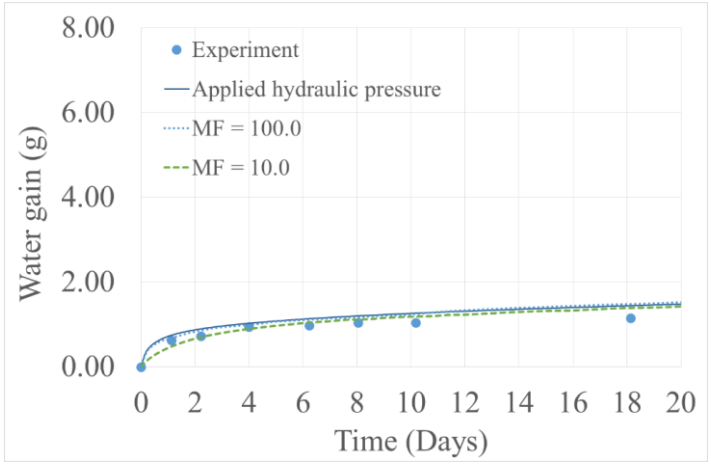

Figure 4-28 Experiment and analysis for water ingression (OPC W/C 40%).

From the results, when magnified factor (MF) equal to 100.0, the water penetrated (water gain) value at the initial state is close to applied hydraulic pressure case and close to experimental results. However, in W/C 0.50 case, when submerged time is increased, analysis results tend to be higher than

experimental results. On the other hand, as discussed in section 4.2.3, rainfall mostly take place for a few hrs. Therefore, it can be inferred that the proposed model, with the MF, can be used to predict water ingression for short periods.

4.3.2. Airborne Chloride Ingression

Section 4.2.1 verified the proposed model by using the data from Ishikawa T. (2012) [3]. The verification showed that the proposed model can be used to predict the amount of chloride penetration in the specimen. However, in the test, the specimens were placed in an oven at 105^{o}C before exposure to accelerate the chloride absorption rate. Such conditions do not, which make the condition in the test was not matched with the real exposure conditions.

Moreover, in the previous experiment, airborne chloride intensity was measured before the chloride penetration test, but, due to the limitation of the equipment, the amount of airborne chloride at each position inside the wind tunnel was not consistent (presented in detail in Appendix I). Thus, the airborne chloride measurement method should be modified.

Additionally, chloride distribution inside the specimen has not been verified. Therefore, an additional test was conducted to confirm that the proposed model can be used to predict both the total airborne chloride ingression and chloride distribution. The differences between previous research and the new proposed experimental method are shown in Table 4-4

.

Table 4-4 Differences between testing methods.

Detail	***Ishikawa T. (2012)***	***Proposed****
Airborne chloride measurement method	Gauze and cotton	Gauze and cotton
Airborne chloride measurement duration*	Measure airborne chloride before mortar specimen exposure/ 4–8 hrs	Measure airborne chloride at the same time as the chloride penetration test/ 1 month
Mortar specimen curing method	Seal curing, 7 days	Air curing, seal curing, and water curing, 28 days
Mortar specimen condition before exposure	Specimen placed in oven (105 ^{o}C) for 2 days	Specimen placed in control room at RH 60, 20 ^{o}C for 28 days
Mortar specimen size	Ø 5 cm, height 5cm	Ø 5 cm, height 10 cm
Exposure duration	7–50 days	50–60 days

**details in appendix I*

The following list details the testing method.

1) <u>Experimental methodology</u>

- <u>Specimen preparation</u>

Mortar specimens, size Ø 5cm x 10 cm, using OPC Type I, were prepared. Mix proportions are shown in Table 4-5

.

Table 4-5 Mix proportions for wind tunnel experiment.

Mix	W/C	Cement (kg/m^3)	Sand (kg/m^3)	Water (kg/m^3)
N40	0.40	675	1340	270
N55	0.55	545	1396	300

Specimens were cured under water, seal, and air conditions for 30 days. After curing, each specimen was dried in the environmental control room (temperature = 20°C, RH = 60%) for 30 days. After drying, the exposure surface was grinded out 1–2 mm with a surface grinding machine to control the quality of the surface and decrease the bleeding effect on the surface.

The grinded specimens were coated with epoxy with the exception of the exposure surface. Figure 4-29 shows coated specimens used in the experiment.

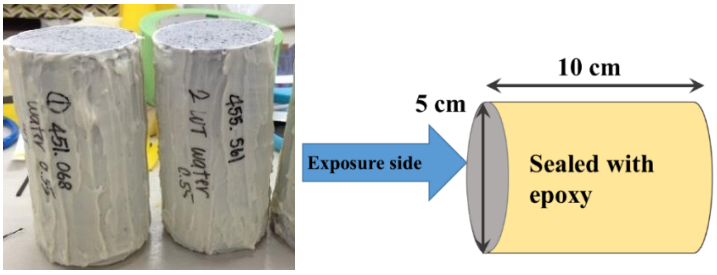

Figure 4-29 Mortar specimen in exposure test.

- Specimen exposure

To determine the amount of airborne salt at the same time as chloride penetration into the specimen, exposure specimens were prepared and installed at various positions.

Mortar specimens coated with epoxy were placed in the middle of a 10 cm diameter mold. In the outer area, gauze and cotton were placed to capture the airborne chloride at each position.

Between the mortar and cotton, a super absorbent polymer (Figure 4-30) was placed to prevent contamination between the mortar specimens and the

cotton. Exposure specimens used in the experiment are shown in Figure 4-32 and Figure 4-31.

After a given exposure period (50 days for W/C 0.55 and 60 days for W/C 0.40), gauze and cotton samples at each position were submerged in pure water to determine the amount of chloride with a titration test.

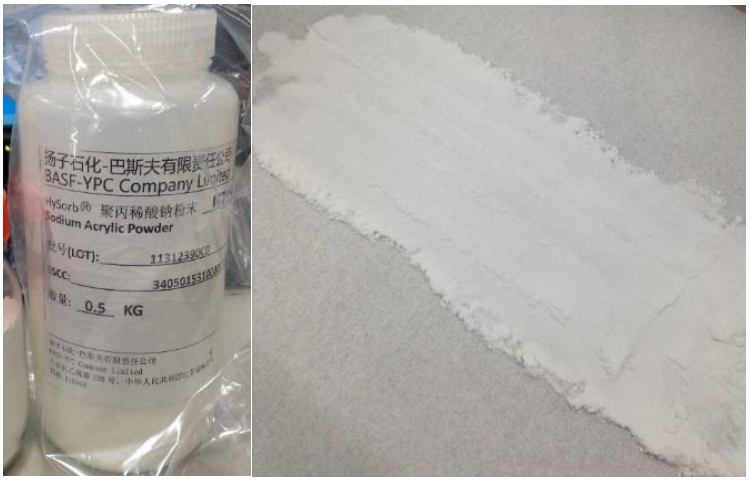

Figure 4-30 Super absorbent polymer (BASF-YPC, Sodium acrylic powder).

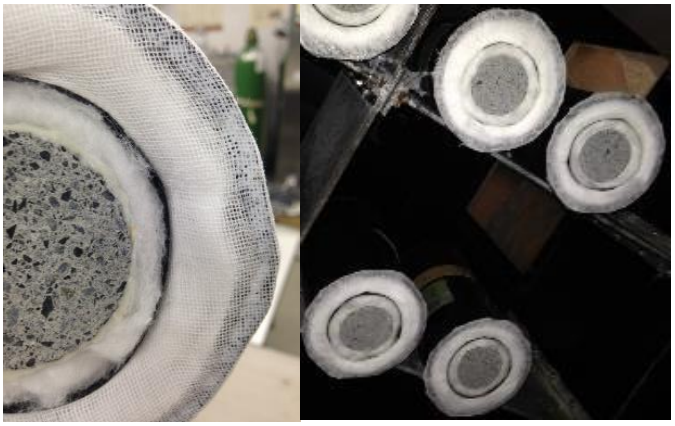

Figure 4-31 Exposure specimens in test.

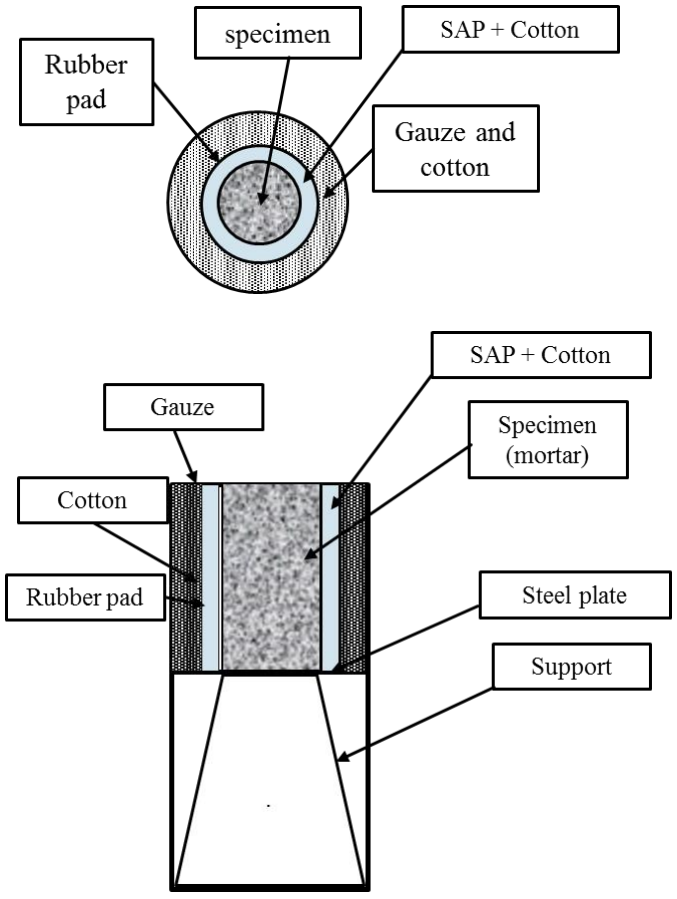

Figure 4-32 Exposure specimen diagram.

- Exposure positions

Exposure positions are the position which airborne chloride flux is consistent, determined by the trial test (details described in Appendix I). Exposure positions are shown in Figure 4-33.

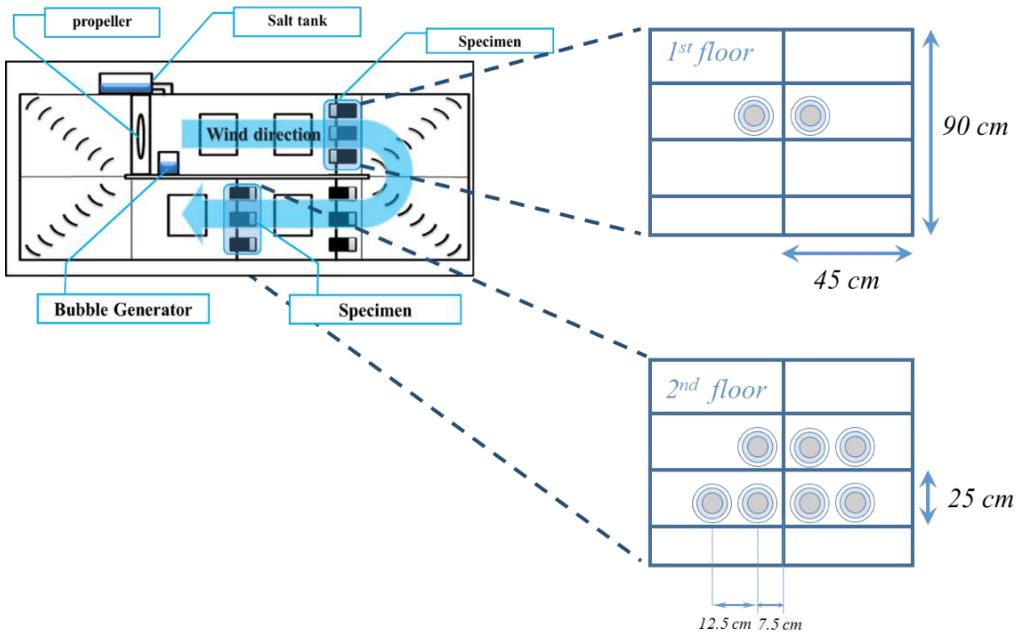

Figure 4-33 Specimen positions.

- Relative humidity measurement

During the test, RH at each position was checked with equipment shown in Figure 4-34. The RH inside the chamber during the test was 89–92%.

Figure 4-34 Relative humidity measurement.

- Measurement of chloride in concrete

After exposure, specimens were removed from the wind tunnel and the chloride content of each specimen was measured. A powder sample was taken by drilling holes into the specimen at intervals of 2–30 mm. Drilling depth and equipment are shown in Figure 4-35 and Figure 4-36, respectively.

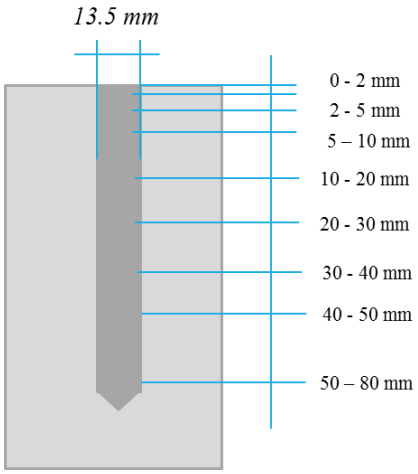

Figure 4-35 Drilling depth.

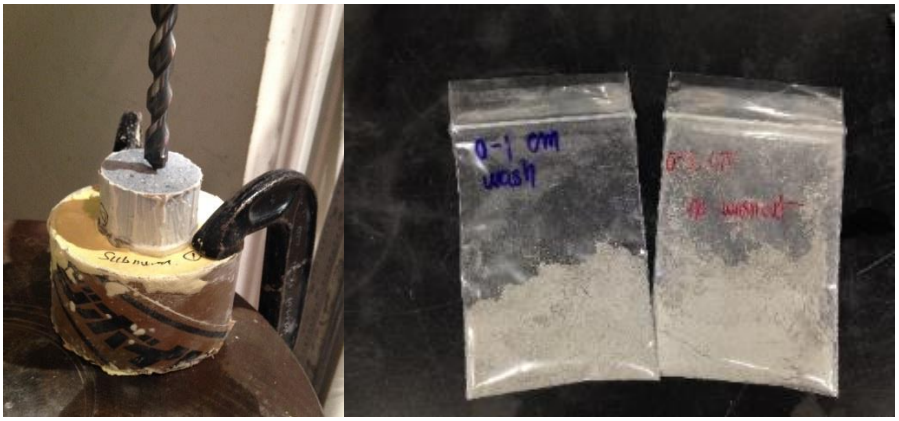

Figure 4-36 Drilling machine and powder specimen for titration.

2) <u>Experimental results and model verification</u>

The experiment showed the flux of airborne chloride ions inside the wind tunnel was between 0.53 and 1.19 mdh (mg/dm^2/hr) depending on the position. The amount of airborne chloride and relative humidity are shown as in Figure 4-37 and Figure 4-38.

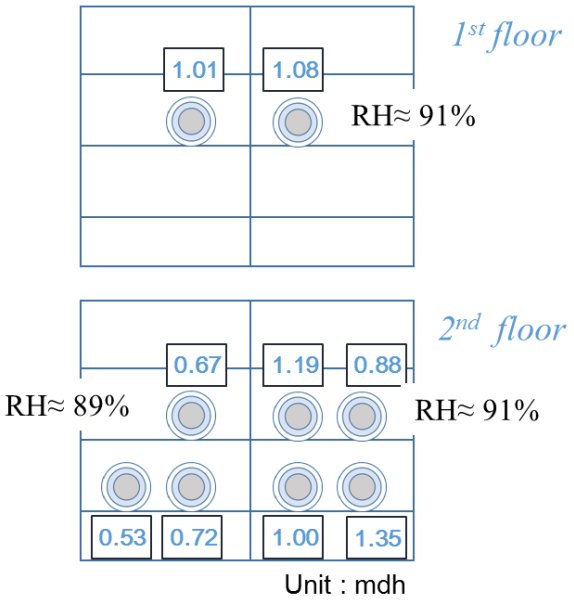

**the specimen on 1st floor was used in trial test.*

Figure 4-37 Chloride ion intensity at each position (For Specimen W/C 0.55).

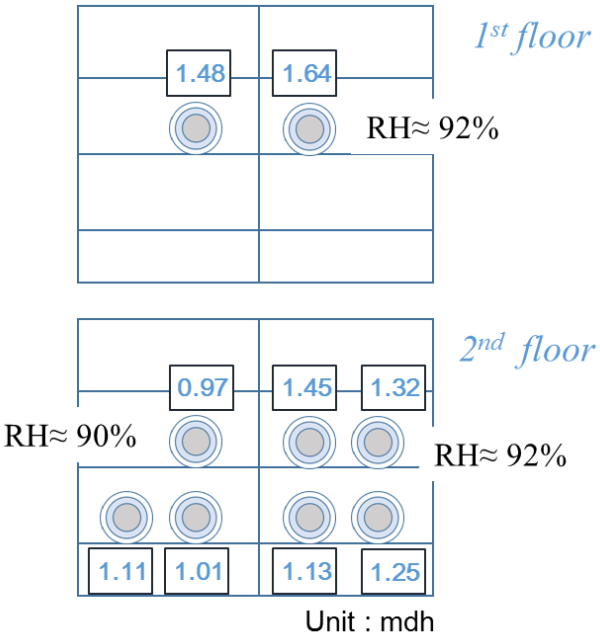

Figure 4-38 Chloride ion intensity at each position (For Specimen W/C 0.40).

During the test, the surface of the specimen is getting wet by airborne chloride flux, as shown in the following figure.

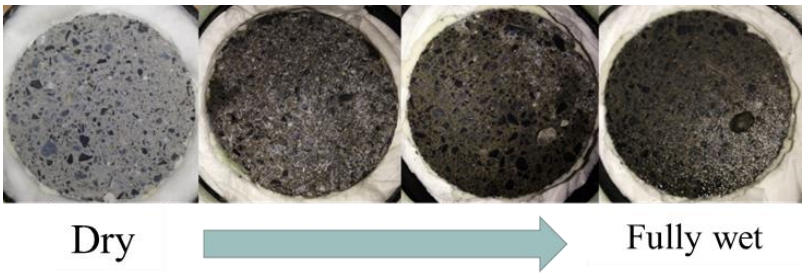

Figure 4-39 Specimen surface after exposure.

The experimental and analytical results of chloride penetration are shown in Figures 4-40–4-45.

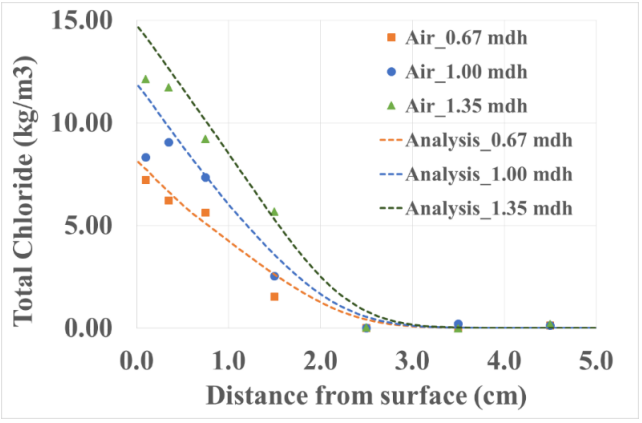

Figure 4-40 Total chloride distribution, W/C 0.55, air curing.

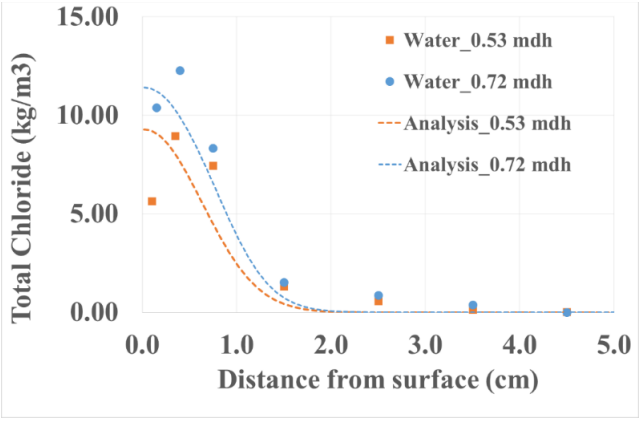

Figure 4-41 Total chloride distribution, W/C 0.55, water curing.

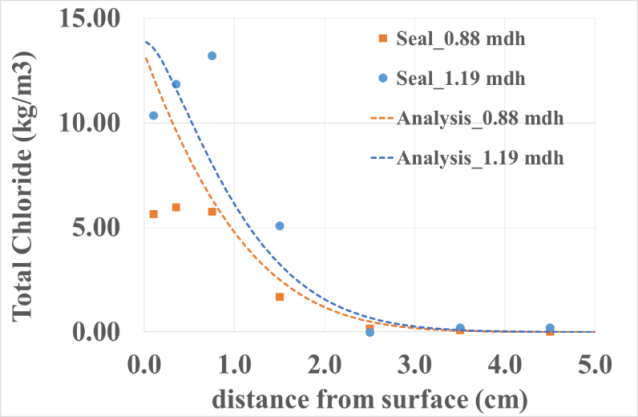

Figure 4-42 Total chloride distribution, W/C 0.55, seal curing.

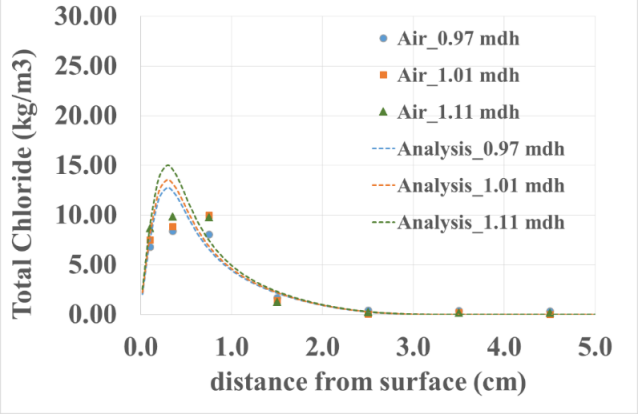

Figure 4-43 Total chloride distribution, W/C 0.40, air curing.

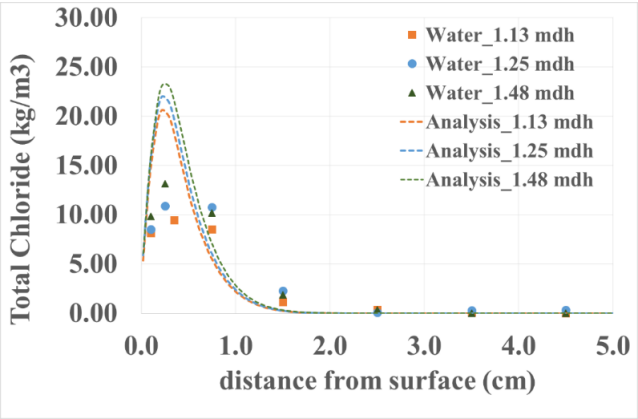

Figure 4-44 Total chloride distribution, W/C 0.40, water curing.

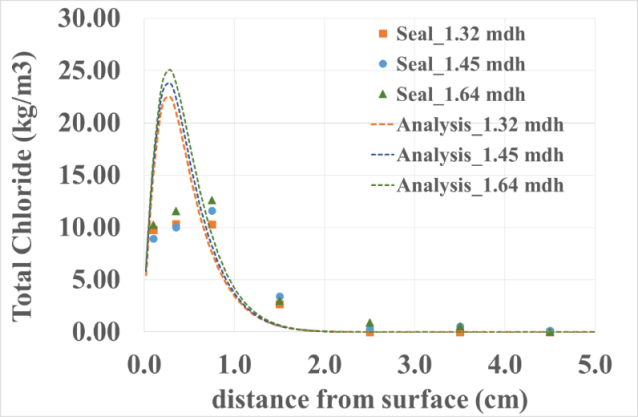

Figure 4-45 Total chloride distribution, W/C 0.40, seal curing.

From the results, the specimen with W/C 0.55, the experimental results show clear difference of chloride distribution when the chloride flux is changed, especially under air curing conditions. On the contrary, for the specimen with W/C 0.40, when the chloride flux is increased, the chloride distribution did not change significantly.

Moreover, the curing method also effects the total chloride distribution. Figure 4-46 shows total chloride distribution in the W/C 0.55 specimen. When the specimen was treated under water curing conditions, although the airborne chloride intensity is higher, the chloride can penetrate into deeper parts more than the air curing specimen, but chloride will accumulate on the specimen's surface.

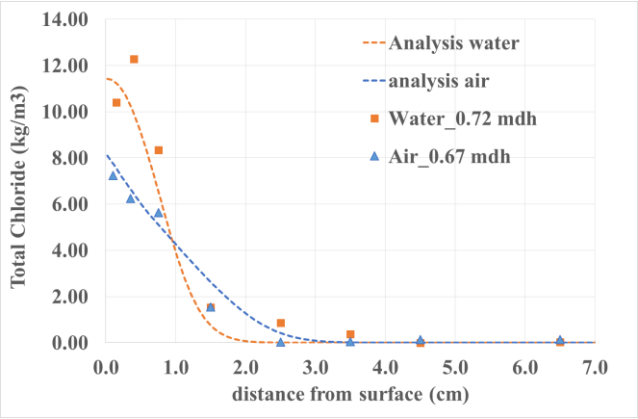

Figure 4-46 Total chloride distribution, W/C 0.55, air and water curing.

Moreover, the chloride profile also differs according to W/C. The experimental results showed that, for W/C 0.50, the total chloride amount at 1.5 cm tended to be higher than for W/C 0.40. On the other hand, for W/C 0.40, the chloride accumulated on the concrete surface but did not penetrate the concrete. The s also showed high chloride concentration on the surface, however, the analysis results are overestimated experimental results for water curing and seal curing with W/C 0.40.

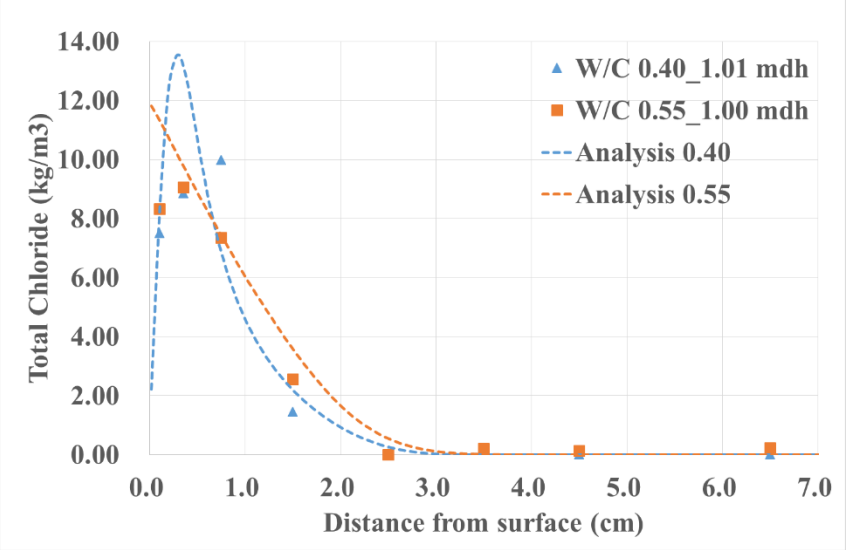

Figure 4-47 Total chloride distribution, W/C 0.55 and 0.40 (air curing).

From the results, the proposed model can be used to calculate chloride distribution under the different level of airborne chloride intensity and different materials properties. However, in low W/C, the proposed model overestimated results. Therefore, a model modification and additional tests are necessary.

4.3.3. Washout effect

Previous research reported that the chloride concentration on concrete structures decreases due to rainfall [13] and chloride inside concrete can be reduced after exposure to pure water for long periods of time [5].

To verify the proposed model and to check the washout mechanism, a washout experiment was conducted. In the experiment, tap water was used to wash specimens' surfaces to reduce the chloride concentration on the surface to 0.

1) Experimental method

- **Specimen preparation**

In the experiment, a water-to-cement ratio (W/C) of 40% and 55% mortar specimens were prepared. After casting, the specimens were kept in an environmental control room for 60 days to reduce the moisture content and submerged in 3% salt water for 90 days. The mix proportions are shown in Table 4-6.

Table 4-6 Mix proportions for washout experiment.

Mix	W/C	Cement (kg/m^3)	Sand (kg/m^3)	Water (kg/m^3)
N40	0.40	675	1340	270
N55	0.55	545	1396	300

- **Testing method**

After submersion in salt water, specimens were put on a slope of 30^o and washed with tap water for 6 and 60 days. The flow of tap water was maintained throughout the test to reduce the chloride concentration on the surface to 0. The testing method is shown in Figure 4-48

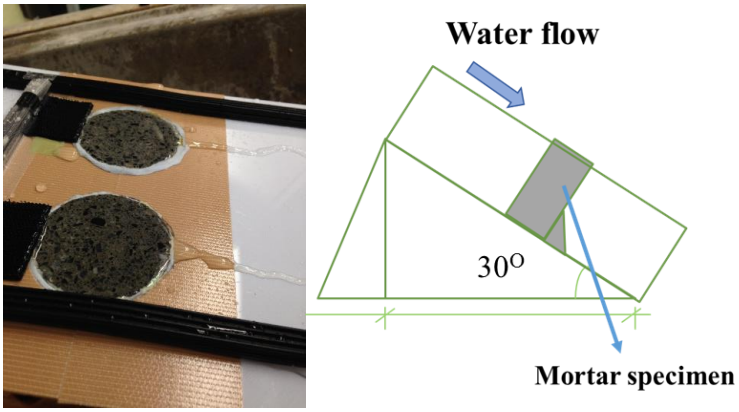

Figure 4-48 Washout experiment.

The speed of water flow used in the experiment was equal to 73 mL/min (equal to rainfall of 5 mm/hr). To check the water flow, a beaker was placed under the slope and the amount of water that flowed over the specimen's surface was measured.

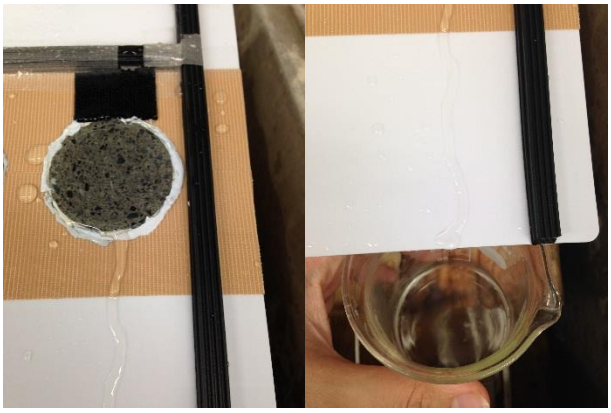

Figure 4-49 Determining water flow.

After the washout test, specimens were taken off the slope and the chloride content in the specimen was measured. A powder sample was taken by drilling into the specimens at 2–30 mm intervals. The drilling depth and drilling equipment are shown in Figure 4-35 and Figure 4-36.

2) Experimental results and model verification

The experiment shows that after being washed with tap water the chloride inside the specimen was significantly reduced by the washout effect. The experimental and analysis results of chloride distribution are shown in Figure 4-50 and Figure 4-51.

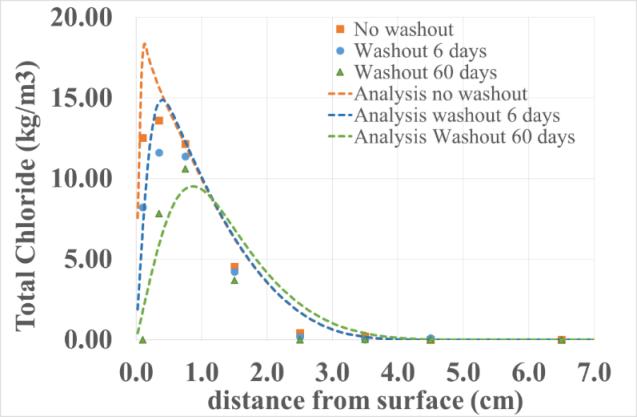

Figure 4-50 Total chloride after washout testing (W/C 0.40).

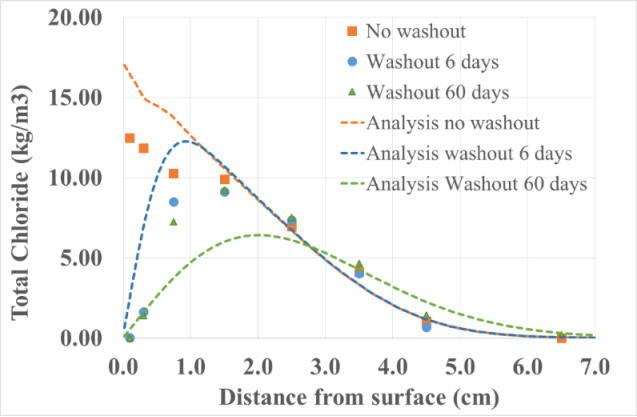

Figure 4-51 Total chloride after washout testing (W/C 0.55).

The results of the 6-day surface washout suggest the proposed model can calculate the reduction of chloride penetration from the washout effect. However, for W/C 0.55, at 0.75–1.5 cm, the prediction from proposed model underestimates the result. This may be because the model overestimates the amount of chloride washout. In the calculation, after long exposures, fixed chloride can be removed with water due to the chloride concentration gradient between the surface and inside the specimen.

In the actual condition, it has been reported that chloride inside cement paste cannot be washed out until there is no chloride inside because fixed chloride inside cannot be washed [5]. However, with the proposed model, if the washout effect occurs for a long time, the chloride inside the specimen will reduce until it is close to 0, as shown in Figure 4-52.

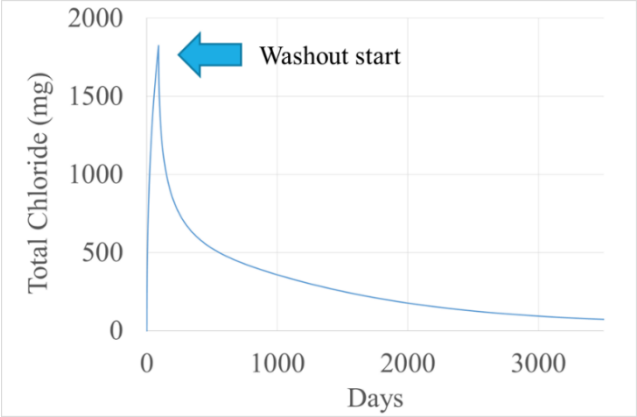

Figure 4-52 Model results when washout effect occurs for a long time (sensitivity analysis with W/C 0.50).

In the calculation, the bound chloride (or fixed chloride) inside the specimen can diffuse out from the specimen due to different gradients of chloride concentration. As discussed, recorded data (Table 4-1) suggests rainfall typically occurs for only a few hrs. Therefore, it can be concluded that the proposed model can be used to predict chloride reduction for a short period.

4.4. Verification with Onsite Measurement Data

The previous section verified the proposed model with experimental results. However, each experiment was tested under controlled conditions. To confirm that the proposed model can be used in actual situation, onsite measurement data from previous research is used for verification.

4.4.1. Model Inputs

To calculate chloride ingression under actual environmental conditions, airborne chloride and rainfall intensity data are needed. In the calculation, the amount of airborne chloride and rainfall must be converted to the water flux (Q_{air_water}), given as an input for the analysis. When concrete is attached to airborne chloride, the water flux (Q_{air_water}) can be calculated from the amount of chloride from recorded by airborne chloride capture equipment [1] with

$$Q_{air\_water} = \frac{Q_{ABS} \times \rho_w}{M_{cl} \times 0.51 \times 1000}, \quad (4\text{-}3)$$

where Q_{ABS} is the amount of airborne chloride (chloride ion) from the observation (kg/m^2.s), ρ_w is the density of water (kg/m^3), M_{cl} is the molecular weight

of chloride, (35.45×10^{-3} kg/mol), and 0.51 is the concentration of chloride in the water particle (mol/l).

When the structure attach to the heavy rainfall and the amount of the water is large enough to produce washout effect, only pure water from rainfall will attach to the concrete surface. Under this condition, the chloride concentration on concrete surface is 0. The value of Q_{air_water} (kg/m^2.s) can be calculated as

$$Q_{air\_water} = \frac{X \times 10^{-3} \times \rho_w}{60 \times 60}, \quad (4\text{-}4)$$

where X is the precipitation value (mm/hr).

4.4.2. Model Assumptions

Past research has been reported that rainfall particles can remove chloride particles from the atmosphere [14]. Furthermore, past observations showed that when specimens exposed to low intensity rainfall (light rain), some rainfall particles contacted the concrete surface and absorbed into concrete but the amount of the water is not large enough to wash the concrete surface. In this case, no washout effect occurs, as shown in Figure 4-53. However, in reality, it is difficult to determine the largest precipitation value that covers a concrete surface and produces the washout effect.

Figure 4-53 Concrete specimen under light rainfall (1-3 mm/hr).

Therefore, to define the *washout point*, or, the point at which rainfall is large enough to create the washout effect, a sensitivity analysis was conducted. The assumptions for the analysis can be divided into three aspects to simulate chloride ingression behavior more realistic manner. The assumptions for the analysis are detailed as follows.

1) <u>Airborne chloride condition (no rainfall)</u>

When there is no rainfall, only airborne chloride can attach to the concrete surface and chloride ions will gradually ingress into the concrete, as shown in Figure 4-54 . The water flux (Qair_water) can be calculate with equation 4-3.

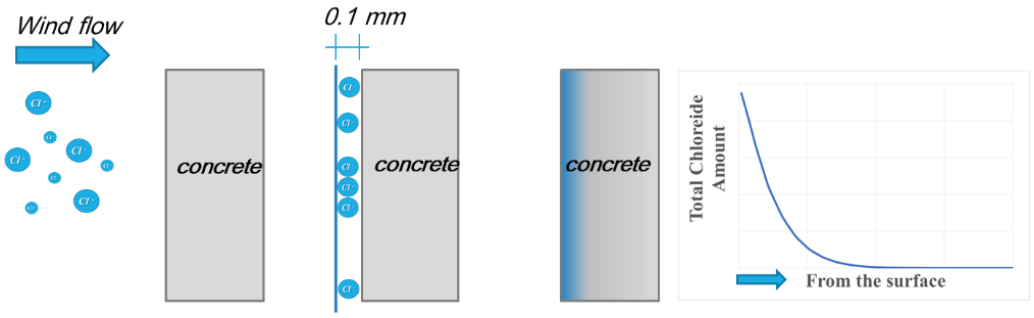

Figure 4-54 Concrete under airborne chloride condition.

2) <u>Light rain (rainfall greater than 1 mm/hr)</u>

The calculation assumes that airborne chloride particles can be blocked by rainfall particles. Therefore the calculation assumes that when the rainfall is greater than 1 mm/hr, but less than the *washout point*, only pure water particles (chloride concentration = 0) can attach to the concrete surface. The amount of water is equal to the amount of water from airborne chloride (equation 4-3). In this step, the water transmission in concrete is close to a humid environment. The washout effect will not occur, but the chloride on the concrete surface is reduced because pure water particles attach to the concrete surface and no chloride ions are in the environment. The pure water particle can reduce the chloride concentration on the concrete surface, as shown in Figure 4-55.

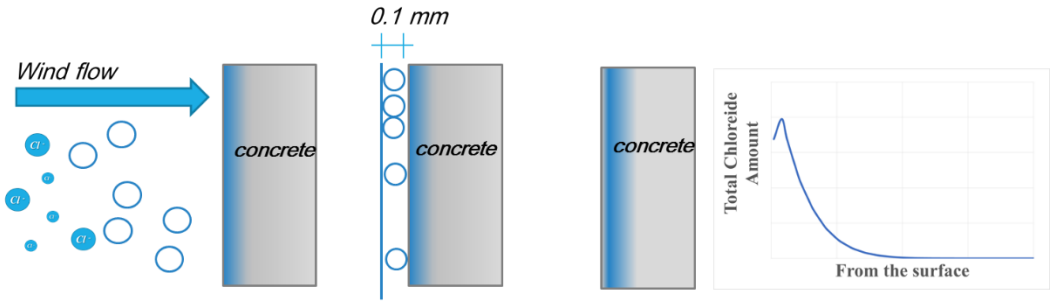

Figure 4-55 Concrete during light rain.

3) Heavy rain (rainfall is equal to washout point)

When a concrete structure is exposed to heavy rainfall and the amount of water is large enough to produce the washout effect (washout point), only pure water from the rainfall will attach to the concrete surface, as shown in Figure 4-56. At this point, the chloride concentration on the concrete surface becomes 0. The value of Q_{air_water} ($kg/m^2.s$) can be calculated with equation 4-4.

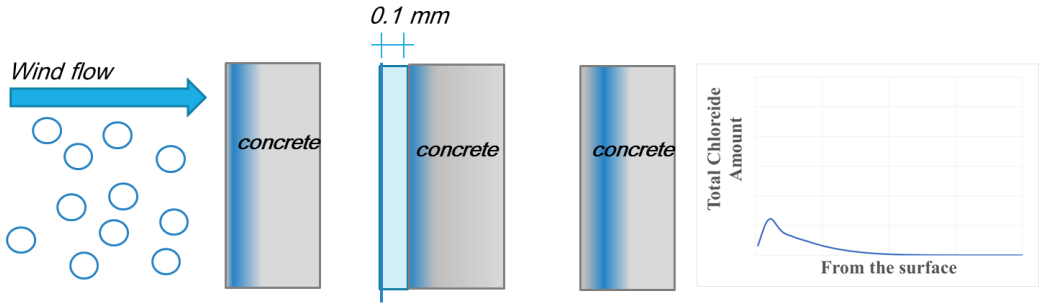

Figure 4-56 Concrete during heavy rain.

To find the appropriate amount of rainfall for the washout calculation, testing data from the PWRI was used [15]. The exposure test used data from between December 10, 1984 and December, 9 1987 in Japan to investigate the amount of airborne chloride and chloride penetration in concrete. The amount of airborne chloride was collected by the tank captured method. Besides the tank, a mortar specimen of the size $10\times10\times10$ cm^3 with a W/C of 57.8% was used to determine the chloride ingression.

For the sensitivity analysis, testing data from close to Shinanokawa River, Niigata prefecture was selected. The RH, temperature, and rainfall intensity/hr were taken from the AMEDAS database at Niigata station. Moreover, it is assumed that when the temperature is lower than 3 ^oC, the precipitation in the AMEDAS database is snow [16, 17]. In cases of snowfall, it is assumed that there is no washout effect and chloride ions can attached to the concrete surface. The analysis was conducted by assuming that the washout effect will occur when the rainfall intensity is equal to 1, 3, and 5 mm/hr.

The sensitivity analysis results are shown in Figure 4-57.

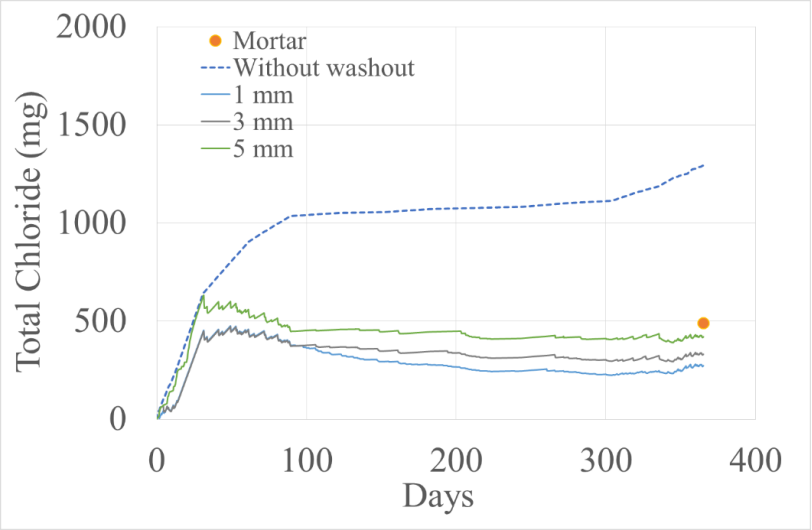

Figure 4-57 Sensitivity analysis for determining the washout point.

The orange dot in the graph in Figure 4-57 is the amount of the total chloride inside the specimen after exposure to airborne chloride conditions for 1 year. Figure 4-57, it can be inferred that when the rainfall intensity is equal to or exceeds 5.0 mm, the washout effect should be taken into account for the calculation. The calculation assumptions can be determined with Figure 4-58.

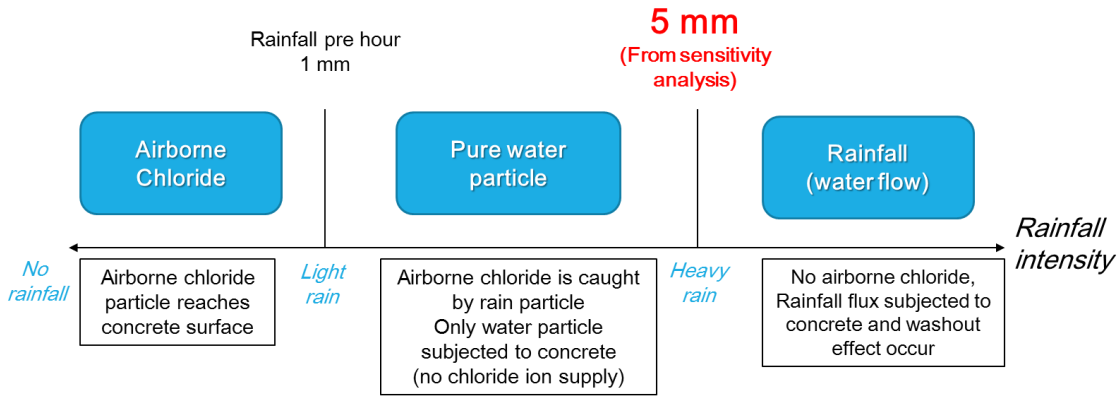

Figure 4-58 Diagram for washout calculation.

The flow of the calculation of airborne chloride penetration into concrete structures under actual environmental condition, after the inclusion of all modifications and assumptions, is shown in Figure 4-59.

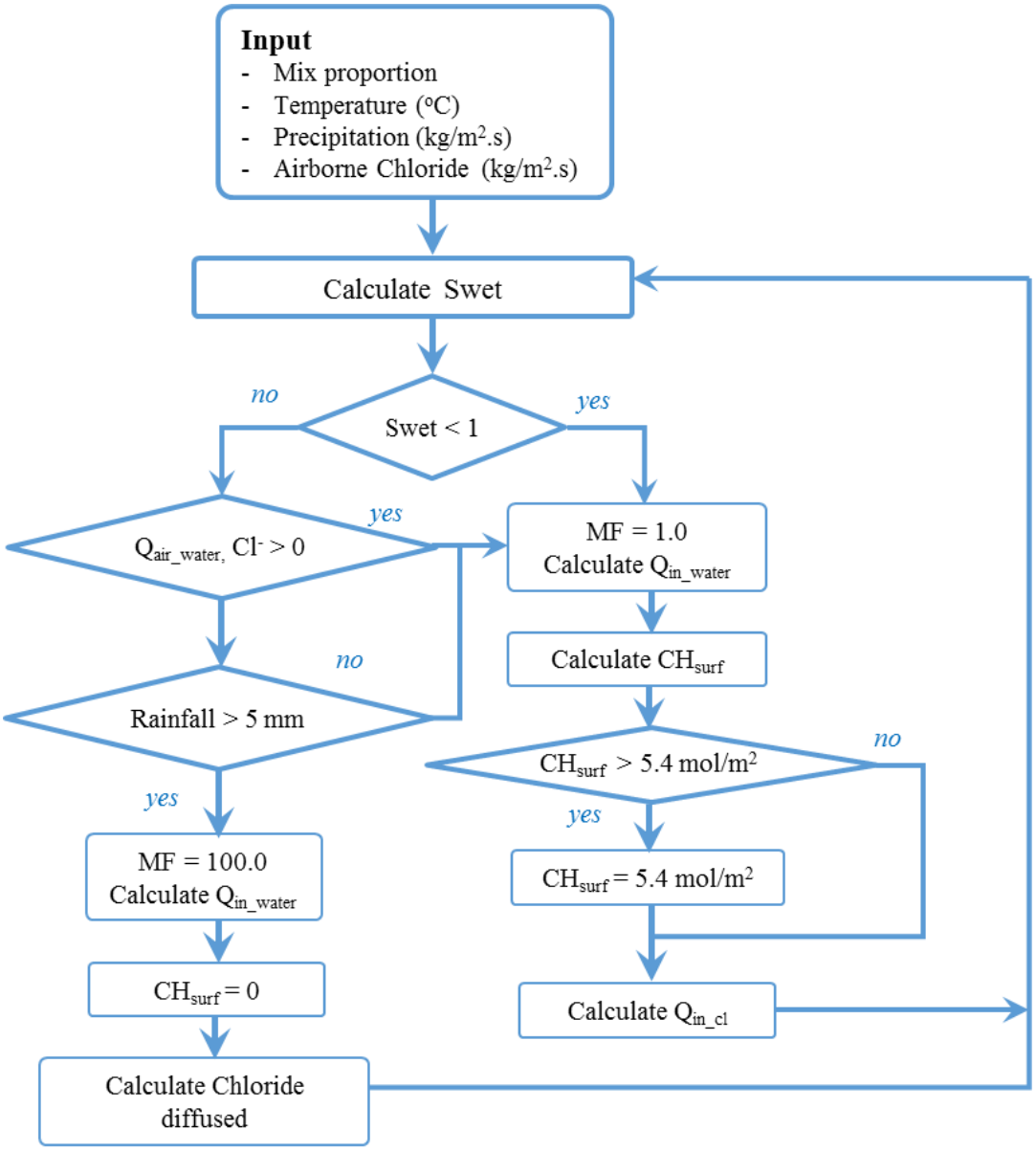

Figure 4-59 Airborne chloride model calculation.

4.4.3. Verification Results

Using the preceding assumptions, verifications with onsite measurement data were conducted. Onsite measurement data were taken from the various research papers. The verifications were done by using the airborne chloride data from different collection methods, detailed as follows.

4.4.3.1. Verification of total chloride penetration with tank collection method in Japan (PWRI; 1984 - 1987) [15]

The first verification used data from experiments conducted by the PWRI between December 10, 1984 and December 9, 1987 in Japan to investigate the amount of airborne chloride and chloride penetration in various regions.

1) Airborne chloride capture method

A tank sample method was used to collect airborne chloride. The amount of airborne chloride was checked every month during the testing period.

Figure 4-60 PWRI airborne chloride capture equipment.

2) Specimen preparation

For the exposure test, test specimens of the size 10×10×10 cm^3 were prepared. Each specimen was placed near the airborne chloride capture equipment. In the experiment, three types of the specimens were used: mortar, normal concrete, and pre-stressed concrete.

The mix proportion and specimen shape are shown in Table 4-7 and Figure 4-61, respectively.

Table 4-7 The PWRI mix proportion for exposure tests.

Mix	W/C	Cement (kg)	Water (kg)	Sand (kg)	Gravel (kg)	% Air
RC	58.4	293	171.2	874	959	5.2
PC	39.0	450	175.7	705	987	4.9
Mortar	57.8	351	203	1681	0	2.3

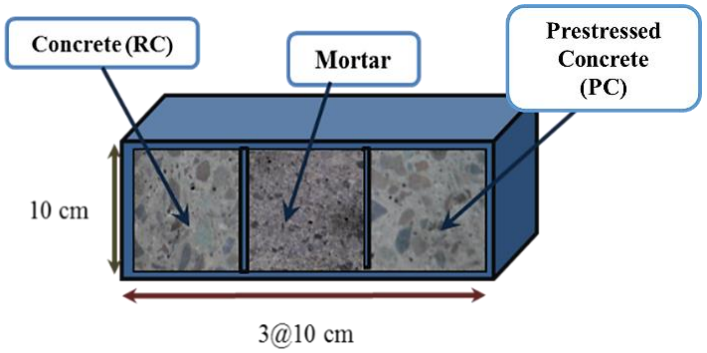

Figure 4-61 The PWRI test specimens (modified from PWRI report) [15].

3) Exposure site

The amount of airborne chloride at each position changes due to wind direction, wind speed, obstacles, and the distance from the seashore [3, 18]. Thus, the amount of airborne chloride for each region and during different seasons differs.

Figure 4-62 and Figure 4-63 show examples of the airborne chloride intensity at Nagaegawa Bridge and Omori Bridge. The chloride intensities at these two positions are different.

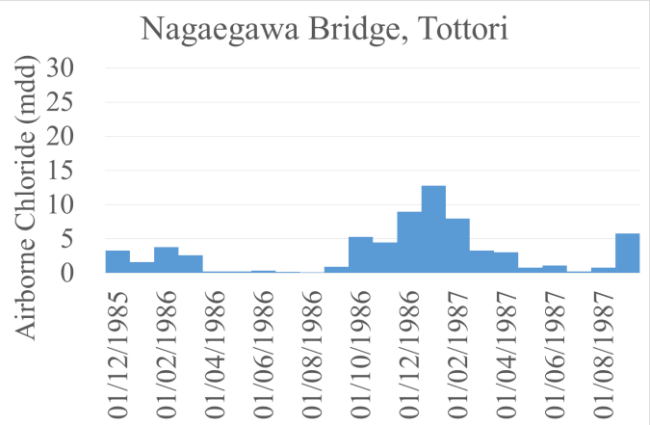

Figure 4-62 Amount of airborne chloride at Nagaegawa bridge, Tottori Prefecture, Japan.

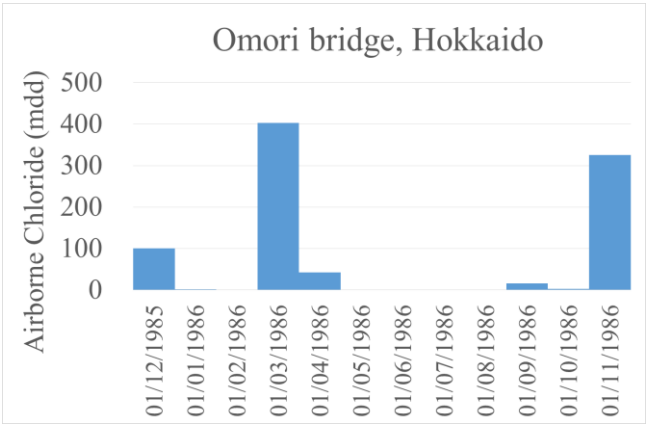

Figure 4-63 Amount of airborne chloride at Omori bridge, Hokkaido Prefecture, Japan.

Furthermore, in Japan, the climate condition varies from subarctic in the north to subtropical in the south. For example, in Okinawa (the southern part of Japan), the temperature is above 20 ^{o}C and the RH is high year round. Meanwhile, in Hokkaido (the northern part of Japan), the temperature is low in the winter and the region experience intense periods of snow. Therefore, for the verification, experimental data was selected around Japan for both Japan Sea and the the Pacific Ocean.

Figure 4-64 shows the exposure locations that selected for the model verification.

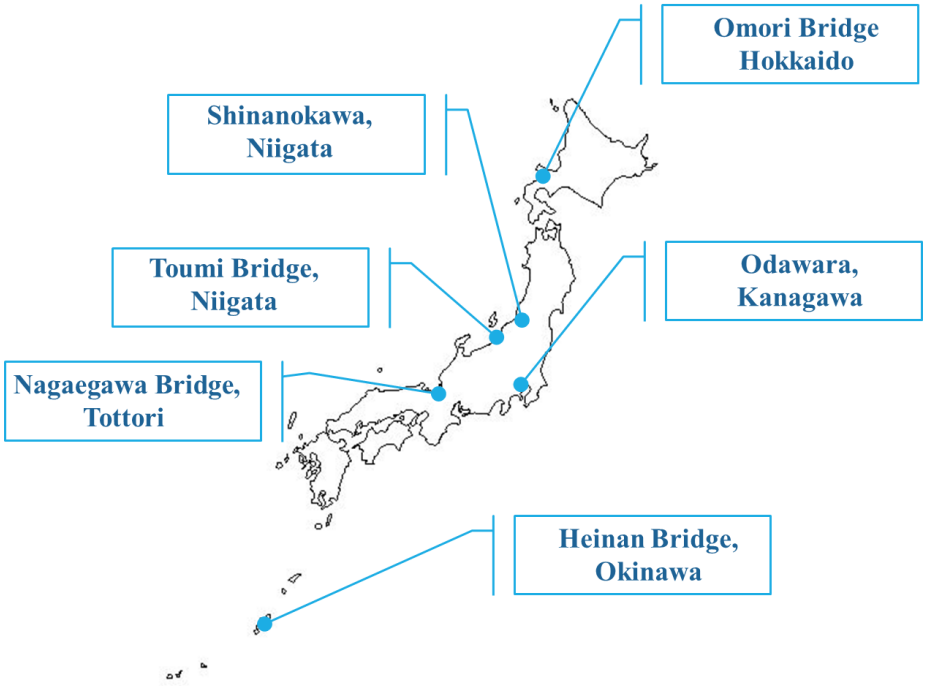

Figure 4-64 Exposure sites in Japan (exposure tested by PWRI).

4) <u>Environmental data</u>

Temperature, RH, and precipitation data received from AMEDAS were used for the analysis.

Data used in the analysis was the recoded data/hr. Each set of data was picked up from the station nearest to the exposure position. The station names are shown in the Table 4-8.

Table 4-8 Stations of AMEDAS for recorded data.

Location	**Station name**		
	Temperature (^oC)	*Relative Humidity (%)*	*Precipitation (mm/hr)*
Shinanokawa	Niigata	Niigata	Niigata
Toumi Bridge	Itoigawa	Takada	Itoigawa
Odawara	Odawara	Yokohama	Odawara
Omori Bridge	Suttsu	Suttsu	Suttsu
Nagaegawa bridge	Tottori	Tottori	Tottori
Heinan Bridge	Nago	Nago	Nago

5) <u>Experimental results and model verification (mortar specimen)</u>

The total chloride penetration into the mortar specimens was calculated with the proposed model. The results of the analysis and the experiment at each position are shown in Figure 4-65–4-70.

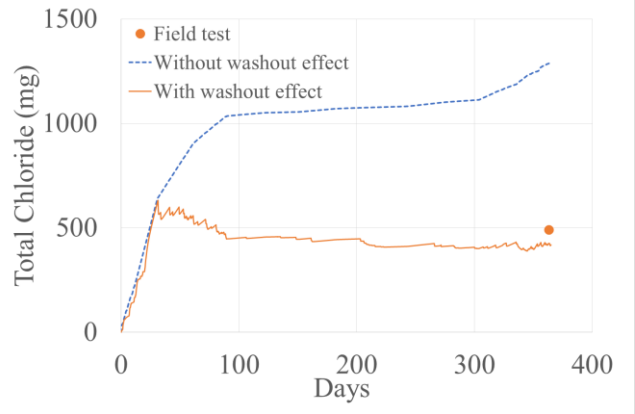

Figure 4-65 Total chloride penetration at Shinanokawa, Niigata Prefecture, Japan.

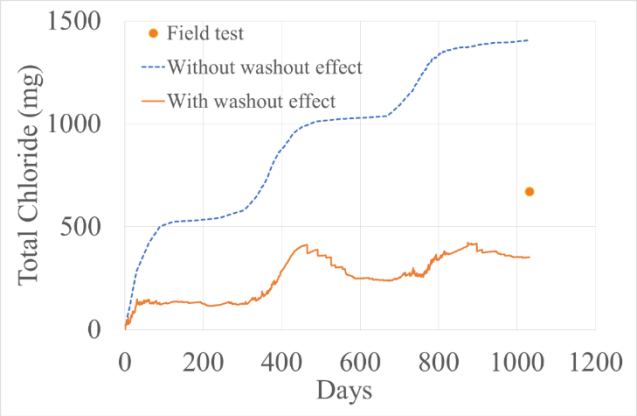

Figure 4-66 Total chloride penetration at Toumi, Niigata Prefecture, Japan.

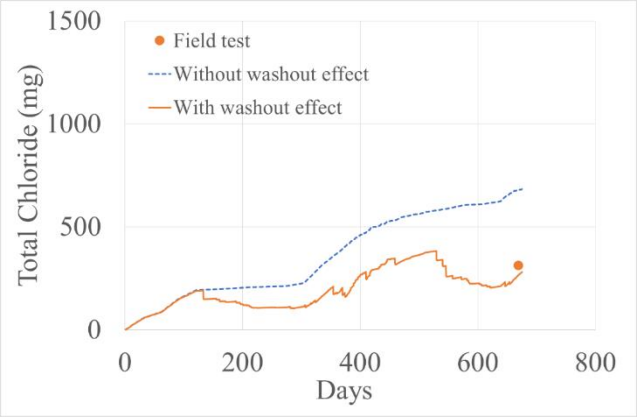

Figure 4-67 Total chloride penetration at Tottori Prefecture, Japan.

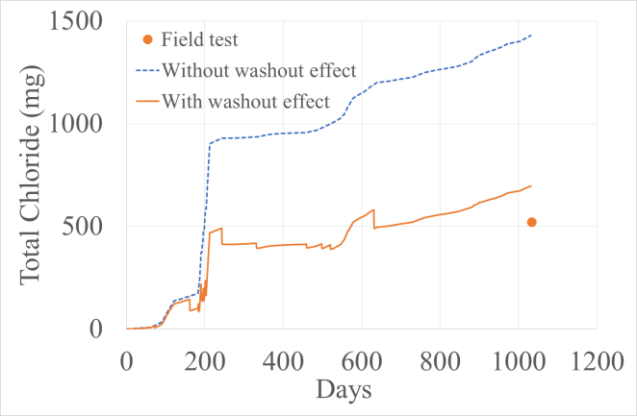

Figure 4-68 Total chloride penetration at Odawara, Kanagawa Prefecture, Japan.

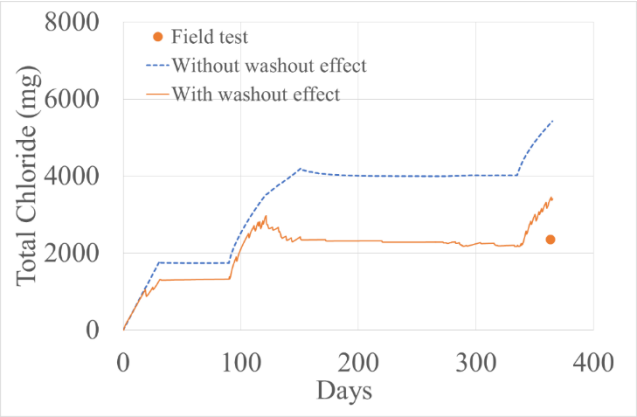

Figure 4-69 Total chloride penetration at Omori Bridge, Hokkaido Prefecture, Japan.

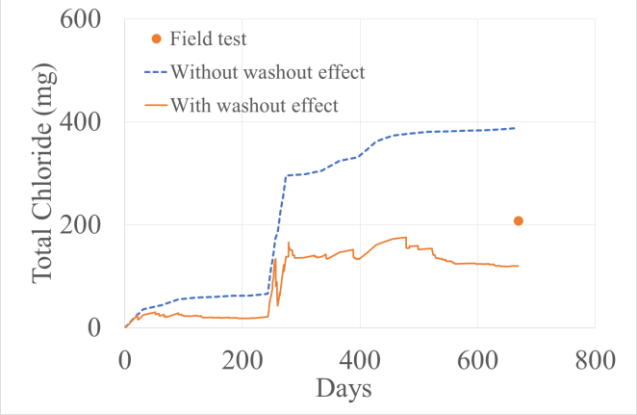

Figure 4-70 Total chloride penetration at Heinan Bridge, Okinawa Prefecture, Japan.

6) Experimental results and model verification (different mix design)

The proposed model as also used to verify the total chloride penetration into specimens with a different mix design, shown in Figure 4-71 and Figure 4-72.

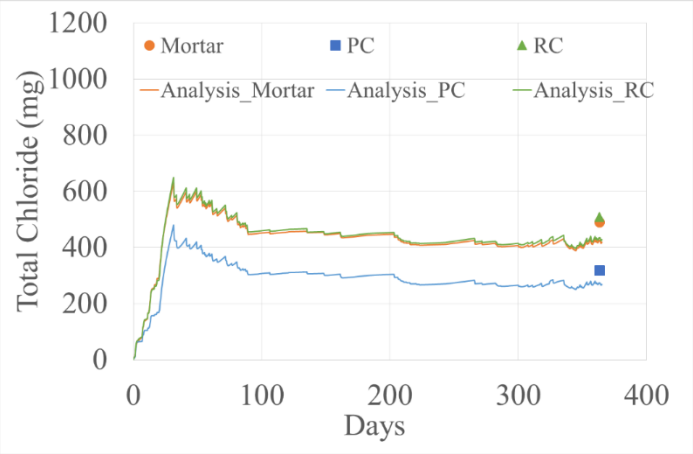

Figure 4-71 Total chloride penetration at Shinanokawa, Niigata Prefecture, Japan (comparison with RC, PC, and mortar).

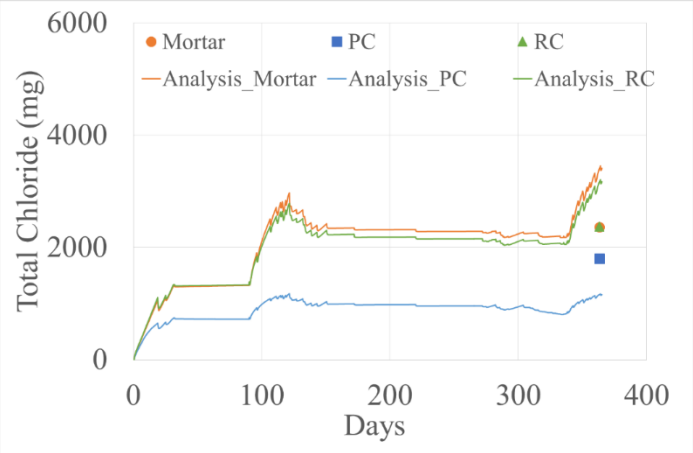

Figure 4-72 Total chloride penetration at Omori Bridge, Hokkaido Prefecture, Japan (comparison with RC, PC, and mortar).

7) Summary

Figure 4-65–4-72 show that, with the actual airborne chloride and metrological data, the proposed model can simulate the chloride penetration and washout effect for specimens under real-world environment conditions. The results show that the proposed model demonstrates a clear difference between chloride penetration under washout conditions and without washout conditions.

Furthermore, Figure 4-72 shows that with a low W/C concrete (pre-stressed concrete; PC), the amount of chloride penetration is lower than in RC. The results show the proposed model can calculate the amount of chloride penetration with different mix design and that results from the analysis have the same trends as experimental results.

The exposure test shows that the analysis underestimates and overestimates values when compared to experimental results. This may be because the methodological data received does not match the condition at the exposure positions. For an example, Figure 4-73 shows the AMEDAS environmental data station and the test location in Okinawa prefecture are in distinct locations. Otherwise, this misprediction may be due to the fact that the assumptions used in the proposed model do not correspond to the actual exposure conditions.

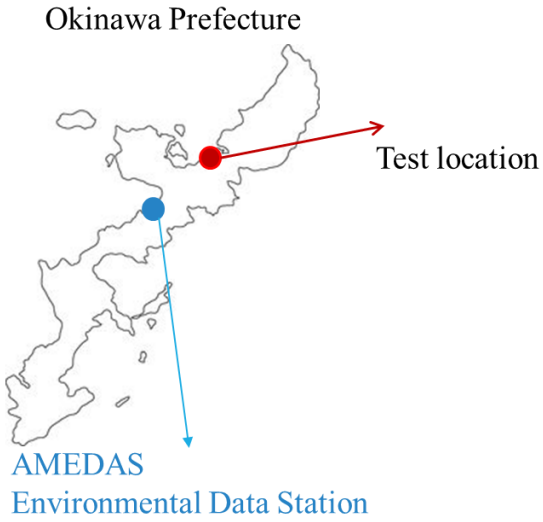

Figure 4-73 Testing and environmental data station location in the Okinawa prefecture, Japan.

4.4.3.2. Verification of chloride distribution with the tank collection method and mortar chip method (Koyanagi; 2014) [19].

This exposure experiment was started in 10 October 2014. For the test, 144 specimens were placed near the coastline. The objective of this exposure test is to

determine the amount of airborne chloride ingression for specimens under different curing condition. The expected exposure time is 10 years.

1) <u>Airborne chloride capture method</u>

In the experiment, the tank sample and mortar chip methods (chloride search [21]) were used to collect airborne chloride. The amount of airborne chloride was checked every month during the testing period (3 months). The airborne chloride collecting equipment is shown in Figure 4-75 and Figure 4-75.

Figure 4-74 Airborne chloride capture tank [19].

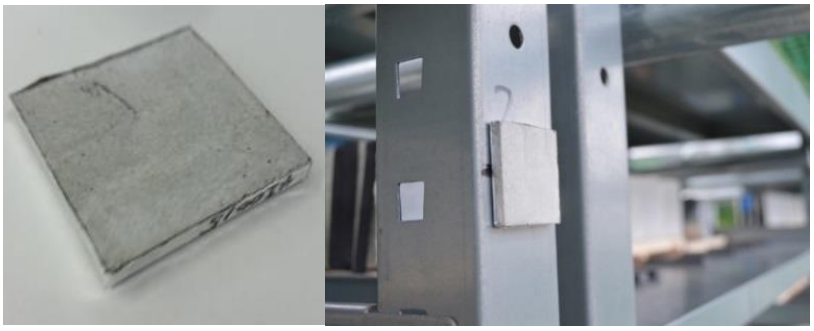

Figure 4-75 Mortar chip used in experiment [19].

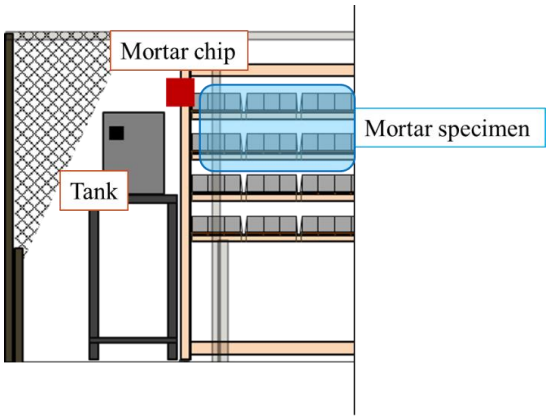

Figure 4-76 Diagram of the chloride capture equipment and mortar specimens [19].

The size of the mortar chip in this test was 40 x 40 mm^2 with a thickness of 5 mm. The amount of airborne chloride from the exposure test is shown in Table 4-9.

Table 4-9 Airborne chloride intensity (exposure site: Yamagata Prefecture).

Duration		**Amount of airborne chloride (NaCl; mdh)**	
from	*to*	*Tank sample*	*Mortar chip (Chloride search)*
10/10/2014	15/11/2014	0.076	0.584
15/11/2014	15/12/2014	0.981	1.396
15/12/2014	13/1/2015	1.679	1.247

2) <u>Specimen preparation</u>

Mortar test specimens of the size 10×10×10 cm^3 were prepared. After curing, each specimen was coated with epoxy and carried to the exposure site, as shown in Figure 4-77 . The mix proportion shown in Table 4-10.

Specimens were cured with different methods:

- Water curing 28 days
- Seal curing 7 days
- Sheet curing 28 days*
- Sheet curing 91 days*

*New curing method using polymer sheet for specimen covering to improve the quality of concrete surface [20]

Table 4-10 Mix proportion for exposure test.

Mix	W/B	Cement (kg)	Fly Ash (kg)	Water (kg)	Sand (kg)	% Air
OPC55	55	691	0	380	1000	2
FA55	55	575	101	372	1000	2

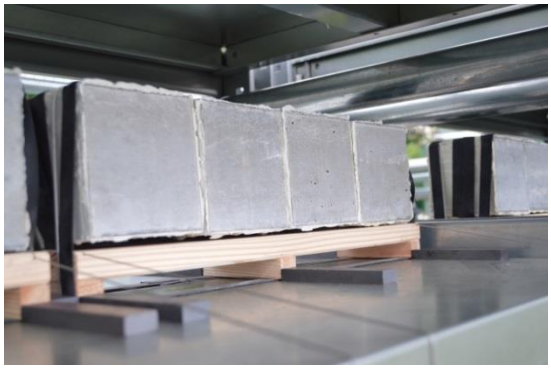

Figure 4-77 Exposure specimens.

3) <u>Exposure site</u>

The exposure site is in the Yamakata Prefecture, Japan. The exposure specimens are 150 m from the seashore (Figure 4-78).

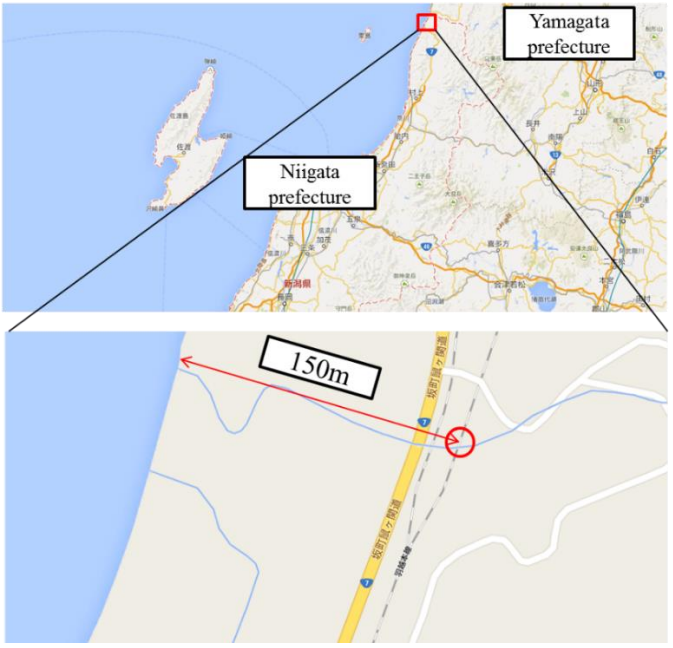

Figure 4-78 Testing location in Yamagata prefecture.

4) Environmental data

Temperature, RH and precipitation data/hr were received from the AMEDAS database. The RH data was from Sakata station. Temperature and precipitation data were from Nezugaseki station.

5) Testing method

After exposure, specimens were cut with 1 cm pitch and ground into a powder for titration.

Figure 4-79 Titration sample preparation.

6) Experimental results and verification

The total chloride penetration into the specimen was calculated with the proposed model. The results of the analysis and the experiment are shown in Figure 4-80–4-83.

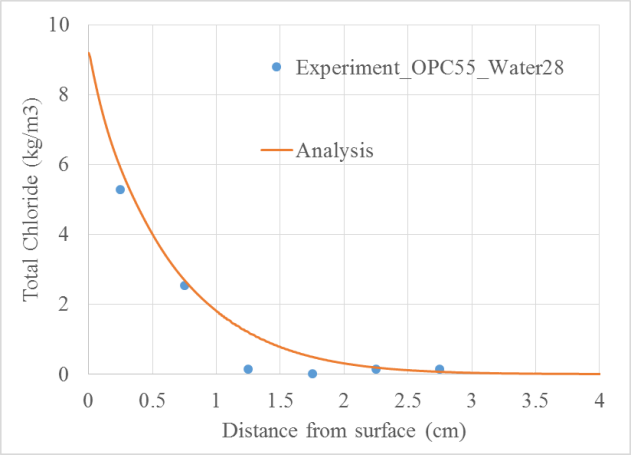

Figure 4-80 Total chloride distribution OPC55, 28 days water curing.

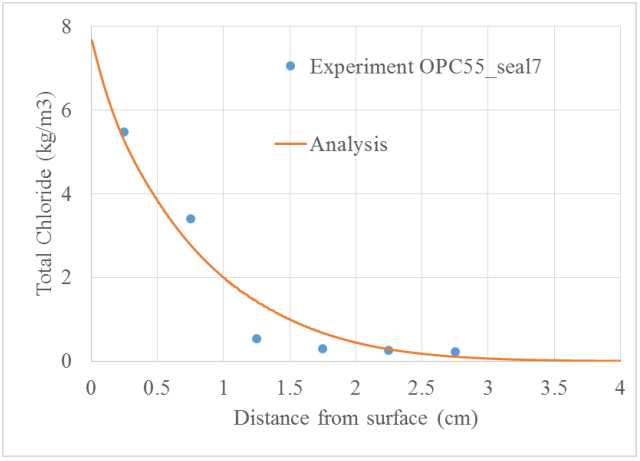

Figure 4-81 Total chloride distribution OPC55, 7 days seal curing.

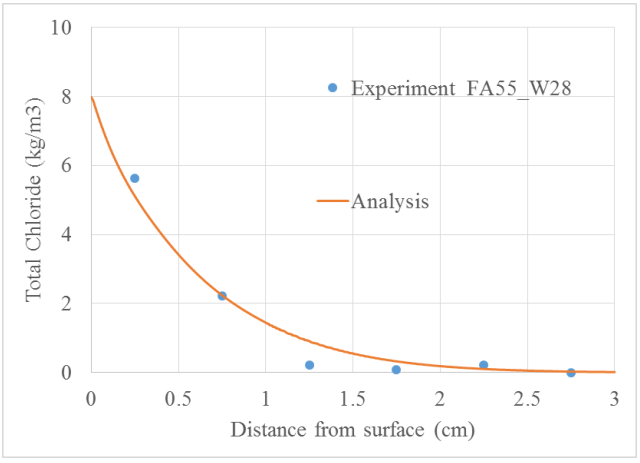

Figure 4-82 Total chloride distribution FA55, 28 days water curing.

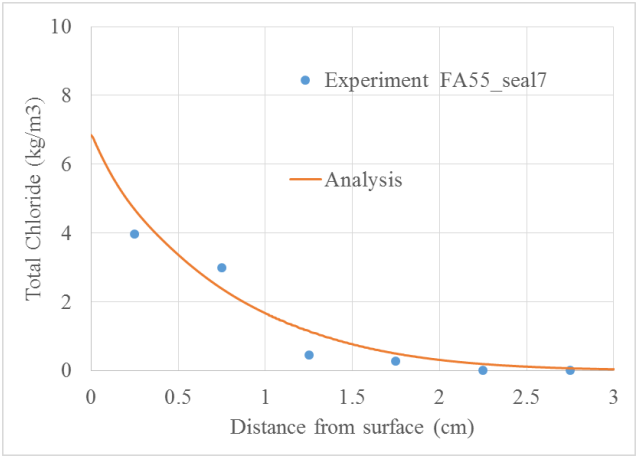

Figure 4-83 Total chloride distribution FA55, 7 days seal curing.

7) Comparison of model results with chloride collection methods

Figure 4-84 shows the analysis results when airborne chloride data from different collection methods is used. From the figure when airborne chloride data from the mortar chip method is used, the chloride distribution from the proposed model underestimates the experimental results. The reason is that the mortar chip specimen can be washed by rainfall, reducing the chloride concentration on the specimen surfaces. Therefore, the amount of airborne chloride from this specimen is lower than for the tank method.

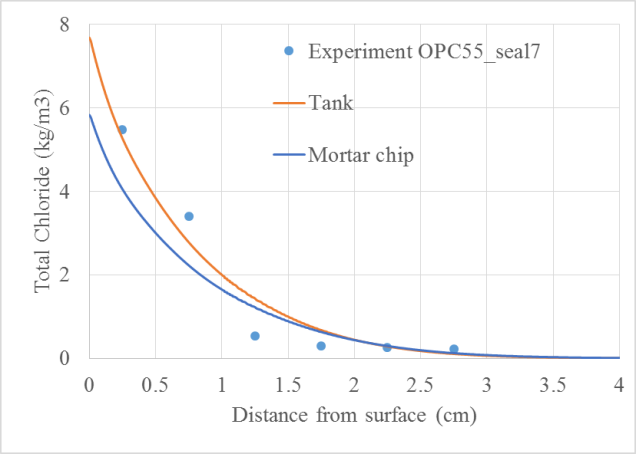

Figure 4-84 Total chloride distribution OPC55, 7 days seal curing.

8) Summary

Figure 4-80–4-83 show that the proposed model can simulate chloride penetration and washout effect of specimen under actual environment conditions and with different mix designs.

Furthermore, the analysis and testing results shows the clear difference between chloride penetration when the specimens are cured with different methods.

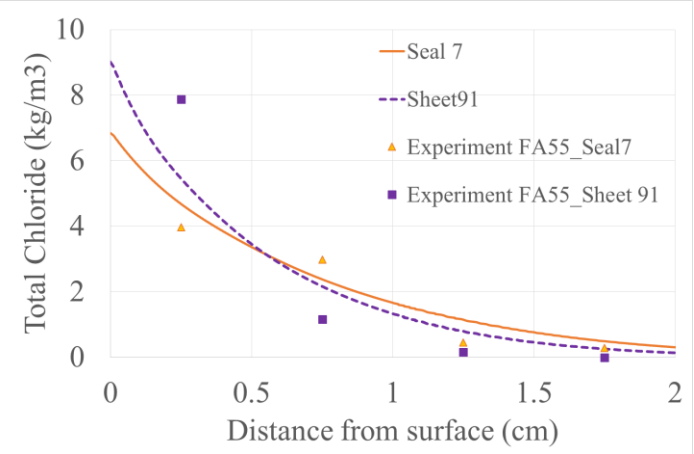

Figure 4-85 Chloride distribution FA55 comparison between 7 day seal and 91 day sheet curing.

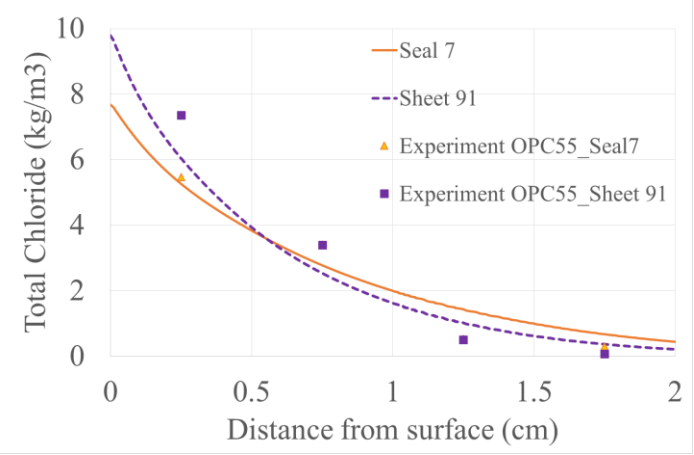

Figure 4-86 Chloride distribution OPC55 comparison between 7 day seal and 91 day sheet curing.

Moreover, chloride penetration in the mortar chip specimen was calculated. The experimental results show that the proposed model underestimates the amount of chloride which can penetrate into the mortar chip. This may be because the mortar specimen and the tank equipment were placed in different positions or because the assumptions in the model do not match the actual mechanism.

In addition, the experiment and model results suggest different airborne chloride measurement methods provide different airborne chloride intensity results. Thus, for the proposed model, a collection method should be carefully selected. For the future research, comparisons between chloride capture

methods should be carefully checked to improve the calculation and proposed model.

4.4.3.3. Verification of total chloride penetration with wet candle method (G.R. Meira et.al; 2006 – 2010) [22, 23, 24]

The objective of this exposure test is to determine the amount of chloride ingression in concrete in João Pessoa, Brazil.

1) <u>Airborne chloride capture method</u>

Airborne chloride in this study was measured with deposition on the wet candle device (Figure 4-87) according to specifications established in the ASTM standard G140.

Figure 4-87 Wet candle equipment set [24]

These devices were placed at a height of 1.5 m from the ground. The chloride deposition on the equipment was collected every month for the testing period. The results of the test are shown in Figure 4-88.

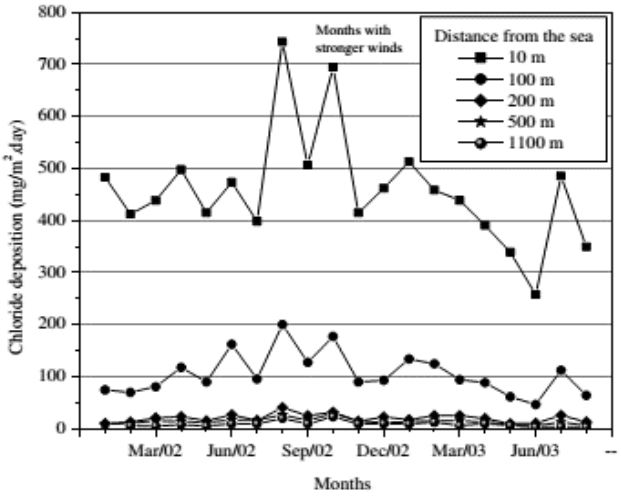

Figure 4-88 Airborne chloride data [24].

2) <u>Specimen preparation</u>

Prismatic concrete columns of $15 \times 15 \times 140\ cm^3$ were cast using Brazilian cement CPIIF (filler-modified Portland). The mix design is presented in Table 4-11.

Table 4-11 Concrete mixtures and properties.

Mix	W/B	Cement (kg)	Gravel (kg)	Sand (kg)
C5	0.57	356	947	812
C6	0.50	406	947	769

After exposure, core samples were taken from the column. Then, the amount of chloride inside the specimen was determined. The testing exposure column layout is shown in Figure 4-89.

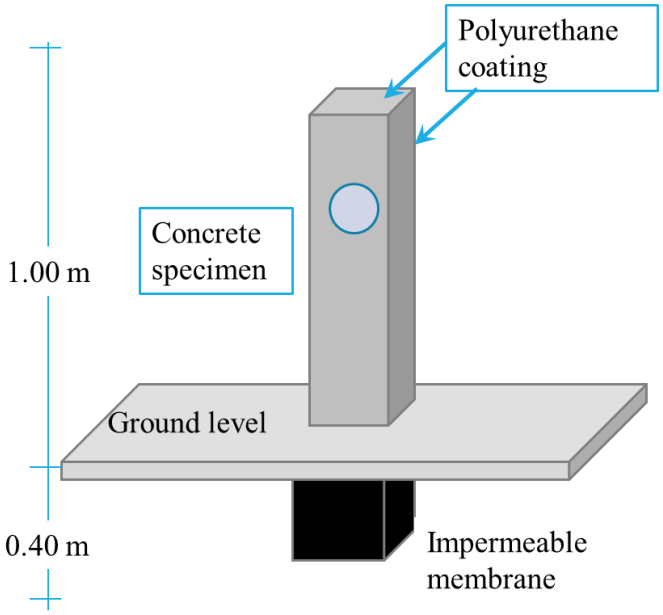

Figure 4-89 Specimen layout (modified from reference) [20].

3) <u>Exposure site</u>

The exposure site is in João Pessoa, Brazil (Figure 4-90).

Figure 4-90 Map of exposure site [20].

4) Environmental Data

Climate data was collected from a Brazilian Government weather station located in the region where the research took place. However, for the model, the environmental data was taken from the reference paper [24]. The environmental data for the analysis in this case are the average data per month (Figure 4-91).

Table 2
Average climatic data for João Pessoa between 1961 and 1990 and during research period

Period	Temperature (°C)		Relative humidity (%)		Rainfall (mm)	
	1961–1990[a]	Research period	1961–1990[a]	Research period	1961–1990[a]	Research period
Jan	25.8	27.5	75	79.5	81.1	115.4
Feb	25.2	27.2	75	79	137.5	193.1
Mar	28.2	27.0	81	81	238.4	263.0
Apr	25.5	26.7	79	78.5	312.9	201.6
May	27.0	27.0	81	81	307.9	178.2
Jun	26.2	25.4	81	85.5	381.5	548.5
Jul	23.7	25.4	87	76	290.2	133.8
Aug	25.4	25.4	75	74.5	202.1	115.0
Sep	27.5	26.5	67	73	40.7	13.4
Oct	27.7	26.5	73	76	57.5	32.7
Nov	27.0	27.1	74	76	44.9	26.0
Dec	24.1	26.6	74	77.5	37.4	30.0
Year	26.1	26.5	76.8	78.1	2132.1	1850.7

[a]*Source*: Brazilian National Institute of Meteorology.

Figure 4-91 Environmental data for the analysis [21].

5) Experimental results and verification

Total chloride penetration into the specimen was calculated with the proposed model. The results of the analysis and the experiment are shown in Figure 4-92 and Figure 4-93.

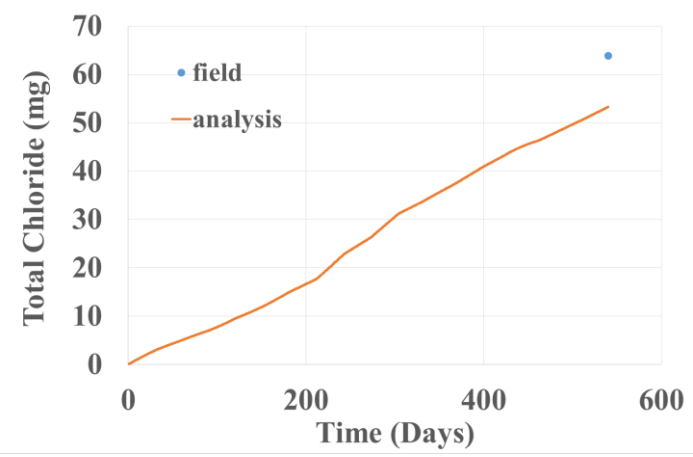

Figure 4-92 Experiment and analysis results, Mix C5.

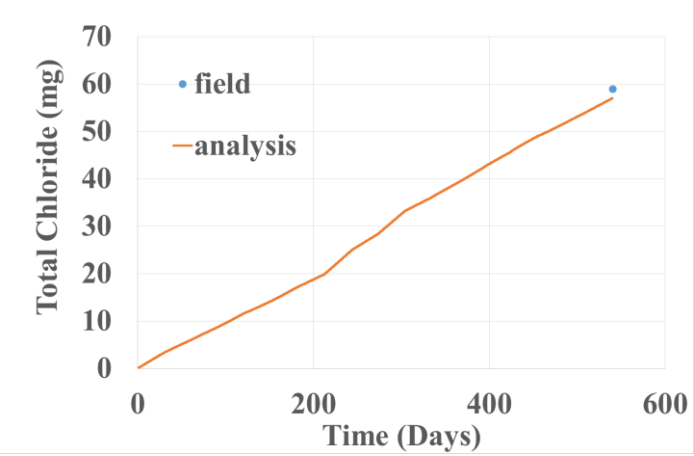

Figure 4-93 Experiment and analysis results, Mix C6.

6) Summary

The analysis results match the experimental results. The proposed model can simulate chloride penetration when the airborne chloride is captured with the wet candle method. However, data for the verification is still limited. Moreover, the available environmental data is not precise. Therefore, further data is necessary to verify the wet candle method.

4.4.3.4. Verification of total chloride penetration with dry gauze method (Hanioka S.; 2011) [22]

The experiment was conducted between January 6, 2011 and November, 21 2011. The objective of this exposure test was to determine the amount of airborne chloride in different locations with the dry gauze method and chloride ingression into mortar specimens at the specific locations.

1) Airborne chloride capture method

The dry gauze method followed the Japanese standard JIS Z 2382 [23]. The device consisted of 10 x 10 cm^2 gauze which was attached to a frame to capture airborne chloride.

Dry gauze specimens were placed at specified positions on a bridge for 2 hrs to determine the amount of airborne chloride at each position (Figure 4-94).

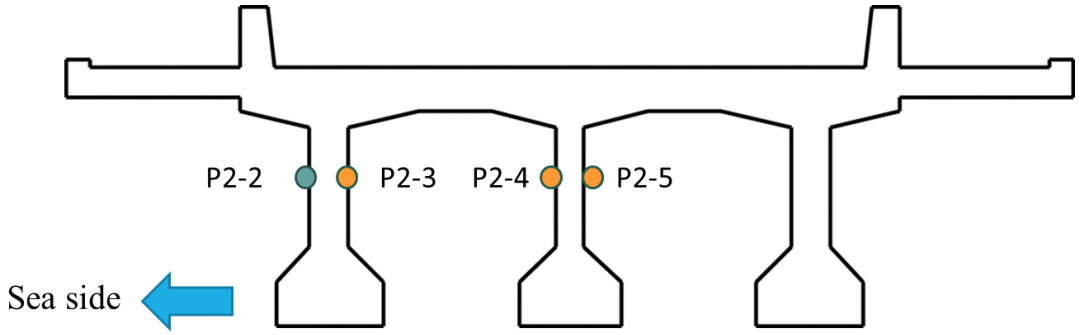

Figure 4-94 Attached positions.

The amount of airborne chloride determined by the test is shown in Figure 4-95.

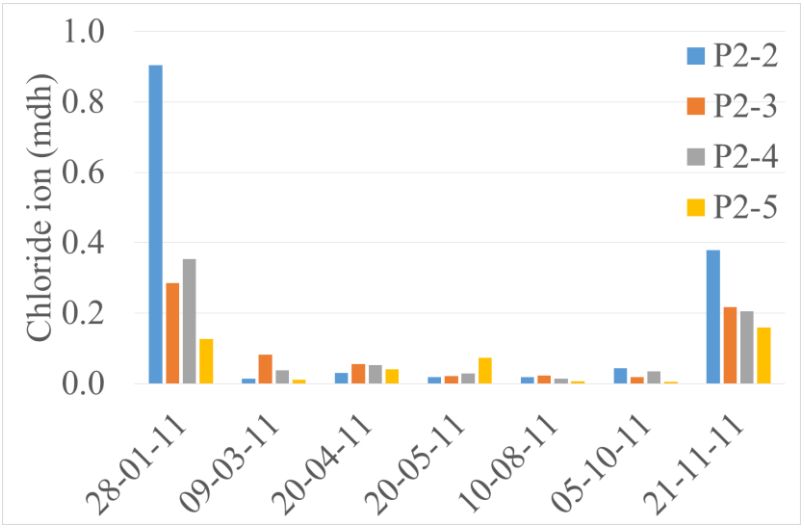

Figure 4-95 Airborne chloride data from the test.

2) <u>Mortar specimen preparation</u>

Cylinder specimens with a Ø 10 cm and a thickness of 1 cm were prepared. After casting, each specimen was cured with water for 28 days. The mix proportion is shown in Table 4-12.

Table 4-12 Mix proportion.

Mix	W/C	Cement (kg)	Water (kg)	Sand (kg)
OPC50	0.50	612.4	306.2	1320

After curing, each specimen was coated with epoxy with the exception of the exposure surface and attached to a plastic board. The set of mortar specimens were placed near the gauze to determine the chloride penetration.

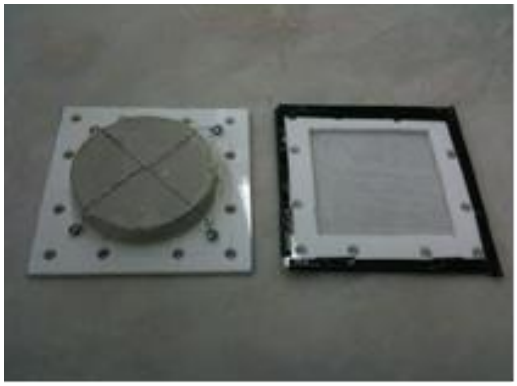

Figure 4-96 Prepared specimen and dry gauze.

Figure 4-97 Mortar and dry gauze attached to the bridge.

The testing period was from January 6 to November 21, 2011. Mortar specimens were placed and exposed to the airborne chloride environment for 1–2 months. The schedule of the exposure time is shown in Table 4-13.

Table 4-13 Specimen exposure schedule.

Season	Date	Duration (days)
S2	January 28–March 9, 2011	40
S3	March 9–April 20, 2011	42
S4	April 20–May 20, 2011	30
S5	May 20–June 24, 2011	35
S6	June 24–August 10, 2011	47
S7	August 10–October 5, 2011	56
S8	October 5–November 21, 2011	48

3) Exposure site

The test was conducted on the Okawa Bridge in Niigata Prefecture, Japan. The bridge is located 150 m from the coastline.

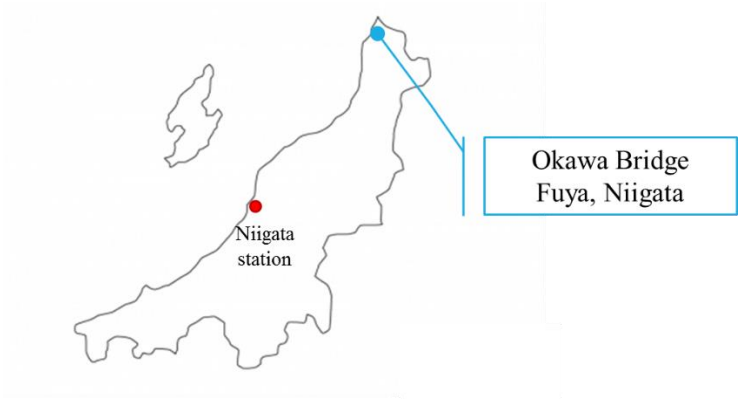

Figure 4-98 Position of Okawa bridge, Niigata Prefecture, Japan.

4) Environmental data

Temperature, RH, and precipitation data per hr were taken from the AMEDAS database. The RH data came from the Sakata station. Temperature and precipitation data are from Nezugaseki station.

The data from the dry gauze exposure test (2 hrs exposure) is the amount of airborne chloride in each season. It is assumed that the amount of measured

airborne chloride continues during the exposure time. The airborne chloride intensity for the calculation at each position is shown as following

Table 4-14 Airborne chloride amount at each position

Season	Airborne chloride (Chloride ion; mdh)			
	P2-2	P2-3	P2-4	P2-5
S2	0.703	0.240	0.283	0.100
S3	0.021	0.070	0.045	0.025
S4	0.022	0.033	0.036	0.062
S5	0.018	0.022	0.029	0.074
S6	0.019	0.023	0.014	0.007
S7	0.034	0.021	0.027	0.006
S8	0.190	0.106	0.110	0.072

5) Experimental results and verification

From the experiment, only the specimens at position P 2-2 were directly attached to the rainfall. Thus, in the calculation, assumed that the washout effect is occur only at position 2-2.

The chloride ingression of the specimens at each position are shown as following;

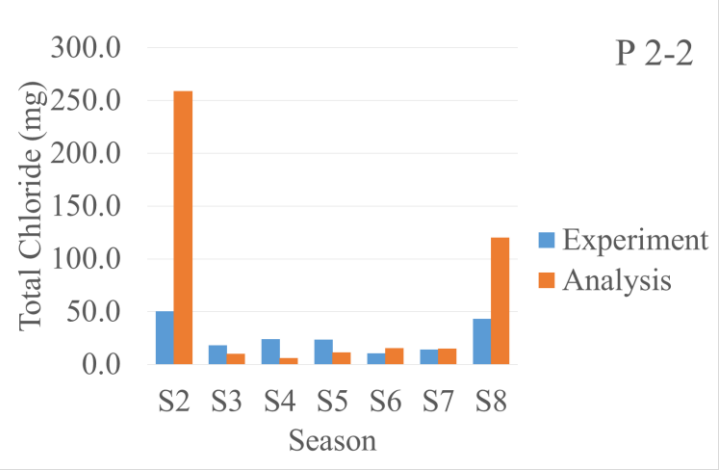

Figure 4-99 Experiment and analysis result at Position 2-2

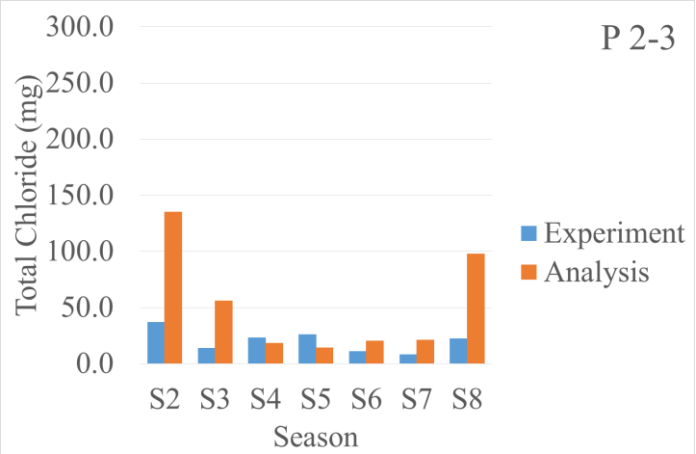

Figure 4-100 Experiment and analysis result at position P2-3

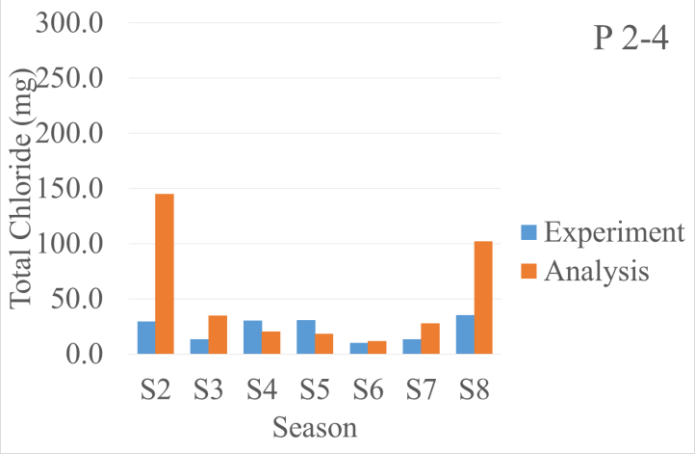

Figure 4-101 Experiment and analysis result at Position 2-4

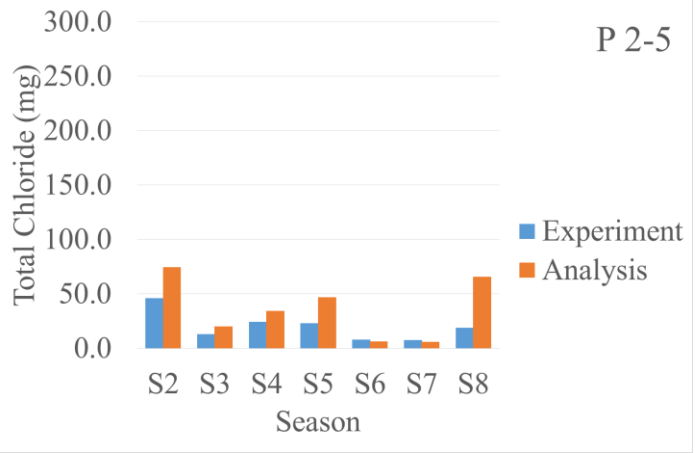

Figure 4-102 Experiment and analysis result at Position 2-5

6) Summary

From the analysis results, the proposed model can be used for calculate the chloride ingression in the mortar in some cases. However in some cases the results show both underestimate and overestimate value.

Dry gauze method can collect airborne chloride on the concrete surface by attached the device on the structure. However, the amount of airborne chloride which can capture by dry gauze is limited by the capacity of gauze itself. In addition, the exposure time in each season was only 2 hours. Hence, the data from dry gauze, in this case, cannot represent the airborne chloride intensity along the exposure time. If the dry gauze method is used, the frequency of the measurement should be increased.

4.4.3.5. Verification of total chloride penetration by Tank collection method in Niigata Prefecture, Japan (Nakamura F. et.al; 2014) [24].

The experiment was conducted during 8 March 2006 – 3 March 2007. The objective of this exposure test is to find the amount of airborne chloride and find the chloride ingression into mortar specimen at the specified position.

1) Airborne chloride capture method

In the experiment, tank sample method was used to collect the airborne chloride. The airborne chloride amount was checked every 1 months along the testing period. The equipment used for collecting airborne chloride is shown as following;

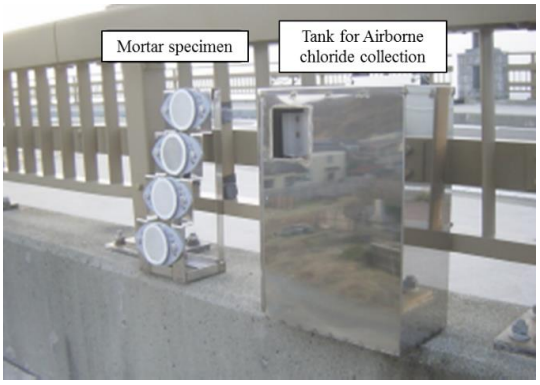

Figure 4-103 Equipment for airborne chloride collection (Modified from the reference)

2) Exposure site

The exposure position site was in Niigata prefecture, Japan. Position 1 is at Nadachi Bridge and position 2 is in the middle part of Niigata at the Isomozaki bridge. Next to the exposure tank, cylinder mortar specimens with a thickness of 1 cm were placed to determine chloride penetration. The exposure duration was 7, 10, and 12 months.

Figure 4-104 Exposure position in the Niigata prefecture.

3) Environmental data

Temperature, RH, and precipitation data/hr were received from the AMEDAS database. For position 1, the environmental data was taken from the Takada station and for position 2 from the Niigata Station.

4) Experimental results and verification

In the calculation, the W/C of the specimen was assumed to be 60%. The experimental and model results are shown in Figure 4-105 and Figure 4-106. For an exposure of 7 months, the model underestimated results in both positions. However, predictions for 10 and 12 months matched the experimental data.

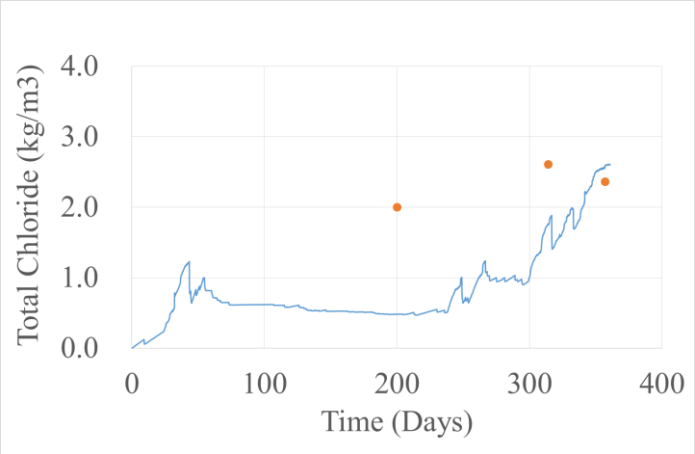

Figure 4-105 Experiment and model results (position 1).

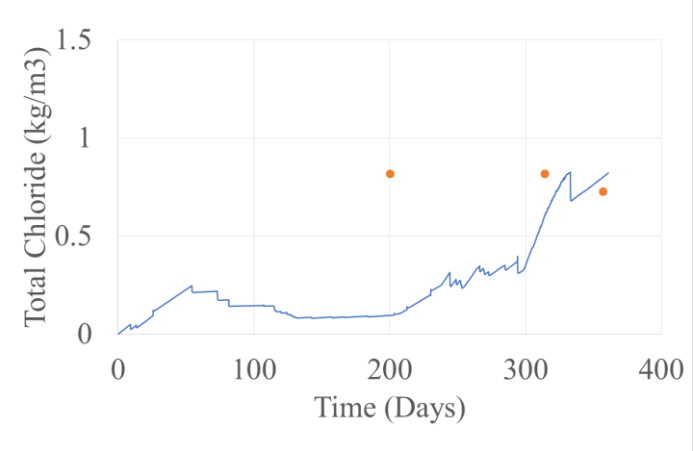

Figure 4-106 Experiment and model results (position 2).

4.5. Summary

To verify the moisture and chloride flux model, a comprehensive experimental series was conducted under controlled conditions. The verification suggests the proposed model can predict water ingression, chloride penetration, and reduction of total chloride from washout under specific conditions.

Additionally, the proposed model was verified using onsite measurement data from various research. In each experimental series, the airborne chloride intensity was corrected with different methods, as shown in Figure 4-107.

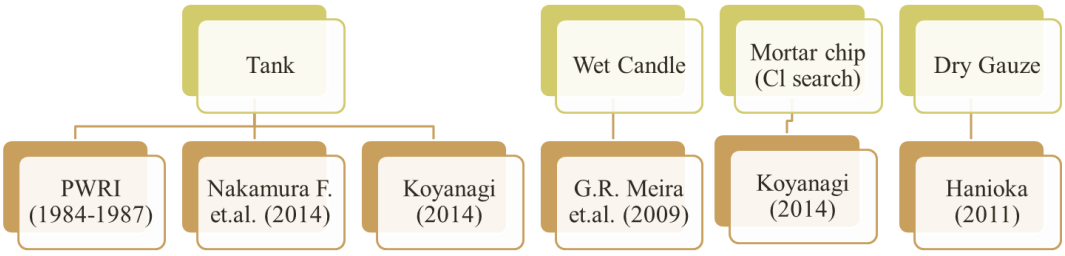

Figure 4-107 Airborne chloride collection methods.

The verification with the tank capture and wet candle method shows that the proposed model can appropriately simulate chloride penetration and washout effects in specimens under actual environment conditions. However, in some cases, the analysis provides dissimilar values when compared with exposure test results. This may be due to the limitations of methodological data, the position of the specimens, because the chloride capture equipment was not close together, or because assumptions used in the calculation did not properly correspond to actual exposure conditions.

Furthermore, with the mortar chip, the model underestimated the experimental results. This may be because the mortar chip specimens can be washed by rainfall, reducing the chloride concentration on the specimen's surface.

Moreover, in verifying the dry gauze method, the results from the model were highly variant compared to results from the tank or wet candle method. With dry gauze, the collection time is short compared to specimen exposure time, thus, it can be concluded that the data from dry gauze, in this case, cannot be representative of the airborne chloride intensity during the test. Therefore, the method for collecting the airborne chloride should be carefully considered and future studies should compare different chloride capture methods to improve calculations with the proposed model.

It can be concluded that when proper airborne chloride and environmental data are available, the proposed model can simulate the chloride concentration in concrete. However, it should be noted that data for the verification of the wet candle and dry gauze methods is limited. Thus, additional tests are necessary to confirm the results.

4.6. Reference

[1] H. Minoo, T. Ishida and T. Ishikawa, "Chloride Ion Ingress Model on the Concrete Surface Under Airborne Chloride Action," in *Japan Concrete Institute Annual Conference*, Japan, 2014. (In Japanese)

[2] J. Barrett, Inorganic Chemistry in Aqueous Solution, Cambridge: The Royal Society of Chemistry , 2003.

[3] T. Ishikawa, "Modeling of airborne chloride penetration flux into concrete," The University of Tokyo, Tokyo, Japan, 2010. (In Japanese)

[4] D. Nuralinah, "Laboratory test and Numerical Analysis of Chloride Ingress into Concrete Subjected to Airborne Salt," Nagaoka University of Technology, Niigata, Japan, 2012.

[5] K. Hong and E. Hooton, "Effects of fresh water exposure on chloride contaminated concrete," *Cement and Concrete Research*, vol. 30, pp. 1199-1207, 2000.

[6] H. Yamashita, T. Shimomura and F. Yamada, "Study of chloride concentration on concrete surface affected by Airborne Chloride.," in *Japan Concrete Institute Annual Conference*, Japan, 2007. (In Japanese)

[7] P. O. Iqbal, "Chloride Transport Coupled with Moisture Migration in Non-Saturated Concrete Exposed to Marine Environment and Application to Cracked Concrete," The University of Tokyo, Tokyo, 2008.

[8] Nicos S. Martys and Chiara F. Ferraris , "Capillary transport in mortars and concrete," *Cement and Concrete Research,* vol. 27, no. 5, p. 747–760, May 1997.

[9] K. Maekawa, T. Ishida and T. Kishi, Multi-Scale Modelling of Structural Concrete, Taylor and Francis, 2008.

[10] T. Ishida, K. Maekawa and T. Kishi, "Enhanced Modeling of Moisture Equilibrium and Transport in Cementitious Materials under Arbitrary Temperature and Relative Humidity History," *Cement and Concrete Research* , vol. 37, pp. 565-578, 2007.

[11] K. Horikiri, "Measurement of airborne salinity by a new method and study on the penetration behavior into concrete," The University of Tokyo, Toyko, 2009. (In Japanese)

[12] "ASTM C1585-04, Standard Test Method for Measurement of Rate of Absorption of Water by Hydraulic-Cement Concretes," *ASTM International*, 2004.

[13] S. Swatekititham, "Computational Model for Chloride Concentration at Surface of Concrete Under Actual Environmental Condition," The dissertation submitted to Kochi University of Technology, Kochi, Japan, 2004.

[14] E. R. Lewis and S. E. Schwartz, Sea Salt Aerosol Production: Mechanisms, Methods, Measurements, and Models : a critical review, Washinaton DC: American Geophysical Union, 2004.

[15] Public Work Research Institute, "Report on Investigation of Airborne Chloride in Japan (III), PWRI report No.2687," 1988. (In Japanese)

[16] Meteorological Research Institute, "The study of Melting of Snowflakes in the atmosphere (Techinical Report No.8)," Meteorological Research Institute, Ibaraki, Japan, 1984. (In Japanese)

[17] Meteorological Office United Kingdom, "Met Office," [Online]. Available: http://www.metoffice.gov.uk/. [Accessed 1 Feburary 2016].

[18] S. Kokubo and H. Okamura, "Calculation Model for Airborne Chloride Ion based on Seawater Particle Generation," *JSCE journal of hydraulic, coastal and environmental engineering*, vol. 65, pp. 259-268, 2009. (In Japanese)

[19] K. Koyanagi, "Combined Effects of Binders and Curing Conditions on Ingress of Chloride Ions into Cementitious Materials," The University of Tokyo, Tokyo, Japan, 2014.

[20] G.R. Meira, C. Andrade, C. Alonso, J.C. Borba Jr. and M. Padilha Jr. , "Durability of concrete structures in marine atmosphere zones – The useof chloride deposition rate on the wet candle as an environmental indicator," *Cement and Concrete Composites*, vol. 32, pp. 427-435, March 2010.

[21] G.R. Meira, C. Andrade, I.J. Padaratz, C. Alonso and J.C. Borba Jr., "Chloride Penetration into Concrete Structure in the marine Atmosphere Zone - Relation ship between deposition of chlorides on the wet candle and chloride accumulate into concrete," *Cement and Concrete Composites*, vol. 29, pp. 667-676, May 2007.

[22] T. Ishida, A. Kita, S. Hanioka, L. A. Ho Thi and Y. Matsuda, "A study on Mechanism of airborne chloride transport and migration into mortar based on onsite measurement," in *Proceedings of the Concrete Structure Scenarios*, 2012. (In Japanese)

[23] Japanese Standards Association, "JSA JIS Z 2382 Determination of pollution for evaluation of corrosivity of atmospheres," 1998. (In Japanese)

[24] F. Nakamura, M. Ikuta, T. Shimomura and T. Hosoyamada, "Field observation and numerical analysis on the adhesion of airborne chloride on concrete surface," in *Proceedings of the Japan Concrete Institute Annual Conference*, 2014. (In Japanese)

Chapter 5
Airborne Chloride Generation and Transportation Model Verification

5.1. Introduction

The previous chapter describes that when properly recorded airborne chloride and environmental data are available, the airborne chloride surface flux model can be used to determine the chloride concentration at specific positions. However, in reality, airborne chloride data is still limited.

The amount of airborne chloride changes due to wind direction, wind speed, obstacles, and distance from the seashore [1, 2]. Thus, airborne chloride intensity for each region and season differ. Furthermore, the amount of airborne chloride can change if the exposure condition changes. In such cases, it is necessary to use the airborne chloride generation and transportation model to calculate the airborne chloride intensity.

Chapter 3 shows the concept behind and the calculation of the amount of airborne chloride. With a modified Kokubo and Okamura model (by Hanioka S., 2011), the amount of airborne chloride can be predicted, but verification of the model is still limited. Thus, additional verifications are necessary to confirm the validity of the model.

5.2. Model assumptions

To calculate the amount of airborne chloride, the exposure position and direction are important parameters to be considered. The exposure direction is assigned as seen in Figure 5-1.

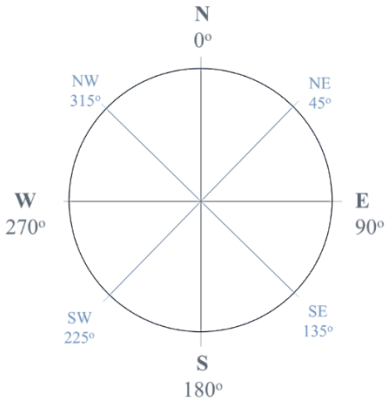

Figure 5-1 The reference plane for exposure direction.

In Figure 5-1, north (N) is assigned as 0° and the angle increases clockwise, for example, east (E) is measured as 90°.

The proposed model can be used to determine the airborne chloride intensity at positions which are directly exposed to the seashore (parallel to the coastline). The calculation assumes that airborne chloride can attach to concrete surfaces when the wind direction is ±67.5 degree from the normal direction, as seen in Figure 5-2.

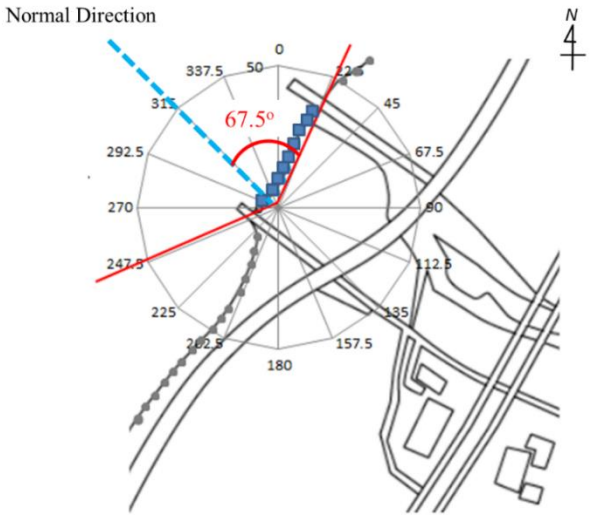

Figure 5-2 Directions at which airborne chloride can attach to target position.

In Figure 4-65, the exposure direction is equal to 315º, therefore, airborne chloride particles can be captured when the wind direction is between 0–22.5º and 247.5–359º.

It has been reported that the amount of the airborne chloride can be reduced by rainfall [3]. On the other hand, Kita A. [4]observed the amount of airborne chloride under different weather conditions in the winter. In the experiment, the amount of airborne chloride was captured with a dry gauze method. The observations showed that during snowfall, the amount of airborne chloride is higher than in other cases due to a higher wind speed (Figure 5-4).

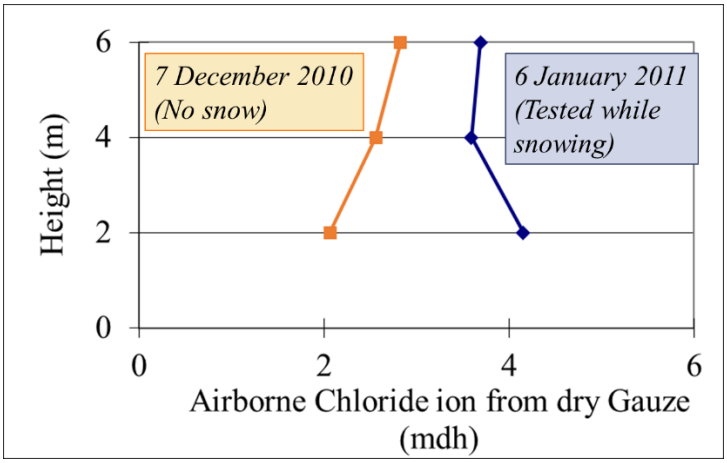

Figure 5-3 Amount of airborne chloride, dry gauze collection by Kita A. (2011).

A snow flake can be transported by wind and attached to a dry gauze device [4], as shown in Figure 5-4.

Figure 5-4 Snow flake on dry gauze.

This observation suggests that the amount of the airborne chloride in an environment is not reduced by snow.

In previous the verification, the reduction of airborne chloride due to rainfall was not considered. For the new verification, it is assumed that airborne chloride particles can be blocked by rainfall particles when rainfall is higher than 1 mm/hr and chloride particles cannot reach a target position, as shown in Figure 5-5.

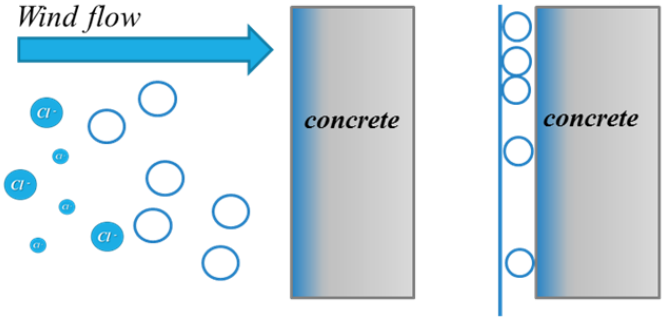

Figure 5-5 Rainfall effect on airborne chloride transportation.

However, in general, recorded data from methodological databases provided the precipitation value. In such cases, precipitation shown in the database can be both snow and rainfall. Thus, to identify the rainfall effect, it is assumed that when the temperature is higher than 3 ^{o}C, the precipitation value in the database is rainfall.

5.3. Verification of the rainfall effect assumption

To verify rainfall effect assumption, airborne chloride determined with previously recorded data from the PWRI was used [5]. The chloride collection method was a tank sample method. For the verification, data from the Toumi Bridge, Niigata prefecture was selected. The results are shown in Figure 5-6.

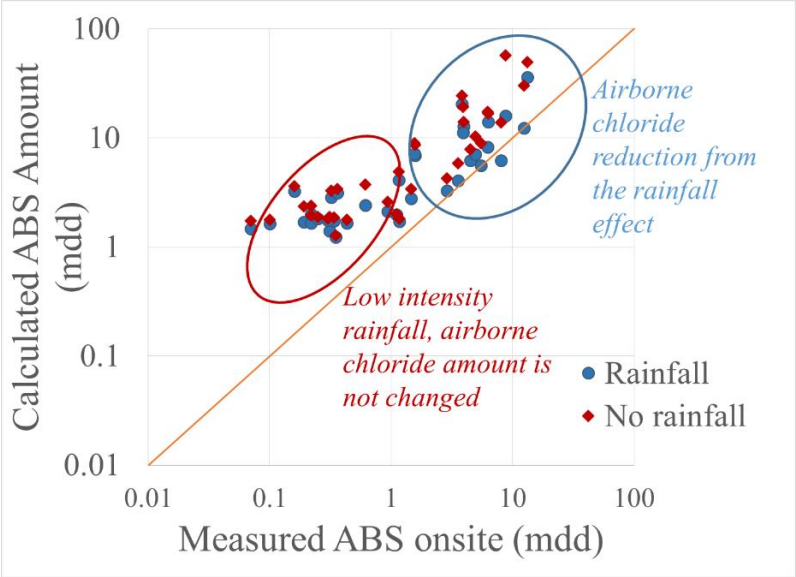

Figure 5-6 Verification results at Toumi Bridge.

Figure 5-6 shows the calculation results with and without the rainfall effect. In the red circle, the amount of airborne chloride between the two cases is almost the same, which mean the rainfall intensity is low during this duration (e.g. in the summer). In the blue circle, the rainfall intensity is high, therefore, the amount of airborne chloride is significantly reduced. The results show that when the calculation includes the rainfall effect, the total amount of airborne chloride is reduced and the calculation results are closer to onsite measurement data.

5.4. Verification of the model

To verify the proposed model, onsite measurement data from previous research with different chloride collection methods was used, as described in the following sections.

5.4.1. Verification of model with tank collection method [5]

For the first verification, the experimental series was conducted by the PWRI between December 10, 1984 and December 9, 1987 in Japan to investigate the amount of airborne chloride and chloride penetration in each region.

1) Airborne chloride capture method

For the test, a tank sample method was used to collect the airborne chloride. The amount of airborne chloride was checked every month during the testing period. The airborne chloride collection equipment is shown in Figure 5-7.

Figure 5-7 The PWRI airborne chloride capture equipment.

2) Exposure site and exposure condition

In Japan, as discussed, the climate varies from subarctic in the north to subtropical in the south. Therefore, recorded data was selected from exposure sites around Japan with different exposure condition.

The exposure position and conditions are the data recorded described in a PWRI report [5]. The distance from the coastline, height, exposure condition, exposure direction, and duration are shown in Table 5-1. The position of the tanks are shown in Figure 5-8.

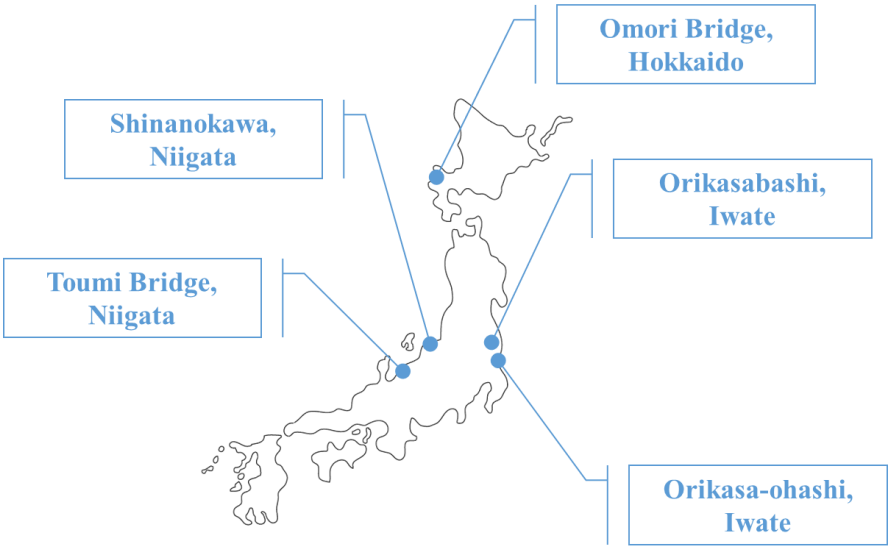

Figure 5-8 Exposure site locations.

Table 5-1 Distance from the coastline, height, and exposure condition.

Position	Distance (m)	Height (m)	Analysis conditions	Exposure direction	Duration (year)
Toumi Bridge	100	6.6	Seashore	337.5º	3
Shinanokawa	100	20.3	Obstacle	337.5º	1
Orikasabashi	400	7.0	Seashore	90º	1
Orikasa-Ohashi	0	3.0	Seashore	90º	2
Omori Bridge	40*	9.0	Obstacle	225º	1

*The distance of the Omori bridge from the seashore is from data by Honma et.al (2005) [6].

3) Environmental data input for the calculation

For the calculation, wave height, tidal cycle, water depth, wind speed, wind direction, and rainfall intensity are necessary.

Environmental data was taken from the previously recorded data from the following databases:

- Wave height, tidal cycle, and water depth are from The Nationwide Ocean Wave Information Network for Ports and Harbors (NowPhas) Database;
- Wind speed and wind direction data received from AMEDAS of the Japan Meteorological Agency.

Data was taken from the station nearest to the exposure position (Table 5-2).

Table 5-2 The NowPhas and AMEDAS stations for previously recorded data.

Location	**Station name**			
	AMEDAS		**NowPhas**	
	Rainfall (mm/hr)	*Wind speed (m/s) and Wind direction*	*Wave height (m) tidal cycle (s)*	*Water Depth (m)*
Shinanokawa	Niigata	Niigata	Niigata-Nishi	Niigataoki
Toumi Bridge	Itoigawa	Itoigawa	Naoetsu	Naoetsu
Omori Bridge	Kamoenai	Kamoenai	Setana	Setana
Orikasabashi	Miyako	Miyako	Kamaishi	Kamaishi
Orikasa-Ohashi	Miyako	Miyako	Kamaishi	Kamaishi

4) Verification results

The amount of airborne chloride at each position was calculated with the proposed model. The results are shown in Figure 5-9–Figure 5-13.

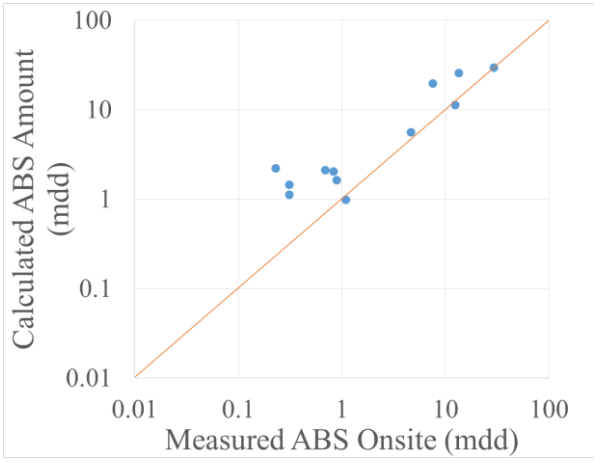

Figure 5-9 Shinanokawa, Niigata prefecture.

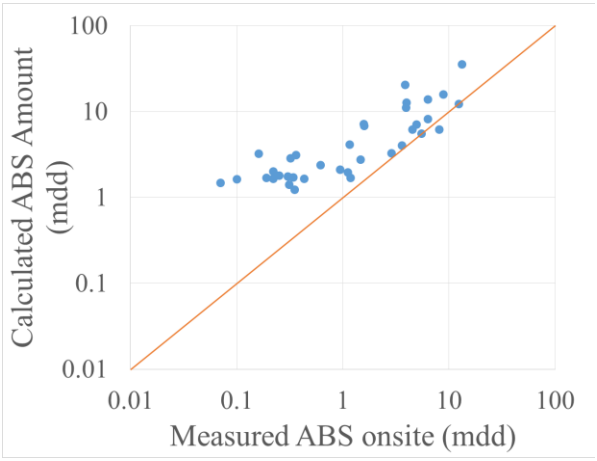

Figure 5-10 Toumi Bridge, Niigata prefecture.

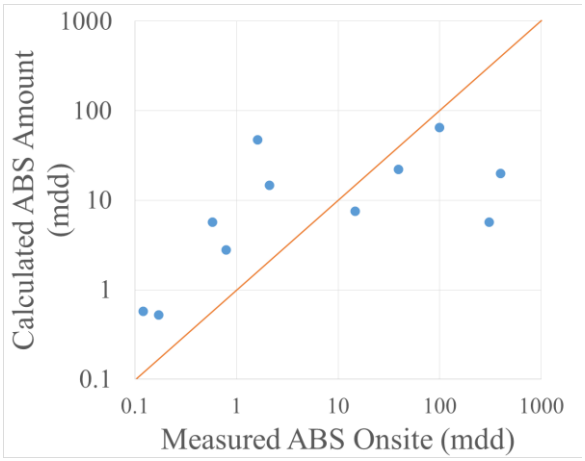

Figure 5-11 Omori Bridge, Hokkaido prefecture.

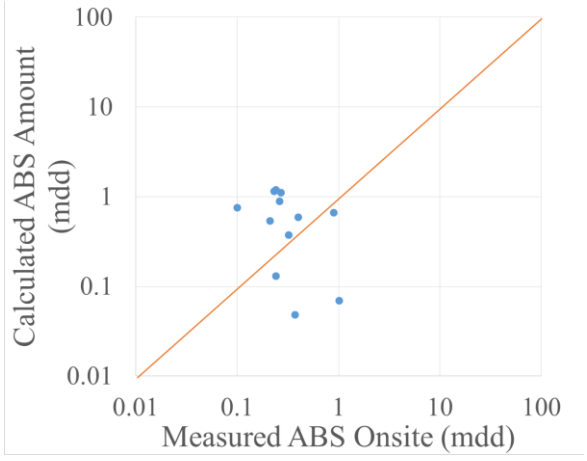

Figure 5-12 Orikasabashi, Iwate prefecture.

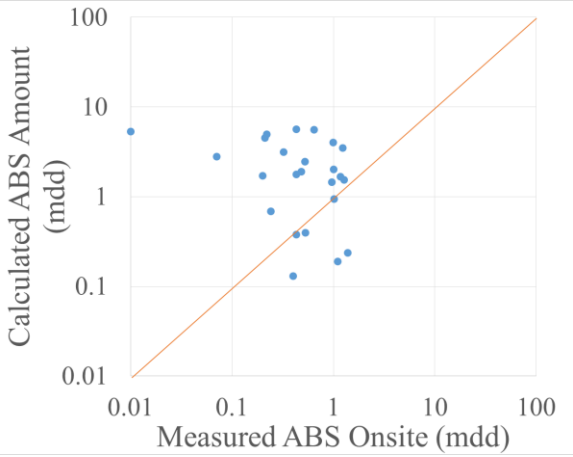

Figure 5-13 Orikasa-ohashi, Iwate prefecture.

5) Summary

From the verification results, the proposed model can be used to predict the amount of the airborne chloride at specific positions when the airborne chloride is captured with a tank sample method. However, for Orikasa-ohashi, the verification results differ from the measurement; compared with other cases, the calculation data is scattered.

In this case, in the PWRI report, the distance of the exposure site to the seashore is 0 m, difficult in actual conditions. Moreover, the exposure conditions are not clear. Therefore, the data may be scatted because the environmental condition does not match the actual exposure condition. Thus, to determine airborne chloride intensity, precise exposure conditions and positions are needed.

5.4.2. Verification of Model with Dry Gauze Method [7, 8]

Hanioka (2011) conducted an experiment to determine the amount of airborne chloride at different heights and distances, as described in Chapter 3. Another objective of this experiment was to determine the amount of chloride that can attach to bridge structures.

The measurement position is in Niigata prefecture at Okawa Bridge. Dry gauze samples were attached at specific positions on the concrete surface to determine the amount of chloride.

1) Airborne chloride capture method

In the experiment, a dry gauze method with Japanese standard JIS Z 2382 was used [9]. The device consisted of a 10 x 10 cm gauze attached to a plastic frame. The dry gauze sample was attached to the surface to capture airborne chloride (Figure 5-14).

The measurement position was on the girder surface, placed on pier No. 2 (Figure 5-15). The distance of the measurement position from the coastline was 150 m and the height of the dry gauze was 12 m from the ground level. The exposure direction was 315°.

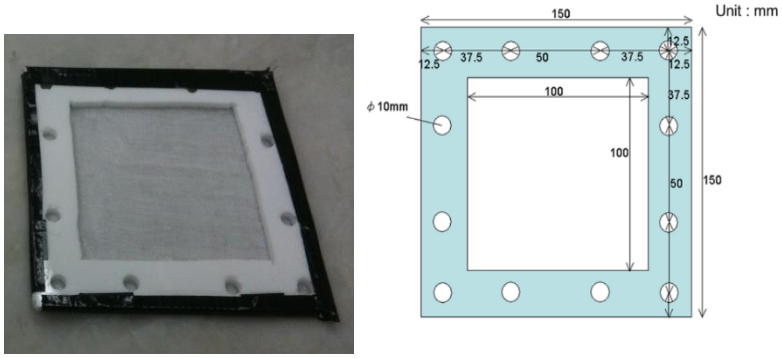

Figure 5-14 Dry gauze [8].

Figure 5-15 Dry gauze attached on the bridge [8].

Exposure was selected at different seasons in 1 year. The exposure time was ~2 hrs. The exposure date, time, and amount of chloride are shown in Table 5-3.

Table 5-3 Exposure date and time.

Date	Time		Chloride amount (mdh)
	Start	*End*	
06-01-11	11:24	13:26	0.541
28-01-11	10:59	14:06	0.904
09-03-11	11:40	13:53	0.013
20-04-11	11:24	13:26	0.030
20-05-11	11:25	13:44	0.018
10-08-11	11:33	13:34	0.019
05-10-11	12:11	14:12	0.044
21-11-11	11:00	13:00	0.408

2) Exposure site

The measurement position was at the Okawa Bridge in Niigata prefecture, Japan. The distance from the bridge to the coastline was 150 m. The position is shown in Figure 5-16 and Figure 5-17

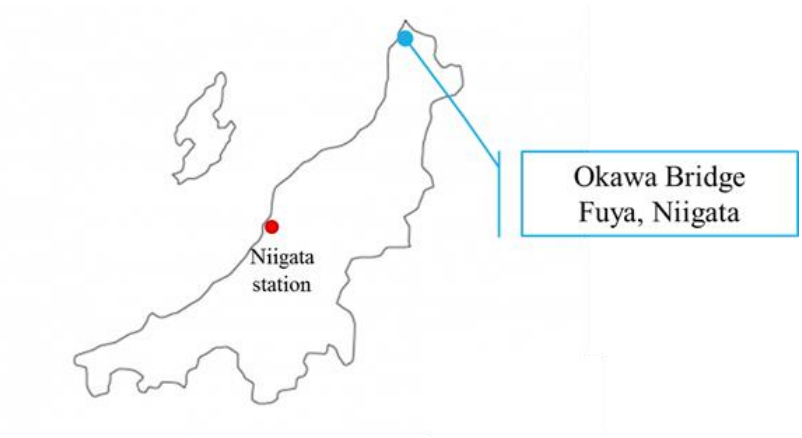

Figure 5-16 Exposure site near Okawa Bridge.

Figure 5-17 Position of Okawa Bridge Pier No. 2.

3) Exposure Condition

The exposure condition was checked with onsite observation and from the a bird's-eye view (Figure 5-18) [7, 8] . Obstacles exist in front of the exposure site. The obstacle positions are shown in Figure 5-19.

Figure 5-18 Map of exposure position (Google maps).

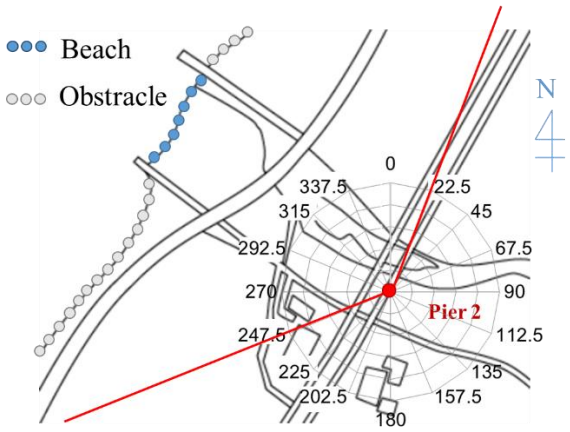

Figure 5-19 Exposure condition near exposure site and the obstacle positions (150 m from the seashore).

Figure 5-20 Environmental condition near exposure site from onsite observations [8].

4) Environmental Data

Data was taken from the following databases:

- Wave height, tidal cycle and water depth are from the NowPhas Database at Sakata station;
- Wind speed and wind direction data received from AMEDAS Nezugaseki station.

5) Verification results

The amount of airborne chloride at Okawa Bridge was calculated as shown in Figure 5-21.

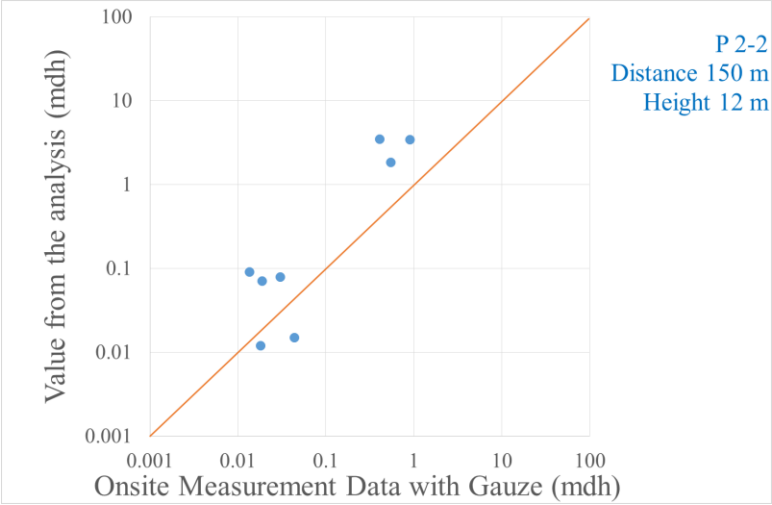

Figure 5-21 Experiment and analysis results at Position 2-2.

6) Summary

The results suggest that when the exposure condition and accurate environmental data are available, the proposed modified Kokubo and Okamura model can be used to calculate the amount of airborne chloride at Okawa Bridge when airborne chloride is measured with a dry gauze method.

5.5. Summary

The verification results show that the proposed model can be used to predict the amount of the airborne chloride at specified positions when the airborne chloride is captured with tank sample and dry gauze methods.

However, verification results in some cases are different from measurements. This may be because environmental conditions do not match the actual exposure condition. Thus, to determine the intensity of airborne chloride, the precise exposure conditions and position are necessary.

Additionally, it should be noted that the proposed model can be used to find the airborne chloride intensity at positions exposed directly to the seashore (parallel to the coastline). Therefore, to find the amount of airborne chloride at different positions on a bridge, the modification of the model or different calculation methods should be considered.

5.6. Reference

[1] N. Bongochgetsakul, S. Kokubo and S. Nasu, "Measurement of Airborne Chloride Particle Sizes Distribution for Infrastructures Maintenance," in *IESL-SSMS Joint Symposium*, Colombo, Srilanka, 2011.

[2] S. Kokubo and H. Okamura, "Calculation Model for Airborne Chloride Ion based on Seawater Particle Generation," *JSCE journal of hydraulic, coastal and environmental engineering*, vol. 65, pp. 259-268, 2009.

[3] E. R. Lewis and S. E. Schwartz, Sea Salt Aerosol Production: Mechanisms, Methods, Measurements, and Models : a critical review, Washinaton DC: American Geophysical Union, 2004.

[4] A. Kita, "Quantification of airborne chloride penetration based on wind tunnel test and field measurement," The University of Tokyo, Tokyo, Japan, 2011. (in Japanese)

[5] Public Work Research Institute, "Report on Investigation of Airborne Chloride in Japan (III), PWRI report No.2687," 1988. (in Japanese)

[6] D. Honma, A. Kubouchi, Y. Yamamoto, A. Hatakeyama and K. Kimura, "Damage Mechanism of Omori Bridge by Typhoon No. 0418 and Measures for Temporary Restoration," *Annual journal of civil engineering in the ocean*, vol. 21, pp. 927-932, 2005. (in Japanese)

[7] T. Ishida, A. Kita, S. Hanioka, L. A. Ho Thi and Y. Matsuda, "A study on Mechanism of airborne chloride transport and migration into mortar based on onsite measurement," in *Proceedings of the Concrete Structure Scenarios*, 2012. (in Japanese)

[8] S. Hanioka, "Verification and enhancement of airborne chloride generation and transportation model based on field measurement," The university of Tokyo, 2011. (in Japanese)

[9] Japanese Standards Association, "JSA JIS Z 2382 Determination of pollution for evaluation of corrosivity of atmospheres," 1998. (in Japanese)

Chapter 6
Verification of Overall Framework to Calculate Chloride Penetration

6.1. Introduction

Chapters 4 and 5, the airborne chloride surface flux model and airborne chloride generation and transportation model have been verified by experimental data and onsite measurement data.

As described in Chapter 4, when correctly recorded airborne chloride and accurate environmental data are available, chloride surface flux models can predict chloride penetration under actual environment conditions. However, in reality, recorded airborne chloride data is limited. Thus, modeling chloride generation and transportation is necessary.

The airborne chloride generation and transportation model can calculate the amount of airborne chloride at specific positions. Then, the calculated airborne chloride amount can be given as the input for the airborne chloride surface flux model. With this method, the total chloride inside the structure can be predicted.

This chapter presents the comprehensive system concept and overall scope. Then, the proposed system is be verified with onsite measurement data from Okawa Bridge.

6.2. Comprehensive System to Predict Airborne Chloride Ingression

When amount of airborne chloride recorded data is available, the chloride concentration inside materials can be calculated through the airborne chloride surface flux model. However, in reality, data about airborne chloride is limited. Thus, in such case, it is necessary to implement the modeling of generation and transportation of airborne chloride particles.

In the previous chapter, an airborne chloride generation and transportation model was verified. The proposed model can predict the amount of the airborne chloride at specific positions by using data concerning wind direction, wind speed, wave height, tidal cycle, and rainfall intensity [1, 2]. According to the verification results, when airborne chloride data is not available, the airborne chloride generation and transportation model can predict the amount of the airborne chloride. This data can then be used as an input for the surface flux model. In this way, the total chloride inside the structure can be predicted (Figure 6-1).

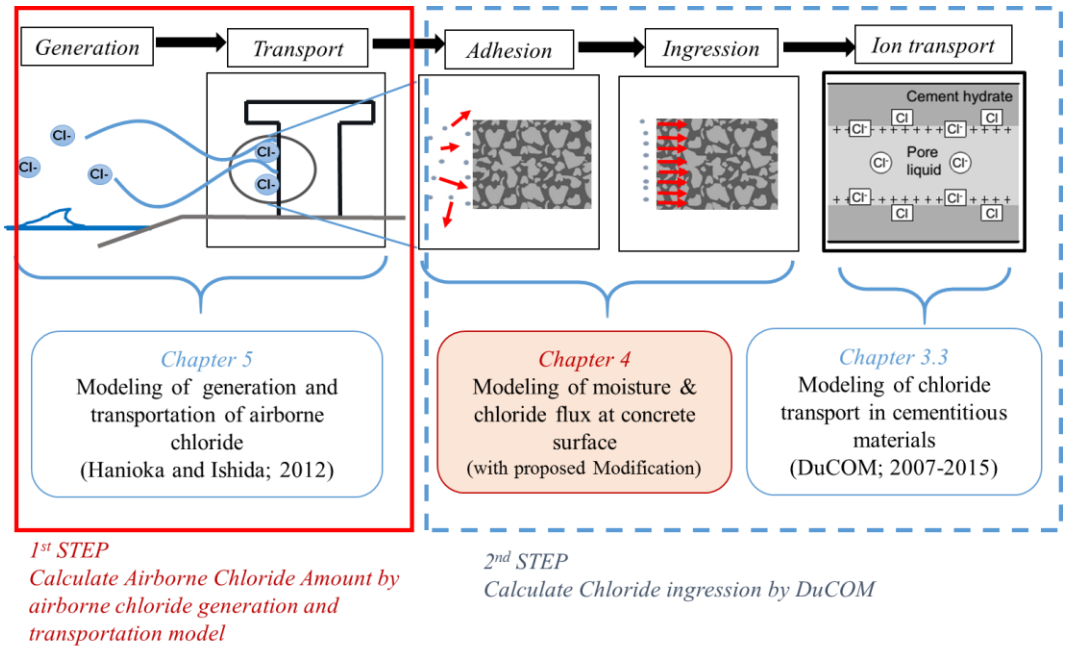

Figure 6-1 Framework to calculate chloride penetration without recorded data concerning airborne chloride.

Figure 6-2 shows the proposed system to calculate airborne chloride penetration. When recorded data concerning airborne chloride is not available, the airborne chloride intensity can be calculated using wind speed, wind direction, rainfall intensity, breaking wave height, tidal cycle, and exposure conditions. The airborne chloride intensity, environmental data, and concrete mix proportions are given as an input into the DuCOM system to calculate chloride ingression.

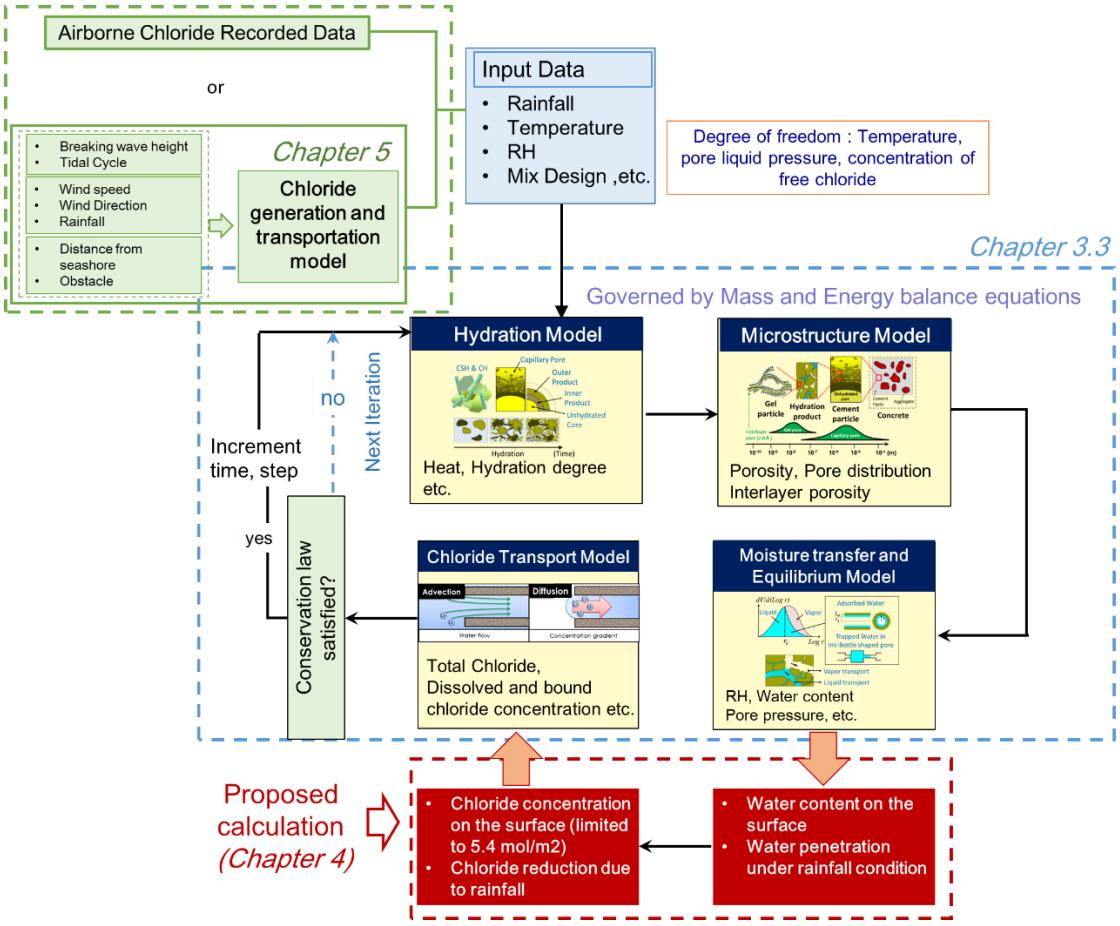

Figure 6-2 System to calculate chloride penetration without recorded data on airborne chloride.

For the verification, chloride penetration data from onsite measurements was used to confirm the validity of the proposed framework

6.3. Verification of Proposed Framework

Yoshida S. et.al [3] observed chloride ingression under airborne chloride conditions at the Okawa Bridge. The Okawa Bridge is a pre-stressed I-Girder bridge located between Fuya and Nezugaseki stations on the JR Uetsu Mainline in the Niigata [refecture. The length of the middle span is 19 m. The distance from the bridge to the coastline is ~150 m.

Okawa Bridge was built in 1974. Due to corrosion problems on the bottom flange, bridge inspection was conducted in 1999. Around 29 cored concrete samples with a size of

Ø5 cm x 6 cm were removed from I-Girder. The amount of chloride ingression was tested at every 2 cm pitch.

For the verification, data from the core samples at the flange and web members in the girder of column No. 2 were used in the analysis. The sample cores were taken from the web and flange as shown in Figure 6-3 [3].

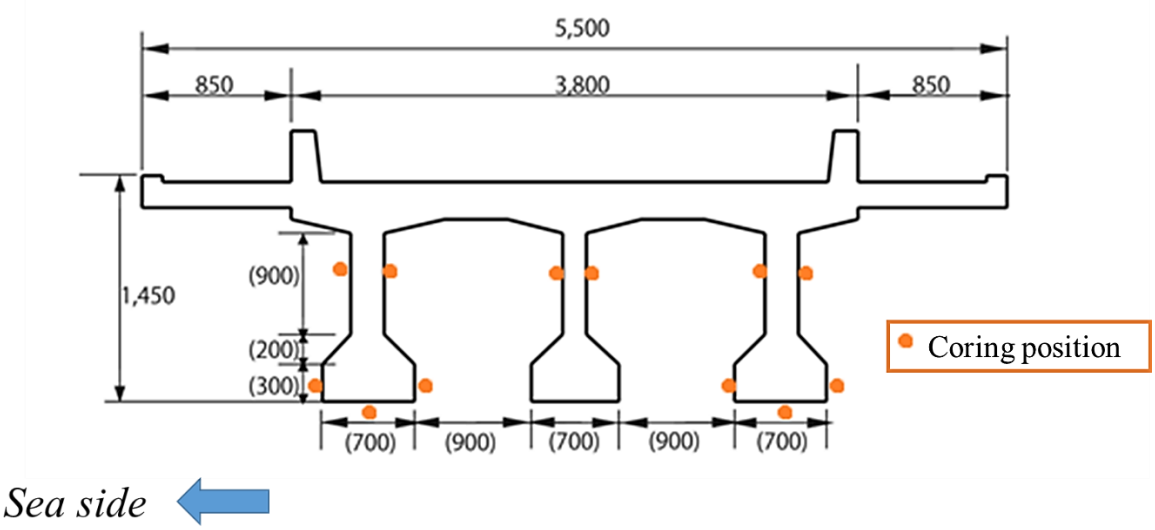

Figure 6-3 Coring position for column No. 2.

Chloride ingression at the flange and the web position of the girder directly exposed to the sea were selected for the verification (Figure 6-4).

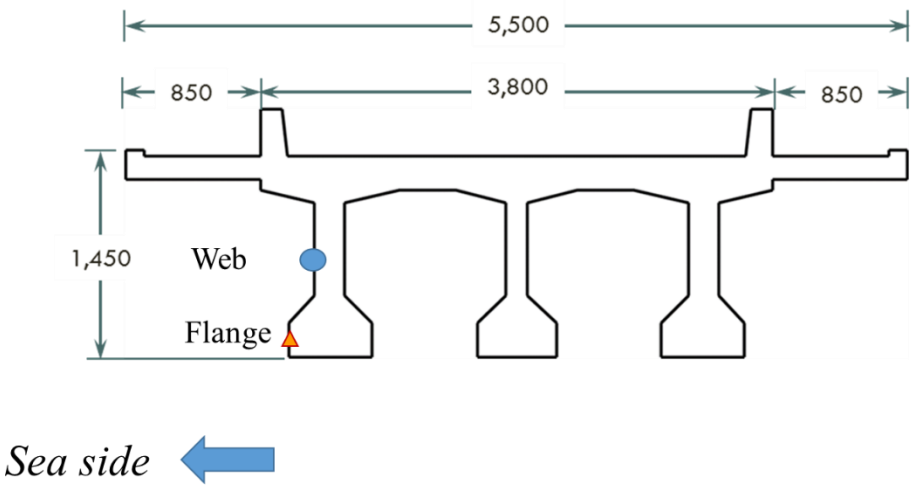

Figure 6-4 Position selected for verification.

Chloride penetration of the sample cores are shown in Figure 6-5 [3]. An onsite survey revealed the coring position to be ~12 m from the ground level [1].

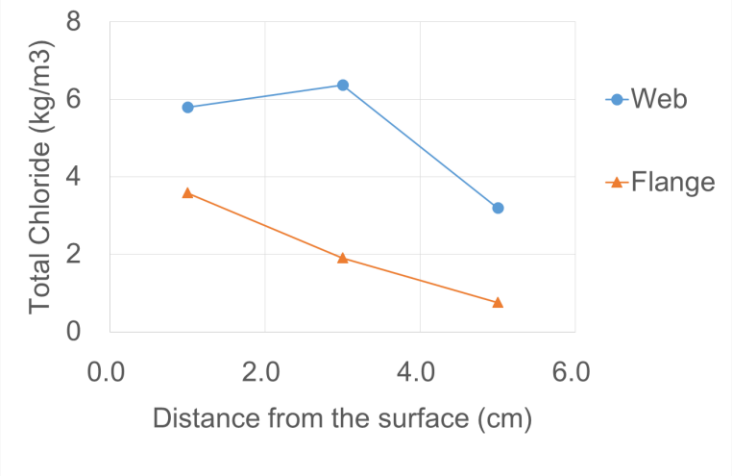

Figure 6-5 Total chloride penetration of core samples.

The observations show the amount of chloride at the flange is lower than the amount at the web position. This may be because rainfall can attach to the flange surface and wash airborne chloride from the surface, reducing the total amount of chloride inside the material.

6.3.1. Assumptions for the Calculation

For this calculation, the assumptions include:

1) when rainfall intensity is equal to 1 mm/hr, the rain blocks chloride particles and only water particles attach on the concrete surface;
2) the washout effect occurs when the rainfall intensity is equal to or higher than 5 mm/hr and only the flange position is subjected to rainfall;
3) the amount of airborne chloride at the web and flange positions is identical;
4) as the mix proportion used in the construction does not appear in previous research, the mix design is that described in Table 6-1.

Table 6-1 Assumed mix proportion for calculation.

W/C	Cement (kg)	Water (kg)	Sand (kg)	Gravel (kg)	% Air
0.45	400	180	780	980	2.3

6.3.2. Exposure Site and Condition

The measurement position is at the Okawa Bridge in Niigata prefecture, Japan. The distance from the bridge to the coastline is 150 m (Figure 6-6).

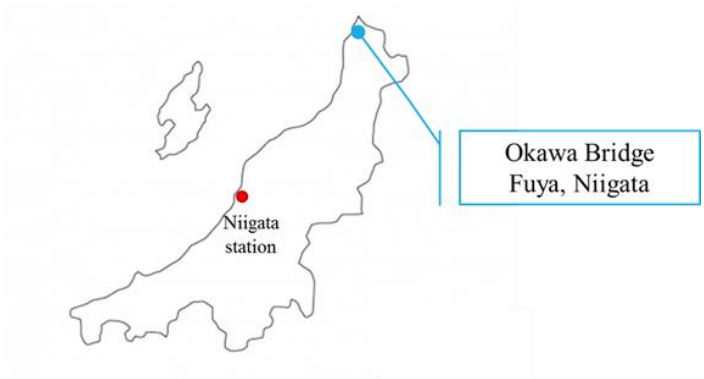

Figure 6-6 Exposure site near Okawa Bridge

Figure 6-7 Position of Okawa Bridge Pier No. 2.

The exposure condition was examined through onsite observations and a bird's-eye view [1, 2]. There are obstacles in front of the exposure site (Figure 6-8).

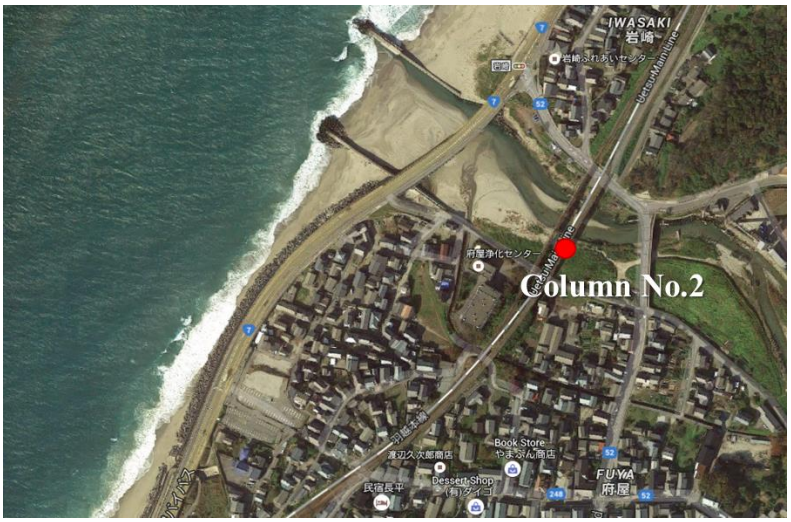

Figure 6-8 Map of exposure site (Google maps).

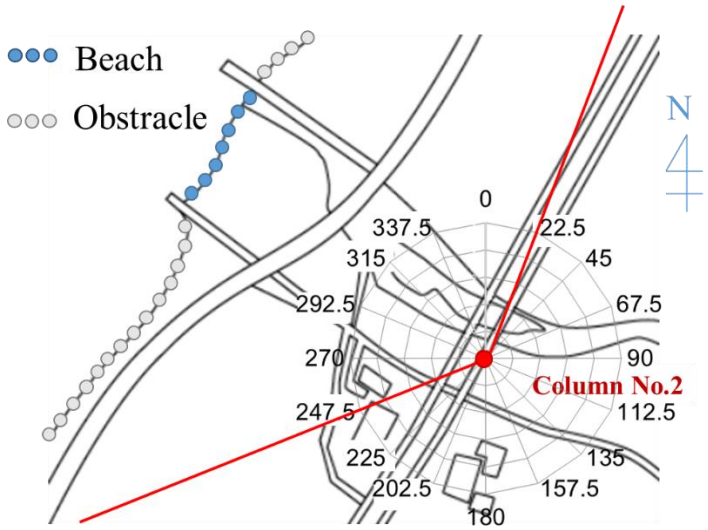

Figure 6-9 Exposure condition near exposure site and obstacle positions (150 m from the seashore).

6.3.3. Airborne Chloride Intensity Calculation

The calculation necessitates data for wave height, tidal cycle, water depth, wind speed, wind direction, and rainfall intensity. This data was taken from AMEDAS and NowPhas databases, as shown in Table 6-2.

Table 6-2 the station for past data recorded

Data	Database	Station
Wind direction	AMEDAS	Sakata (1975–1976) Nezugaseki (1977–1999)
Wind speed		Nezugaseki (1977–1999)
Precipitation		Sakata (1975–1976) Nezugaseki (1977–1999)
Wave height	NowPhas	Sakata (1975–1999)
Tidal cycle		

With this previously recorded data, the airborne chloride intensity was calculated (Figure 6-10).

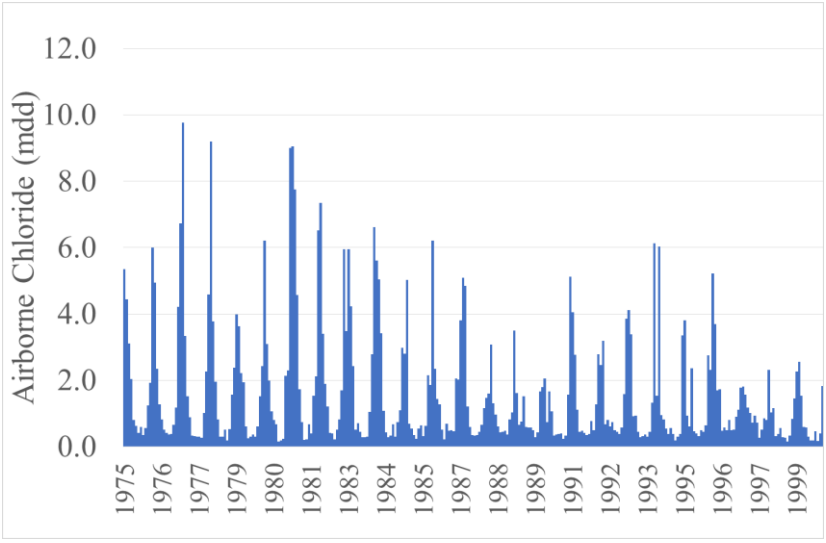

Figure 6-10 Airborne chloride intensity from the calculation (1975 – 1999).

In the calculation, the amount of airborne chloride each year changed due to different wind directions, speed, and wave height. Figure 6-11–6-15 show the difference in airborne chloride intensity each year.

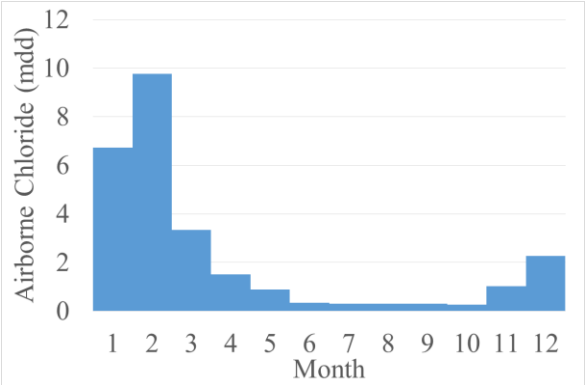

Figure 6-11 Airborne chloride intensity (1977).

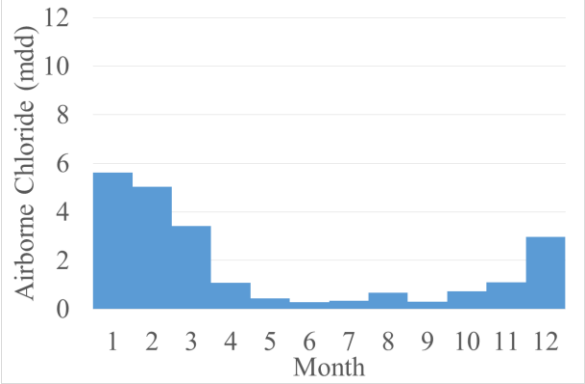

Figure 6-12 Airborne chloride intensity (1984).

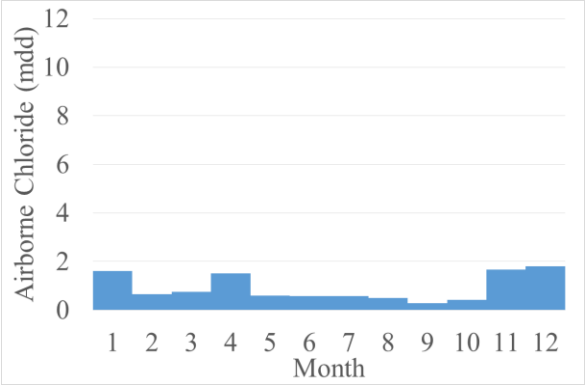

Figure 6-13 Airborne chloride intensity (1989).

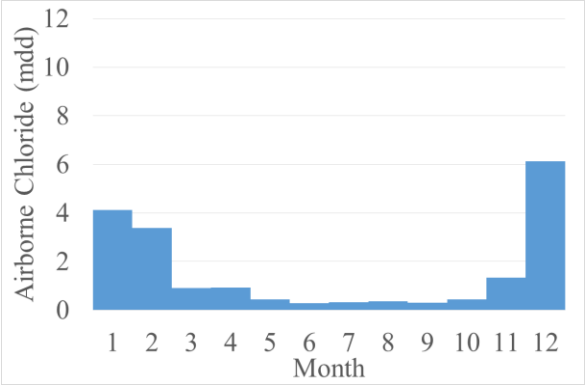

Figure 6-14 Airborne chloride intensity (1993).

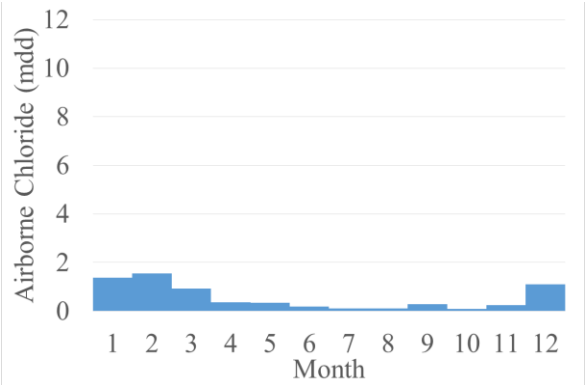

Figure 6-15 Airborne chloride intensity (1999).

The results show that the amount of airborne chloride during the exposure time was not constant. The amount of the airborne chloride changed due to environmental factors. Therefore, though previously recorded airborne chloride data is available, such records may not always be the most viable option for determining the chloride concentration of concrete structures.

6.3.4. Verification Results

The previous section described the calculation of the mount of airborne chloride between 1975–1999 with the airborne chloride generation and transportation model. This data is used as an input to calculate chloride ingression with the airborne chloride surface flux model.

To calculate chloride penetration, environmental data is needed. In this case, hourly temperature, relative humidity, and rainfall intensity data was received from the AMEDAS database, as shown in Table 6-3.

Table 6-3The AMEDAS station for data.

Data	**Station**
Relative humidity	Sakata (1975–1999)
Temperature	Sakata (1975–1976) Nezugaseki (1977–1999)
Precipitation	Sakata (1975–1976) Nezugaseki (1977–1999)

The total chloride ingression according to the calculations is shown in Figure 6-16 and Figure 6-17.

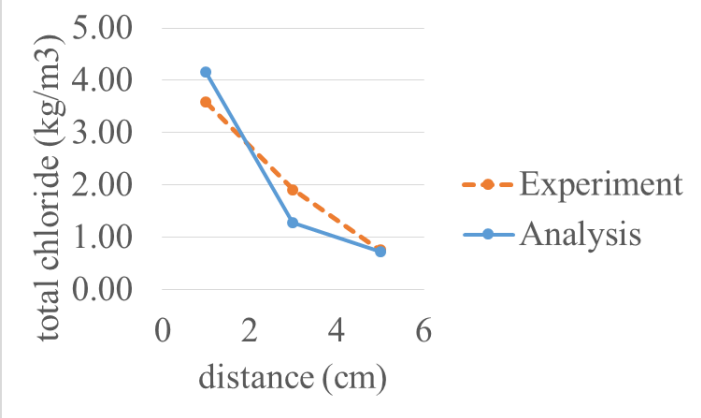

Figure 6-16 Total chloride penetration at flange.

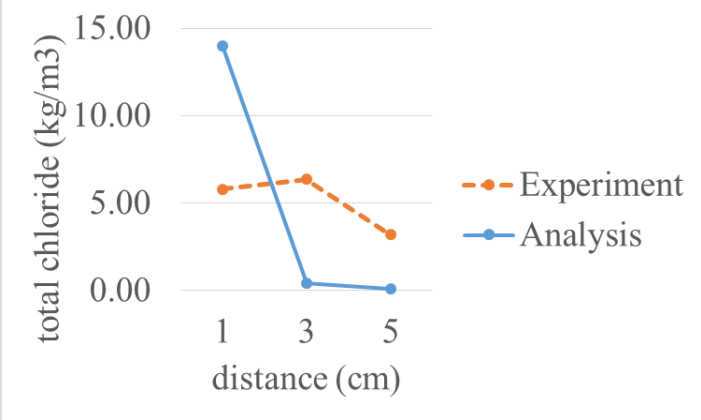

Figure 6-17 Total chloride penetration at web.

The verification reveals that the proposed comprehensive system can calculate the total chloride at the flange position though analysis results for the web position are do not match onsite measurement data.

This may be due to the assumed threshold value (r_{thre}) in the chloride ion transportation model [4]. In previous research, when the chloride ion transportation model is used to calculate chloride penetration for OPC, the chloride ion does not move in pores below ~80% relative humidity [4]. When the structure is not exposed to rainfall, the concrete remains dry.

At the flange position, it was assumed that the structure is subject to rainfall. Thus, the relative humidity inside the material is higher than at the web. In the calculation for the web position, the concrete is dry and chloride ions cannot penetrate deep into structure. The relative humidity and chloride distribution inside the materials from the calculations are shown in Figure 6-18 and 6-19.

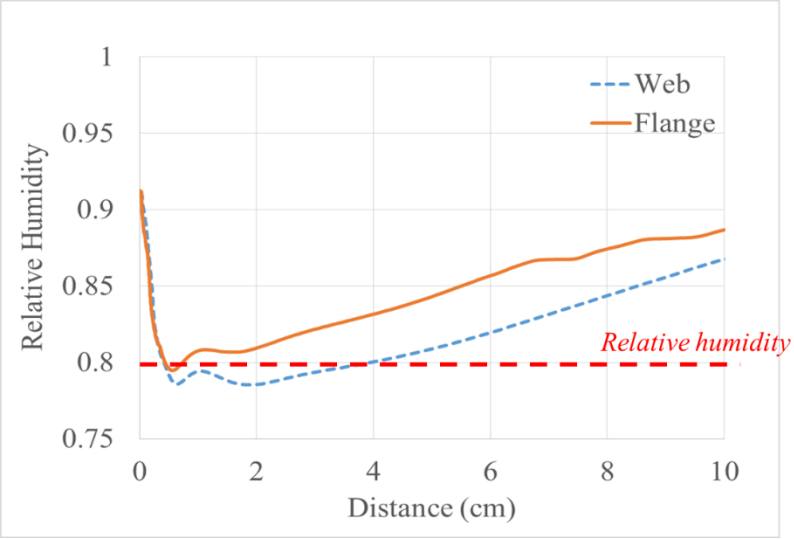

Figure 6-18 Relative humidity in materials after 25 year exposure.

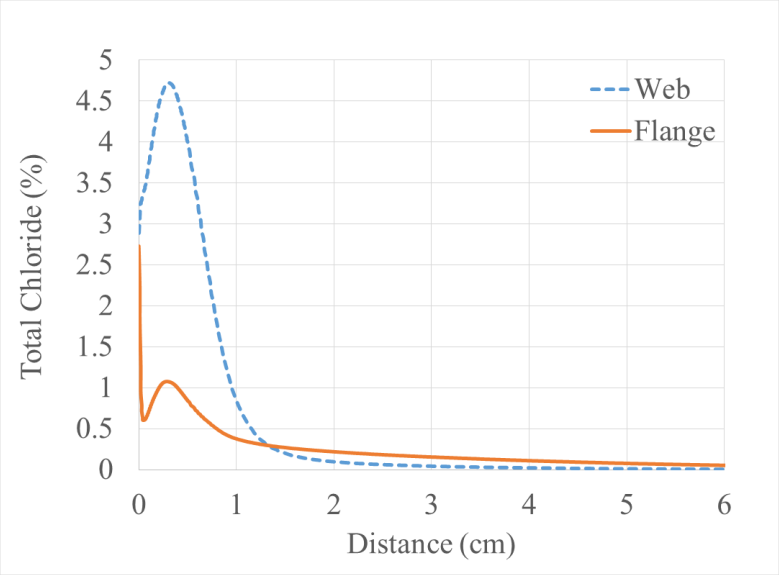

Figure 6-19 Chloride distribution in material after25 year exposure.

According to the calculation at the web position, the relative humidity for 0.5–4 cm is lower than 80%. Therefore, the chloride cannot penetrate further.

The analysis results show that for the proposed framework, when concrete remains in a dry environment, such as concrete under a roof slab covering, chloride ingression cannot be properly predicted. Thus, the examination of chloride ion transportation in unsaturated concrete should be considered in the future.

6.4. Conclusion

The current study presents a comprehensive framework for calculating airborne chloride penetration. This framework can determine the amount of the airborne chloride generated by breaking waves, transported by wind flow, and its ingression in concrete. The proposed framework was verified with exposure tests under actual environmental conditions.

From the verification results, the proposed comprehensive system can calculate the total chloride at a flange position. However, the analysis results at a web position did not match onsite measurement data. This may be due to limitations of the proposed system which cannot calculate chloride penetration in unsaturated concrete. Thus, continued examination of chloride ion transportation should be considered.

6.5. *Reference*

[1] S. Hanioka, "Verification and enhancement of airborne chloride generation and transportation model based on field measurement," The university of Tokyo, 2011. (in Japanese)

[2] T. Ishida, A. Kita, S. Hanioka, L. A. Ho Thi and Y. Matsuda, "A study on Mechanism of airborne chloride transport and migration into mortar based on onsite measurement," in *Proceedings of the Concrete Structure Scenarios*, 2012. (in Japanese)

[3] S. Yoshida, K. Shikiya and H. Kobayashi, "The application of Cathodic corrosion protection method on PC bridge repairing," *SED : Structural engineering data*, vol. 12, pp. 48-57, 1999. (in Japanese)

[4] Y. Takahashi and T. Ishida, "Modeling of chloride ion ingress and liquid water movement in mortars and concretes with low water-to-cement ratio," in *International Conference on Sustainable Construction Materials and Technologies 3*, Kyoto, Japan, 2013.

Chapter 7
Conclusion and Suggestions for Future Study

7.1. Conclusion

In a marine environment, the deterioration of RC structures is caused by airborne chloride attack. For this reason, infrastructure in coastal areas often require repair or reconstruction due to corrosion. Therefore, the reliable prediction of airborne chloride penetration into concrete structures is necessary to evaluate the service life of these structures.

Chapter 3 presented a comprehensive system to this end. The comprehensive system considers the amount of chloride generation and ingression by connecting three numerical models, which are the chloride ion transportation model, a moisture and chloride surface flux model, and a airborne chloride generation and transportation model. The current study reviewed and verified each model.

According to the verification results, the chloride ion transportation in cementitious materials model can predict the amount of chloride ingression in concrete under submerged condition. However, when the chloride ion transport model is combined with the moisture and chloride surface flux model, the model overestimates experimental and onsite measurement results. Therefore, a modification of the model was considered necessary.

Chapter 4 presented a modification of the moisture and chloride surface flux model. The limitations of chloride concentration on the surface, washout effect, and water absorption behavior were taken into account in the calculation. A comprehensive experimental series was conducted to verify the moisture and chloride surface flux model. According to the verification, the proposed model can predict chloride ingression, water ingression, and the amount of chloride washout under controlled conditions.

Furthermore, onsite measurement data from previous research was used to verify airborne chloride ingression under actual environmental conditions. Verification with tank capture and wet candle methods show that the proposed model can appropriately simulate chloride penetration under actual environmental conditions.

With the mortar chip method, the model underestimates experimental results. This may be because the mortar chip can be washed by rainfall, reducing the chloride concentration on the specimen surface reduced.

Moreover, for the dry gauze method, the model results were highly variant compared to others method. The chloride collection time with the dry gauze in the current study was short compared to specimen exposure time. It can be concluded that airborne chloride data from the dry gauze method was not representative of the amount of airborne chloride during the specified exposure time. Therefore, airborne chloride collecting methods should be carefully selected.

When both properly recorded airborne chloride and adequate environmental data are available, the proposed model can properly simulate chloride penetration into structures. However, in reality, airborne chloride data is limited. Thus, in such cases, it is necessary to model the generation and transportation of airborne chloride particles.

In Chapter 5, the airborne chloride generation and transportation model was verified with onsite measurement data. According to the verification, the chloride generation and transportation model can predict the amount of airborne chloride at specific locations under different exposure conditions. The amount of airborne chloride from the calculation can be given as the input for the airborne chloride surface flux model.

Chapter 6 discusses the verification of the proposed comprehensive system with onsite measurement data from the Okawa Bridge. The results suggest the proposed comprehensive system can calculate the total chloride penetration for positions subject to rainfall (flange). However, model results for positions unexposed to rain (web) are poorly predicted. This may be because of limitations in calculations from the chloride ion transportation model for unsaturated concrete. Thus, understanding of chloride ion transportation in cementitious materials should be expanded.

7.2. Suggestion for Future Research

With the proposed comprehensive system, chloride ingression in airborne chloride environments can be predicted. However, there are still some limitations to the calculation. A number of suggestions for future research can be made.

1) Airborne chloride ion generation and transportation model

- The proposed model can predict the amount of airborne chloride with the tank sample method. However, for calculation results when the exposure position is close

to the seashore (Orikasa-Ohashi), verification results were different from the measurement. Therefore, the study of airborne chloride generation and transportation in positions close to the seashore should be considered.

- The proposed model can calculate the amount of the airborne chloride for sites directly exposed to the seashore but, in reality, airborne chloride can be transported to different areas by wind flow. Therefore, a model which can calculate the amount of airborne chloride at different positions should be considered.

2) Moisture and chloride surface flux model

- When airborne chloride was collected with different methods, data differs and may affect the model results. Thus, the relationship between the amount of airborne chloride determined by each method should be considered.

- Moreover, data for the verification with the wet candle and dry gauze methods is limited. Thus, additional tests are necessary to confirm the results.

- For the calculation, it is assumed that the washout effect occurs when the rainfall intensity is equal to or higher than 5 mm/hr. This assumption is from the sensitivity analysis. However, the mechanism under actual environmental conditions should be examined to ensure the validity of the model.

3) Chloride ion transportation model

- The verification results show that when concrete is exposed to rainfall the proposed comprehensive system can calculate the amount of chloride penetration. However, when the concrete is under dry conditions, the proposed system cannot predict chloride penetration. This may be due to limitations in the chloride ion transportation model. Thus, future modifications in the chloride ion transportation model should be considered.

Appendix I
Wind Tunnel Experiment

1. *Introduction*

To simulate airborne chloride environmental condition in the laboratory, a wind tunnel has developed [1, 2, 3] . Inside the wind tunnel, a salt bath and a bubble generator were installed. The salt bath was filled with NaCl solution, concentration 3% (0.51 mol/L). The bubble generator was placed inside the salt water bath to generate small salt particles.

A propeller was installed behind the salt bath to generate the air flow inside the chamber. The air flow will transport the airborne chloride particle inside the wind tunnel. The average wind speed in this test is around 1.5 m/s.

By this concept, the airborne chloride exposure environment can be simulate. However, this method has some limitations. Therefore, the experimental methodology was modified to increase the accuracy of the experiment.

2. *Limitation of previous method*

In the previous experiment, the airborne chloride amount was measured before testing chloride penetration in mortar specimen. The flow of the experiment is shown as following

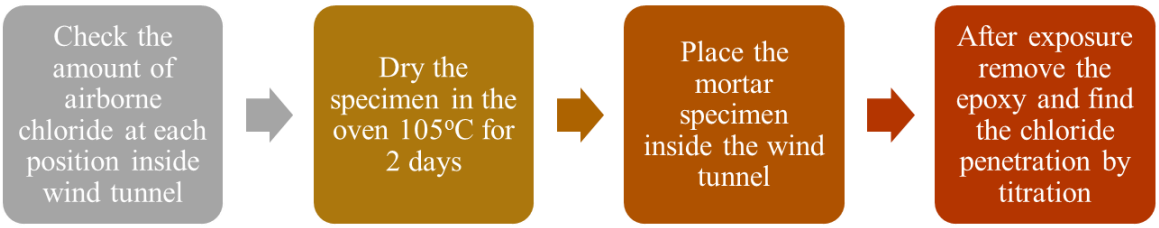

Figure I-1 Total chloride penetration experiment process by Ishikawa T.

To find the amount adhesion airborne inside the chamber gauze and cotton specimens were installed at various positions as following.

Figure I-2 Gauze and cotton specimen in the test.

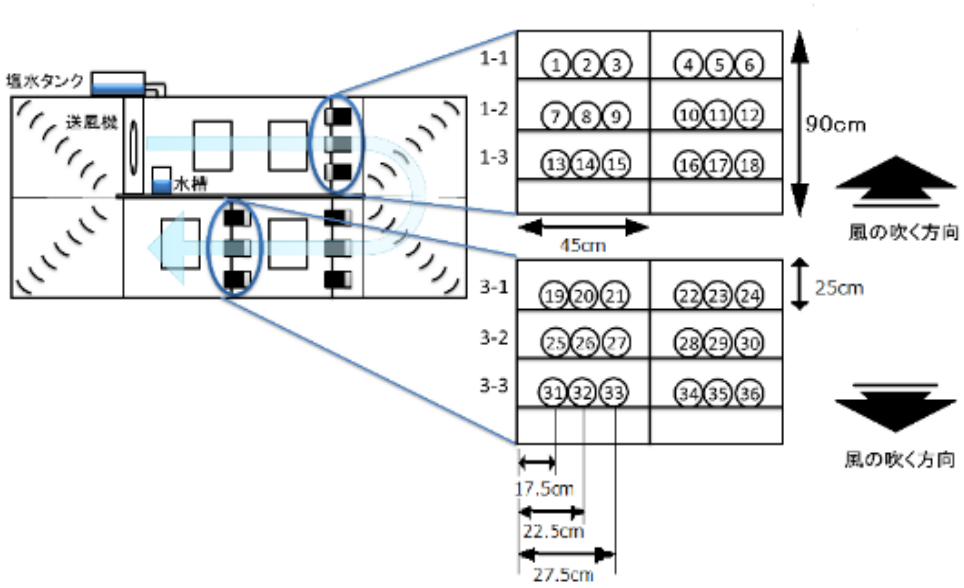

Figure I-3 The position of the specimen in the test.

After exposure (4–8 hrs), gauze and cotton samples at each position were submerged in pure water and titrated to determine the amount of chloride at each position [3].

The wind speed at each position in the wind tunnel can change due to the obstacle inside. Additionally, if the level of the salt water is changed, the amount of airborne chloride at each position is also changed. Because of these factors, the amount of airborne chloride at each position inside the wind tunnel is not constant during the test [1].

Figure I-4 shows the amount of airborne chloride at each position. From the results, although the exposure time are almost the same (3.2 – 4 hours) but the airborne amount differ.

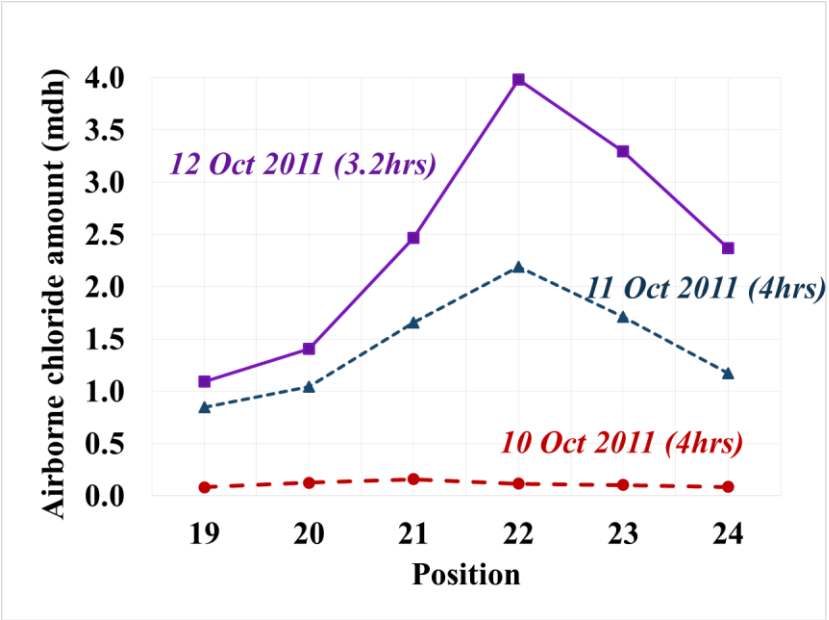

Figure I-4 The amount of the airborne chloride at position 19 – 24.

Moreover, another trial test was done by using colored salt water. Instead of normal salt water, the black ink was added into salt water bath as show in Figure I-5

Figure I-5 Colored salt water.

Inside the wind tunnel the cotton and gauze specimen was placed at each position to observe the concentration of airborne chloride at each position by detecting the intensity of black color on each specimen. The position of specimen is shown in Figure I-6.

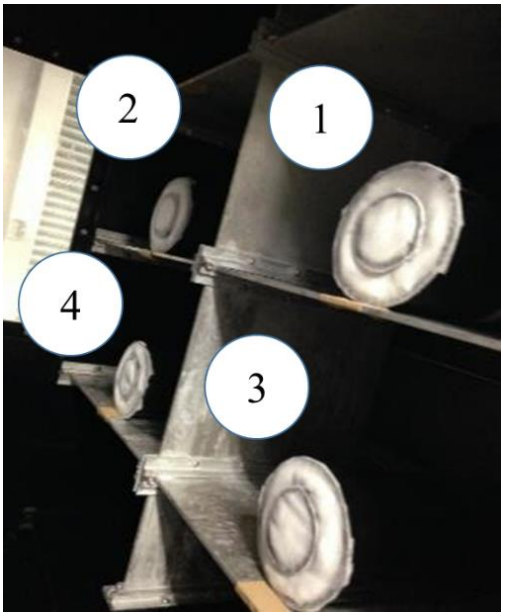

Figure I-6 Specimen position.

After 4 - 6 hours exposure the color intensity was observed as show in Figure I-7 and Figure I-8.

Figure I-7 Color intensity inside the wind tunnel.

Figure I-8 Black color in the wind tunnel after test.

From Figure I-8, in the middle part of the chamber, the amount of airborne chloride is higher than on the side.

Moreover, with the existing equipment, to control the wind speed or the airborne chloride flux at each position are difficult. Thus, the exposure specimen should be modified.

3. Modified Method

3.1. Limit testing area

Figure I-8 showed the result that the airborne chloride intensity in the middle and on the side are completely different. Therefore, the area which suitable for the experiment are limited.

To scope the testing area, the trial and error test was conducted by using colored salted. The cotton and gauze specimen was placed in the different place and check the consistency of the color on the specimen. If the color on the specimen are consistence, that area can be used in the experiment.

Figure I-9 Example of the consistency color on the testing specimen.

Figure I-10 Different of the color after the test.

After the test, the area which can be used in the experiment is the blue highlight zone as following

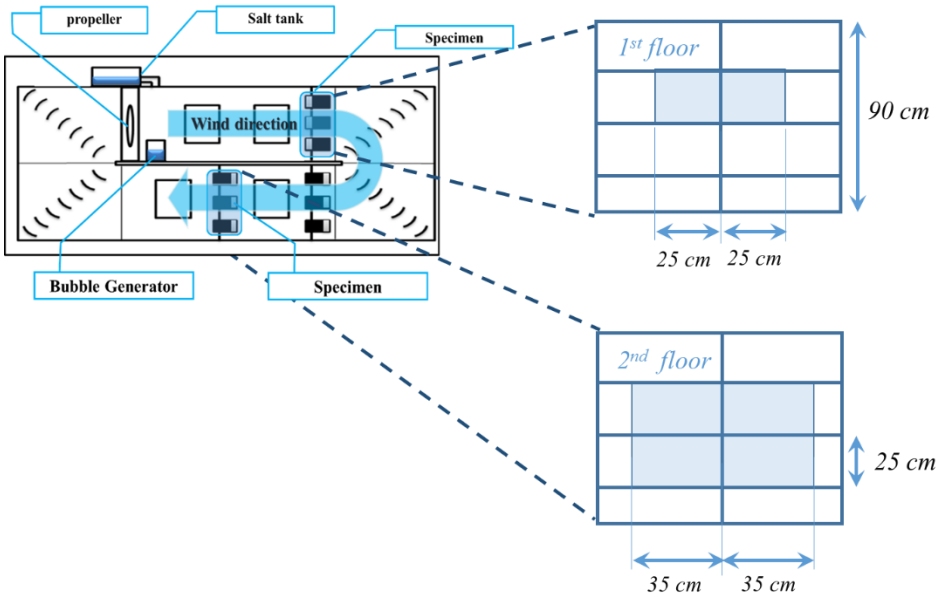

Figure I-11 The suggested area for exposure experiment in wind tunnel.

3.2. Exposure specimen

As mention in the previous section, with the existing equipment, to control the wind speed or the airborne chloride flux at each position are very difficult. Thus a new exposure specimen was made. The objective of using the new specimen is to measure the amount of the airborne chloride and the amount of airborne chloride ingression at the same time. With this method, although the airborne chloride flux during the test is not consistence, but the total airborne chloride amount can be captured.

In the new method, a mortar specimen will be placed in the middle of cylinder mold (Ø 10 cm x 20 cm). Then, gauze and cotton will be placed around the mortar specimen to capture airborne chloride particles. The concept of the proposed specimen are shown as following

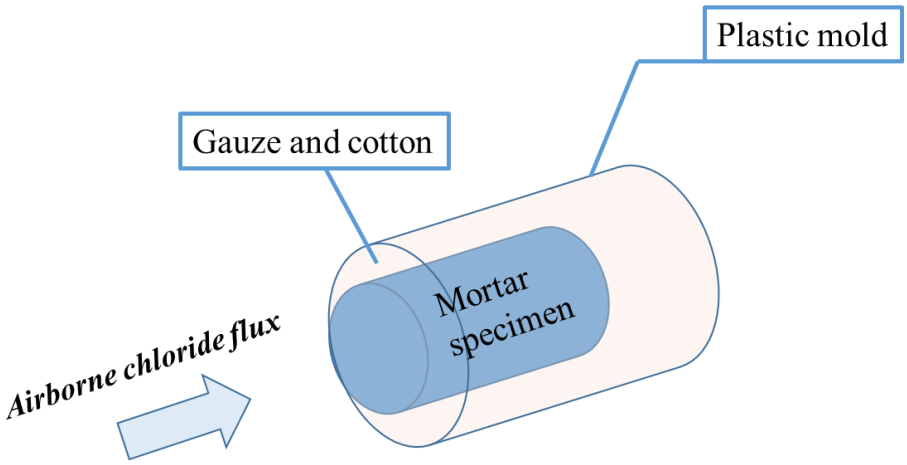

Figure I-12 Concept of proposed exposure specimen.

To verify the concept the mock up specimen was made with 2 cylinder mold, size Ø5cm x 10 cm and Ø10cm x 20 cm. The smaller mold was placed inside the bigger mold. In each mold, cotton and gauze were filled as shown in Figure I-13 and Figure I-14.

Figure I-13 Mock up specimen (top view).

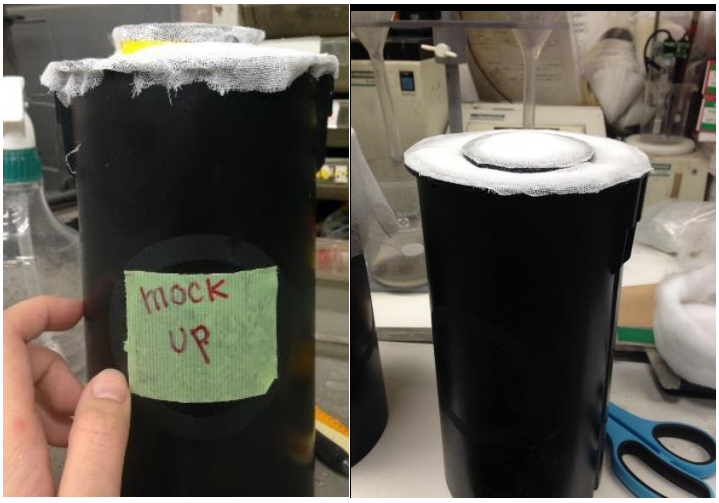

Figure I-14 Mock up specimen (Side view).

The mockup specimens were place in the wind tunnel and capture the amount for the airborne chloride, to check the amount of the adhesion chloride in the inner part and the outer part or the specimen. If the airborne chloride amount are the same, it can be inferred that this concept can be used in the experiment.

The test series to verified this concept are shown as following

1) The level of mortar specimen

For the first test, the appropriate level of mortar specimen was check. To prevent the contamination between inner part and outer part, the different level of 2 inner mold and outer mold was made as shown in Figure I-15. Case I, the inner mold level is higher than the outer mold 0.5 cm. Case II, the inner mold level is higher than the outer mold 0.2 cm. Case III the inner mold level and the outer mold are controlled at the same level.

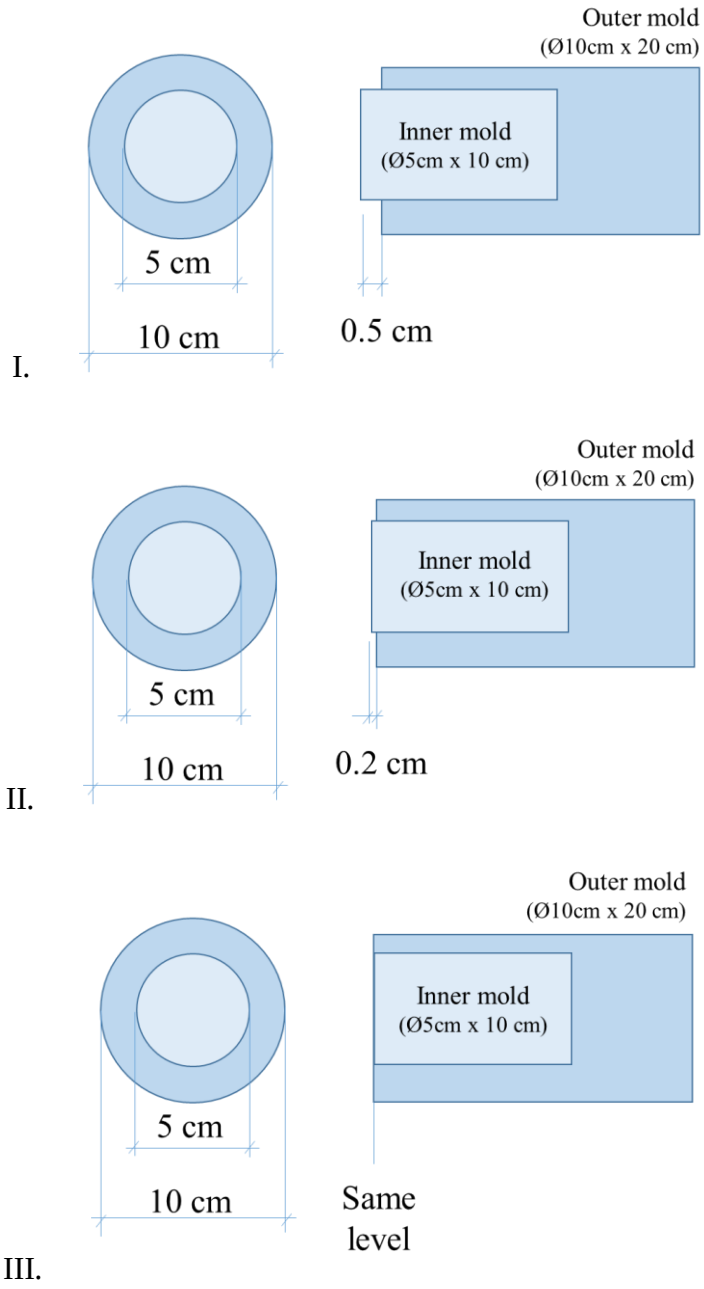

Figure I-15 Layout of the specimen

Then, each specimen was placed inside the wind tunnel for 4 hours to find the amount of airborne chloride. The testing results are shown in Table I-1−I-3.

Table I-1 The amount of airborne chloride after exposure (Case I 0.5 cm gap).

Position	**Inner (mg/cm^2)**	**Outer (mg/cm^2)**	**Different (%)**
1	0.320	0.000	- 100%
2	0.032	0.046	43 %
3	0.019	0.000	-100%
4	0.100	0.170	70%

Table I-2 The amount of airborne chloride after exposure (Case II 0.2 cm gap).

Position	**Inner (mg/cm^2)**	**Outer (mg/cm^2)**	**Different (%)**
1	0.299	0.0498	67%
2	0.040	0.037	-8 %
3	1.609	1.620	1%
4	1.474	1.881	28%

Table I-3 The amount of airborne chloride after exposure (Case III 0.0 cm gap).

Position	**Inner (mg/cm^2)**	**Outer (mg/cm^2)**	**Different (%)**
1	0.0199	0.0188	-5%
2	0.0140	0.0129	-8%
3	0.3505	0.3547	1%
4	0.3505	0.3547	1%

From the results, when the gap between inner and outer part is reduced, the chloride amount from inner and outer part are also reduced. When the level of the inner and outer mold are the same (Case III, 0 cm gap) the difference of airborne chloride flux are less than 10%. Thus, in the experiment the mortar specimen and the mold should be controlled at the same level.

However, when the mortar and the outer mold are controlled at the same level the contamination in the gauze and cotton specimen can occur.

In the trial test, the mortar specimen was casted and coated with epoxy. Then, around the specimen was cover by gypsum and placed in the middle of the cylinder mold (Ø10cm x 20 cm) as following

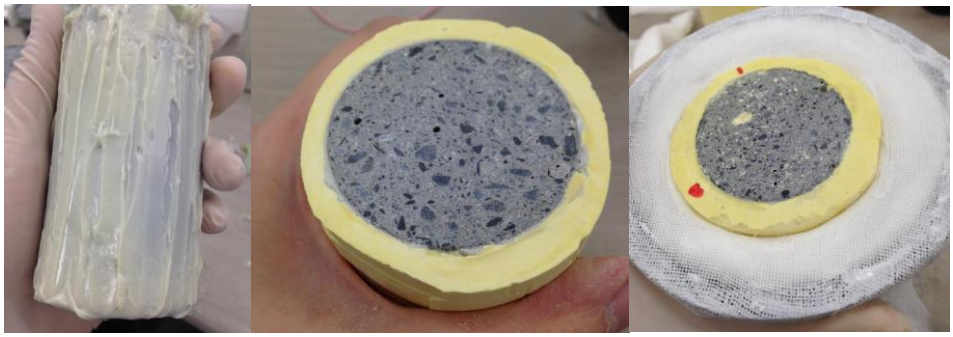

Figure I-16 Testing Specimen.

The testing specimen was placed in the wind tunnel. The testing specimen after exposure is shown in Figure I-17. After the exposure, the airborne chloride which cannot absorb into mortar was accumulate in the bottom part of the specimen and absorbed into the cotton. In this case, the airborne chloride flux can be overestimated. Therefore, the exposure specimen should be modified.

Figure I-17 Testing specimen after exposure (2 days).

2) Applied Super Absorbent Polymer (SAP)

Super Absorbent Polymer (SAP) is the materials which can absorb large amount of water. In the exposure specimen, SAP materials will be placed between the mortar and cotton to prevent the contamination of the salt water.

The step in making exposure specimen are shown as following

- Ø7 cm x 10 cm mold was made by the rubber pad as following

Figure I-18 Rubber mold size Ø7 cm x 10 cm.

- The mortar specimen (size Ø5 cm x 10 cm) coated with epoxy was placed in the middle of the rubber mold and the SAP material was rap by high quality tissue and filled in the space between rubber mold and mortar specimen.

Figure I-19 Specimen filled with SAP materials.

- The rubber mold and mortar specimen was placed in the plastic mold size Ø10cm x 20 cm. Inside the Ø10cm x 20 cm mold the space between plastic mold and rubber mold was filled with cotton and gauze as following

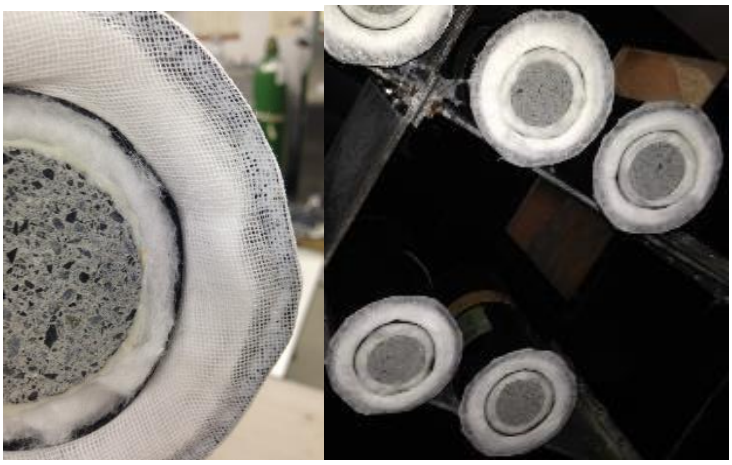

Figure I-20 Exposure specimen in the test.

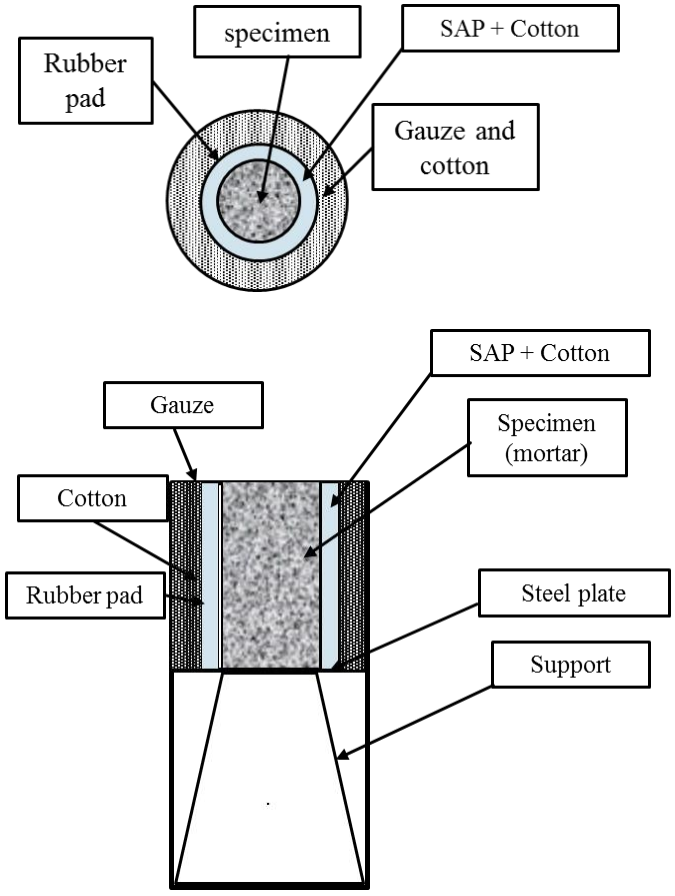

Figure I-21 *Exposure specimen layout.*

In the experiment, the SAP was Sodium acrylic powder base from BASF chemical company.

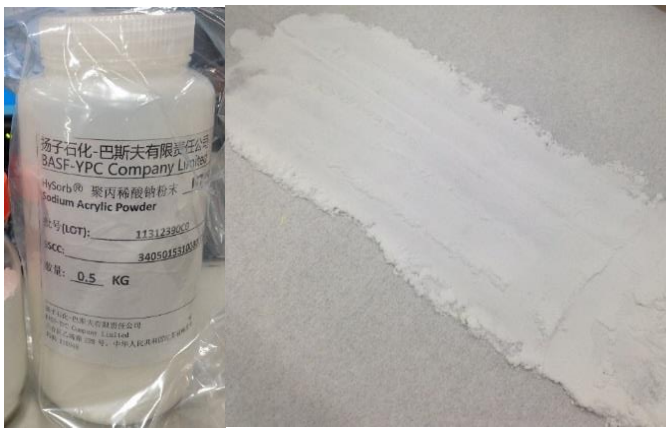

Figure I-22 Super absorbent polymer.
(BASF-YPC, Sodium acrylic powder)

This set up was checked by placed the exposure specimen in the wind tunnel. After the exposure, when the specimen attach to the airborne chloride around 5-7 days, the SAP materials will expand a little bit and change from the powder to the gel. At this stage the SAP materials can be changed to prevent the contamination.

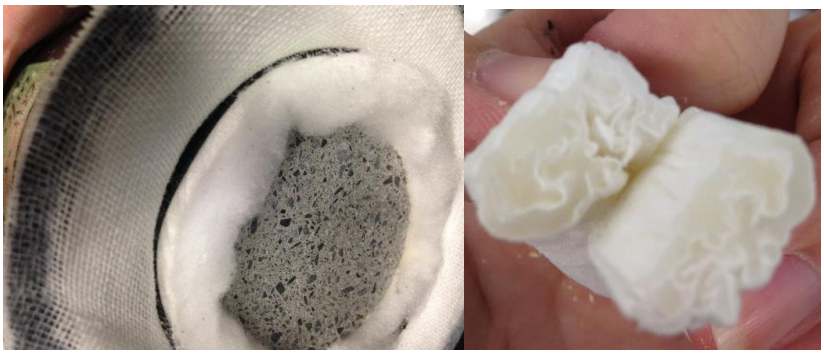

Figure I-23 Super absorbent polymer after exposure.

3) Specimen position

From the experiment and from the analysis*, the position in placing specimen are also important.

If the specimen was placed on the shelf, the chloride concentration on the specimen surface will not uniform because the wind cannot flow pass through the specimen as shown in Figure I-24

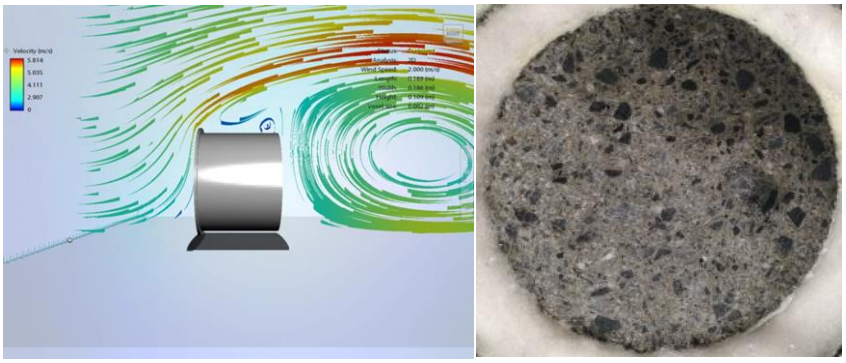

Figure I-24 Non-uniform airborne chloride flux on the surface.

However, if the specimen was lifted and left the space between the floor and the specimen, the wind speed and airborne chloride concentration on the specimen surface will become more uniform as show in Figure I-25.

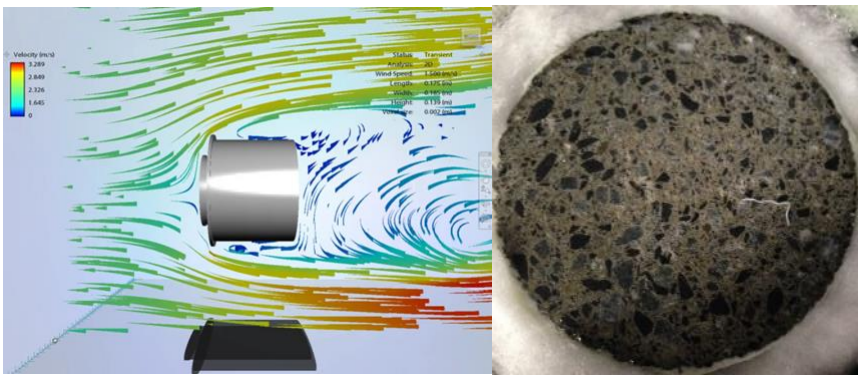

Figure I-25 Uniform airborne chloride flux on the surface.

**The analysis was made by Flow Design Program by AutoDesk.*
Flow Design Program is a virtual wind tunnel for visualizing airflow around the object.

However in the experiment, it is difficult to lift the specimen from the shelf, thus the specimen was shift forward to let the wind can flow in the bottom of the specimen as following

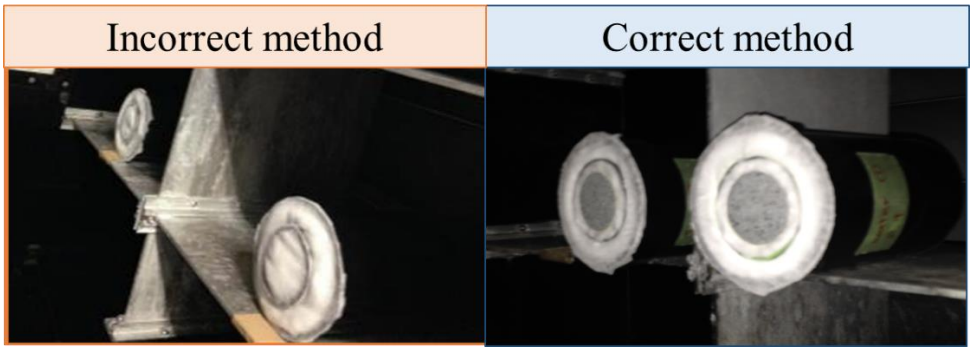

Figure I-26 Suggested specimen position.

3.3. Consistency of the chloride ingression

After exposure, to check the consistency of chloride ingression, the mortar specimen was drilled in the different position to find the total chloride ingression.

Figure I-27 Drilled specimen and driller.

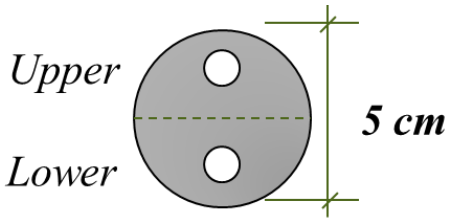

Figure I-28 Drilling position.

The chloride ingression results are shown in Table I-4 and Table I-5. From the results, the amount of chloride penetration by using the proposed method give the uniform chloride ingression results.

Table I-4 Airborne chloride ingression in W/C 0.55 specimen.

Date	**Curing Condition**	**Exposure time**	**Position**	**Sample (g)**	**Cl- (kg/m3)**
20 Nov 14	Air cure W/C 0.55	14 Days	Upper	3.235	0.1233
			Lower	3.569	0.1250

Table I-5 Airborne chloride ingression in W/C 0.40 specimen.

Date	**Curing Condition**	**Exposure time**	**Position**	**Sample (g)**	**Cl- (kg/m3)**
5 Feb 15	Water cure W/C 0.40	21 Days	Upper	4.113	0.3218
			Lower	4.200	0.4326

4. Summary

The airborne chloride flux inside the wind tunnel are not uniform. In addition with the existing equipment, to control the wind speed or the airborne chloride flux at each position are difficult. Thus, the exposure specimen and the testing method should be modified.

The proposed method has been verified by various experiment as mention in the previous section. From the verification, the proposed method can give the acceptable results. Therefore the proposed exposure specimen and testing method are used to verify the airborne chloride ingression in this research.

The different between past research and the new proposed experimental method are shown as following

Table I-6 Comparison between the previous and new proposed method.

Detail	***Ishikawa T. (2012)***	***New proposed***
Airborne chloride measurement method	Gauze and cotton	Gauze and cotton
Airborne chloride measurement duration*	Measure airborne chloride before mortar specimen exposure/ 4-8 hours	Measure airborne chloride at the same time with chloride penetration test/ 1 month
Mortar specimen curing method	Seal curing 7 days	Air curing, seal curing and water curing 28 days
Mortar specimen Condition before exposure	The specimen was putted in oven (105^{o}C) for 2 days	The specimen was putted in control room at RH 60, 20^{o}C for 28 days
Mortar Specimen size	Ø 5 cm, height 5cm	Ø 5 cm, height 10 cm
Exposure Duration	7 – 50 days	50 - 60 days

5. Reference

[1] K. Horikiri, "Measurement of airborne salinity by a new method and study on the penetration behavior into concrete," The University of Tokyo, Toyko, 2009.

[2] A. Kita, "Quantification of airborne chloride penetration based on wind tunnel and field measurement," The University of Tokyo, Tokyo, Japan, 2009.

[3] T. Ishikawa, "Modeling of airborne chloride penetration flux into concrete," The University of Tokyo, Tokyo, Japan, 2010.